

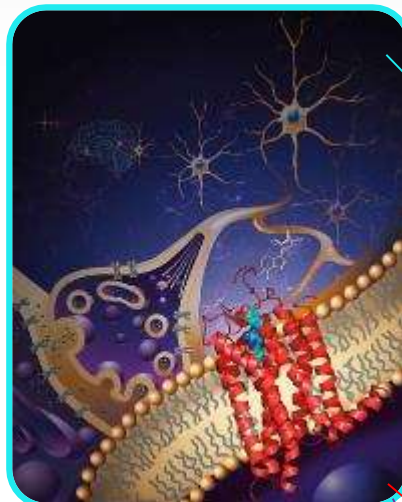
Computational Modeling of GPCRs: Towards Understanding Receptor Signaling for Biology and Drug Discovery

Vsevolod (Seva) Katritch



GPCRs in Human Biology & Pharmacology

800 GPCR are receptors for:



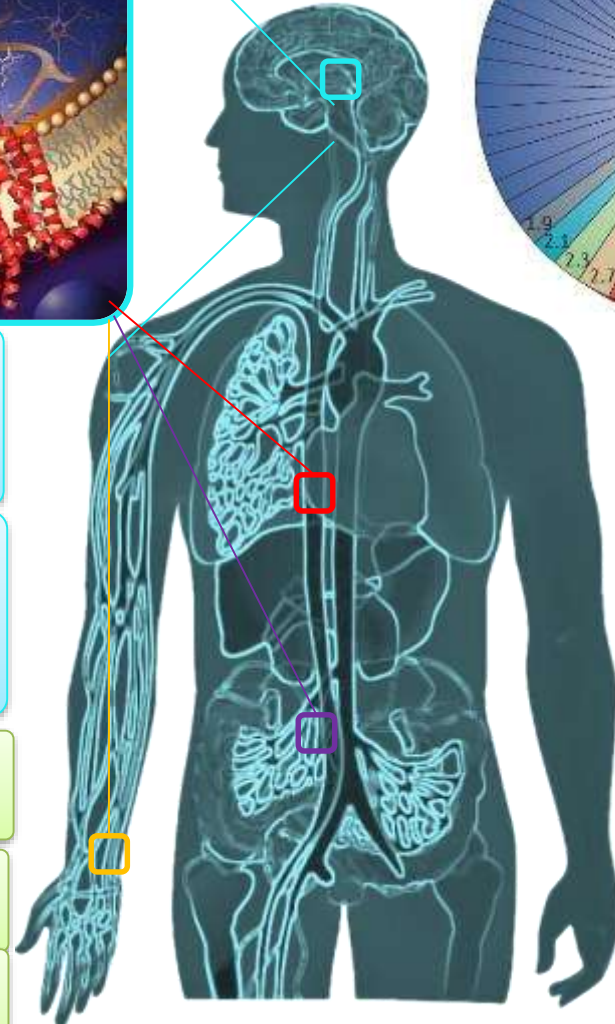
Neurotransmitters
(adrenaline, dopamine, histamine, acetylcholine, adenosine, serotonin, glutamate, anandamide, GABA)

Hormones & Neuropeptides
(opioid, neuropeptidin, glucagon, CRF, galanin, orexin, oxytocin, neuromedin, melanocortins, somatostatin, ghrelin, TRH, TSH, GnRH, PTH, THS, LH... >30 total)

Immune system
(chemokine, sphingosine 1 phosphate)

Development
(Frizzled, Adhesion)

Sensory
Light, Taste, Olfactory (388)



Nat Rev Drug Disc 5:993 (2006)

>30% of all drugs

GPCR Targets:
>120 established
> 800 potential

Disorders Targeted Clinically

Psychiatric, Learning & Memory, Mood, Sleep, Drug Addiction, Stress, Anxiety, Pain, Social Behavior...

Cardiovascular, Endocrine, Obesity, Immune, HIV, Reproductive ...

Neurodegenerative and Autoimmune Disease ...

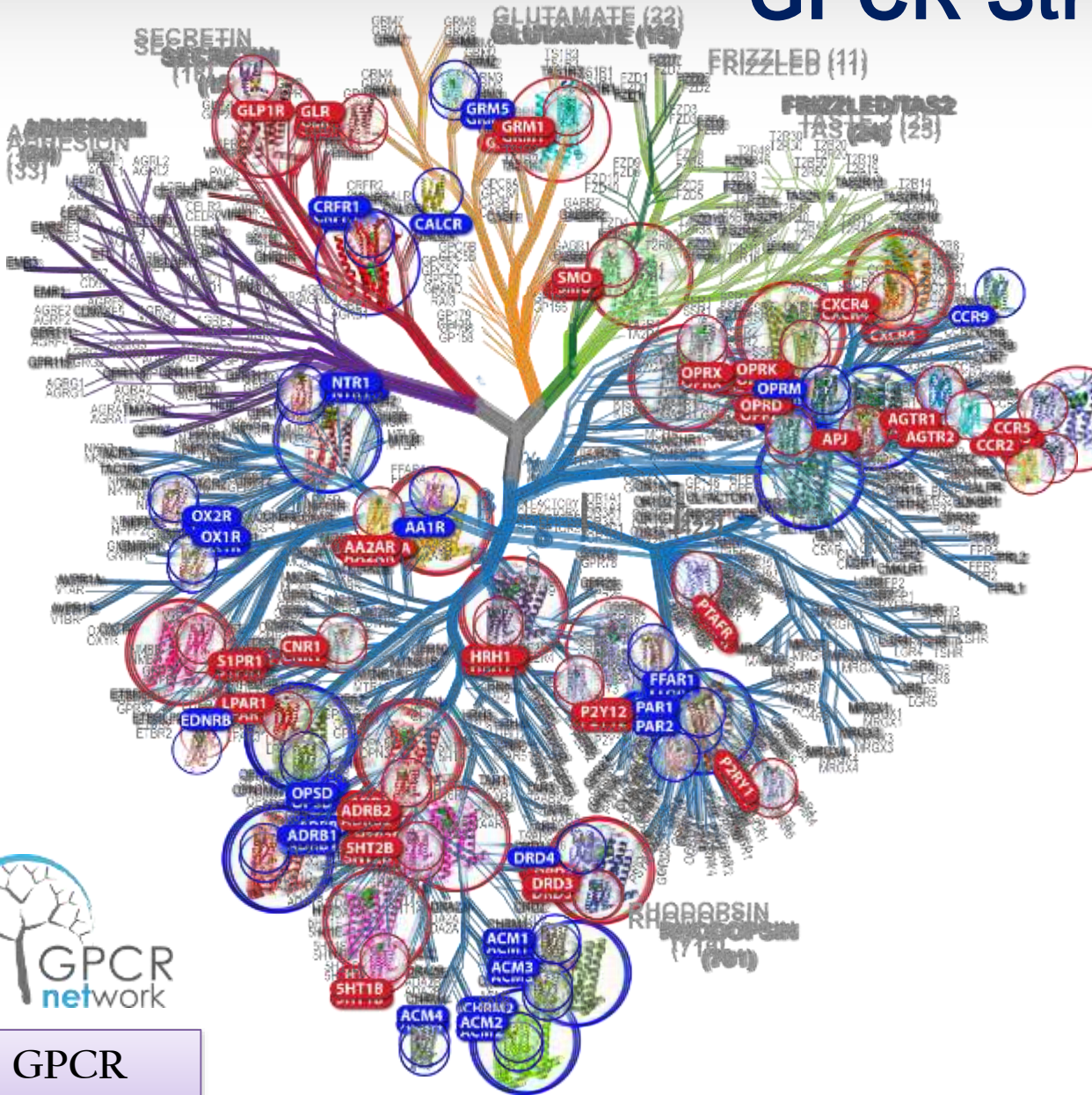
Brain Development, Regenerative Med.

Cancer

GPCR Structure and Function



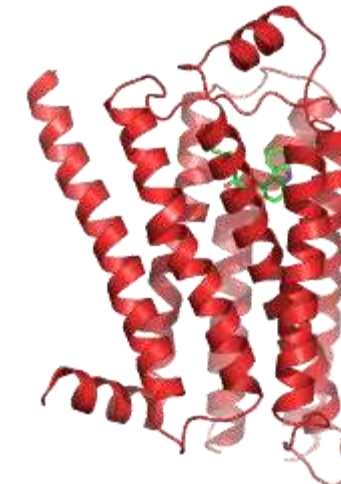
GPCR
Consortium



Thousands of
Ligands -
Chemical
Diversity

>800 Different
Human
Receptors
(largest family
in human genome)
Share 7TM Fold
But Diverse
Structural Features

Dozens of
Effectors



We use structure
and modeling
to learn:

- Molecular Recognition
- Signaling Mechanisms

and to design:
New tool compounds
New receptor properties

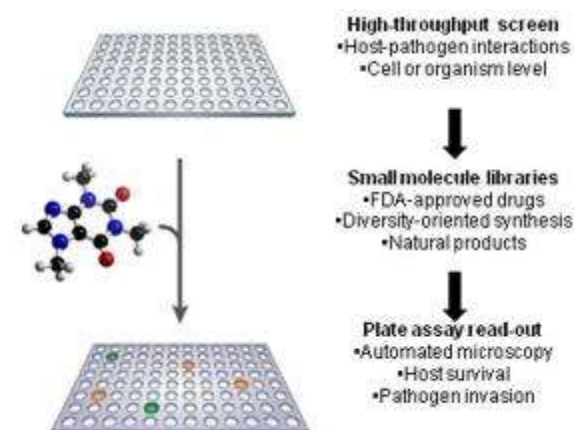
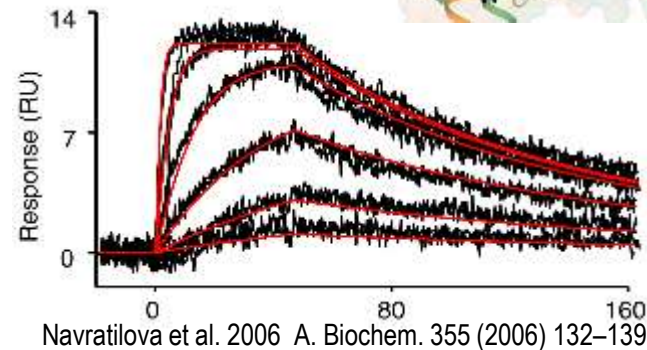
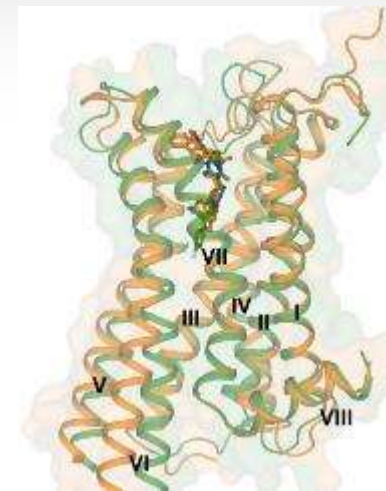
Katritch et al 2013 *Annu Rev Pharm. Tox.* **53**, 531-556
Stevens et al. 2013, *Nat Rev Drug Discov.* **12**: 25–34

Outline

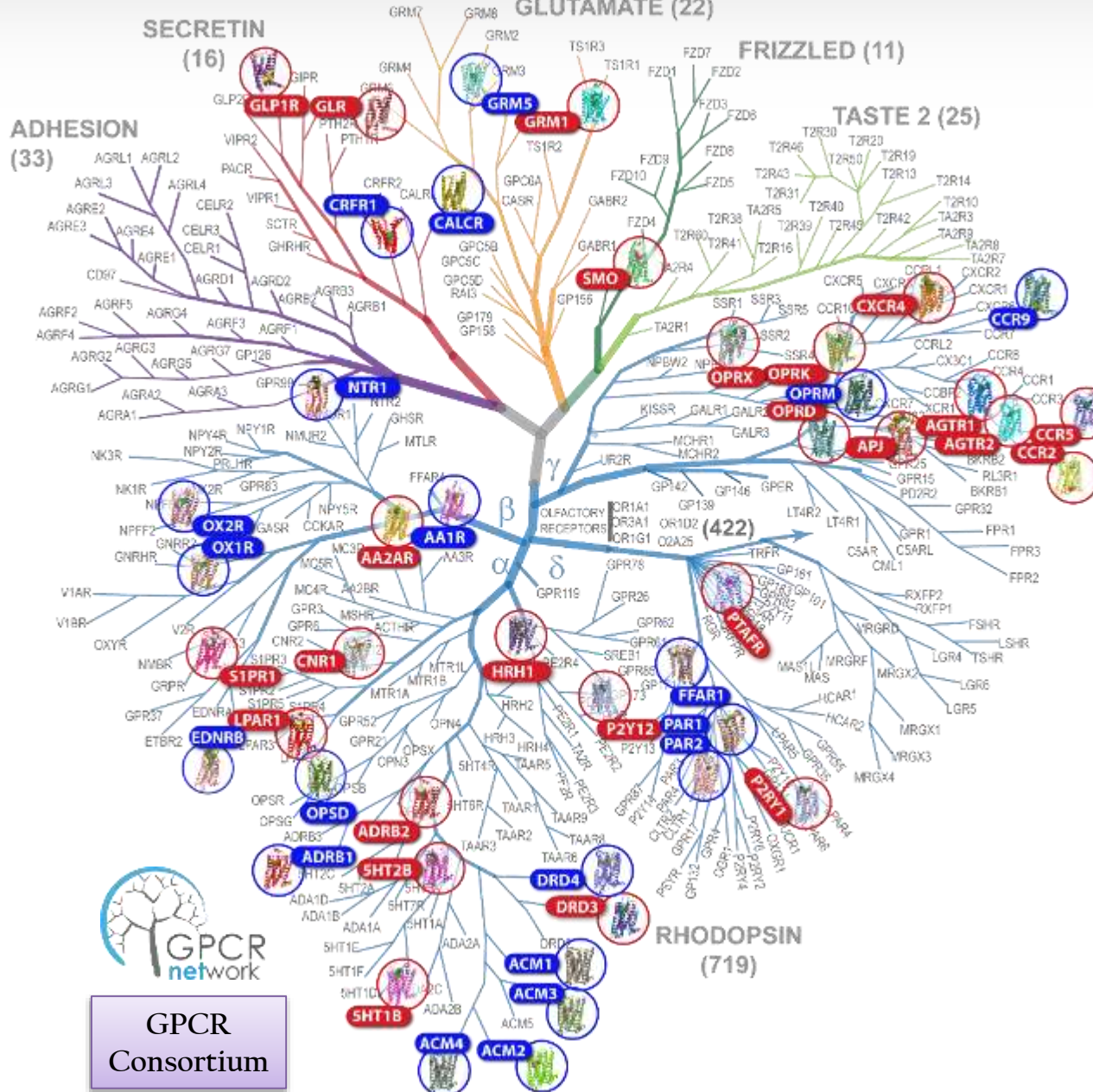
- Rational prediction of stabilizing mutations:
CompoMug
- New insights into GPCR function and allosteric mechanisms
- Structure-Based ligand discovery for GPCRs

Why Stabilizing GPCRs?

- Crystallography:
 - Synergistic with fusions and truncations
 - Reduces heterogeneity
 - Allows stabilization of active or inactive states
 - Allows co-crystallization with low-affinity ligands
- Biophysical characterization
 - SPR
 - NMR
- Drug discovery
 - More robust assays for HTS
 - NMR-based ligand screening
 - Ligand soaking for large-scale SBDD



GPCR Structure and Function



- > 250 structures
- > 55 unique GPCRs

All required some protein engineering:

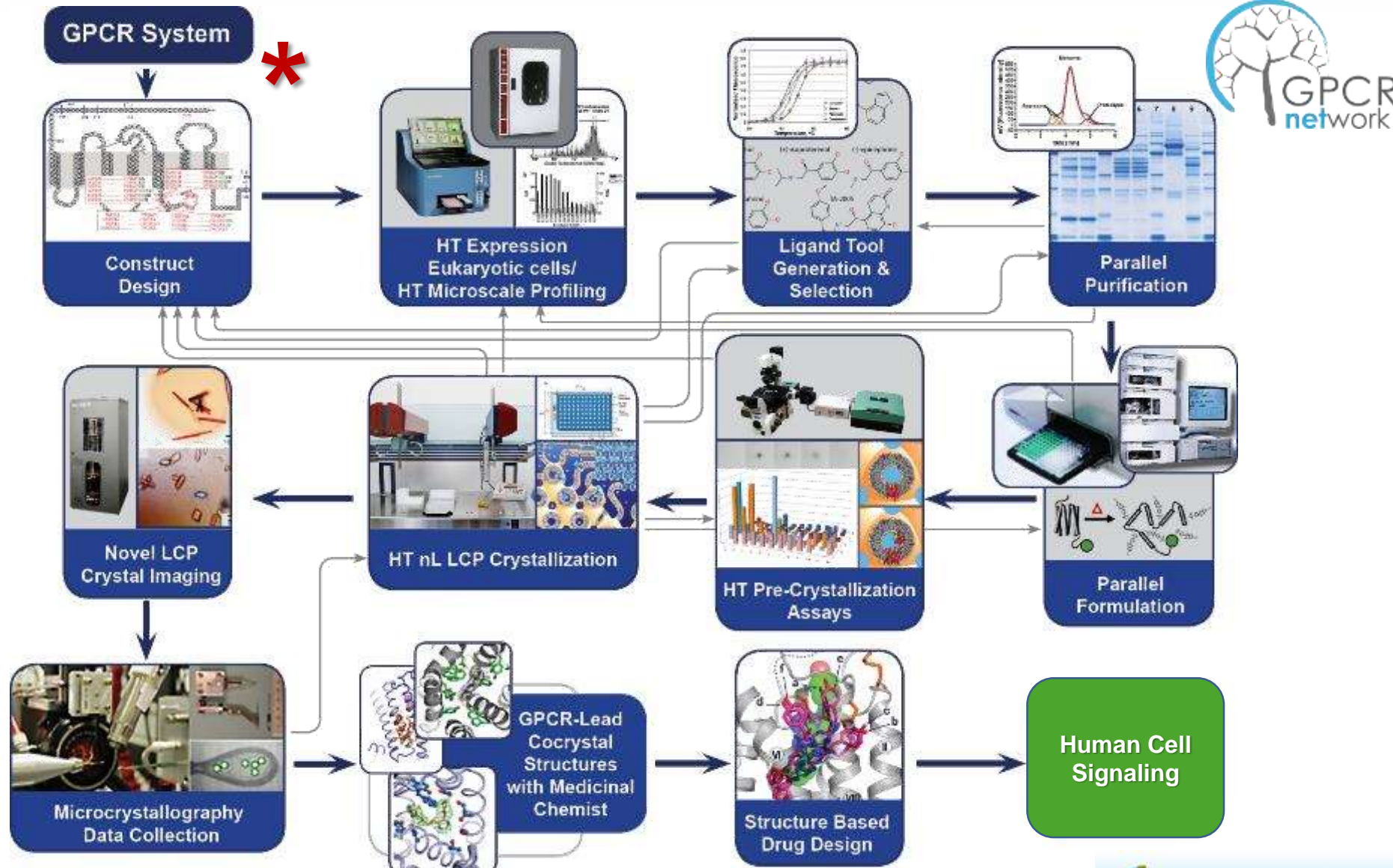
- 47 with fusion proteins
- 36 with mutations
- 25 with both
- All have truncations



GPCR Network Structure-Function Pipeline



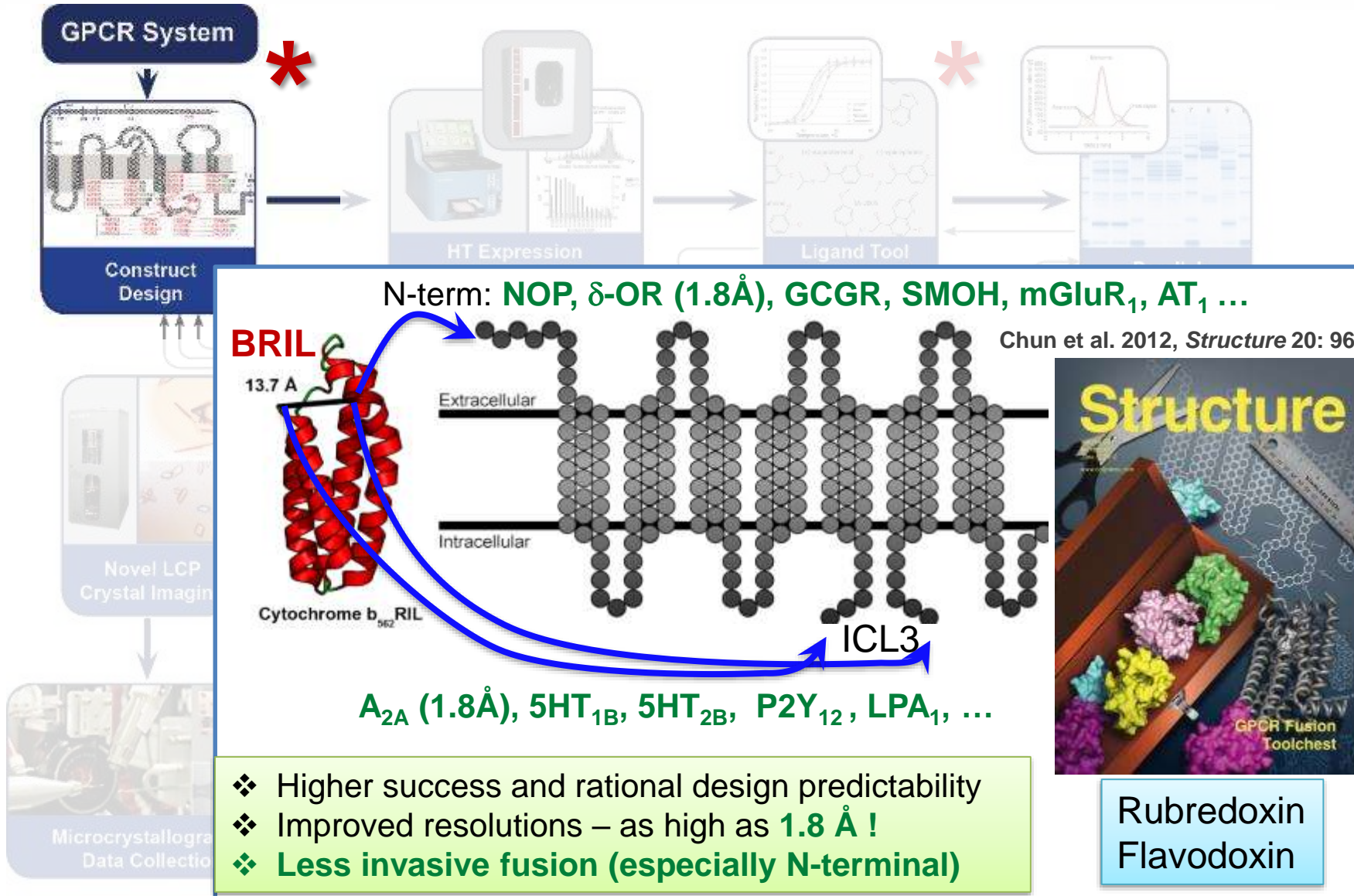
Multistage iterative process

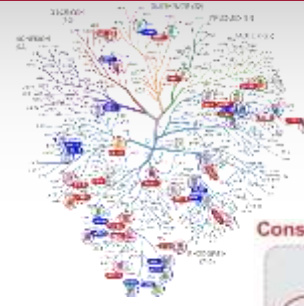


GPCR Network Structure-Function Pipeline

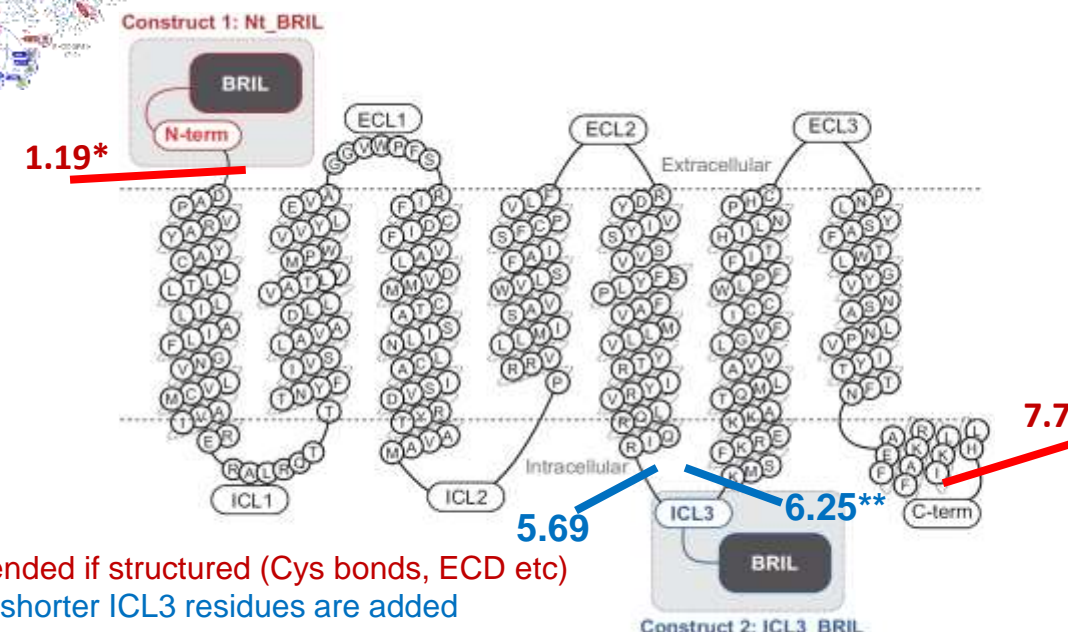


New Rationally Designed Protein Fusions



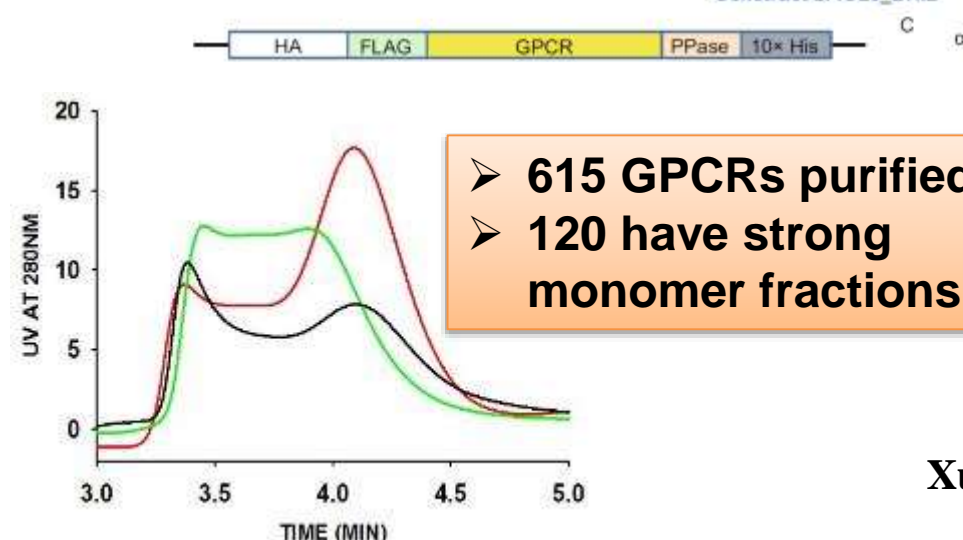


Initial Constructs: GPCR-826 project



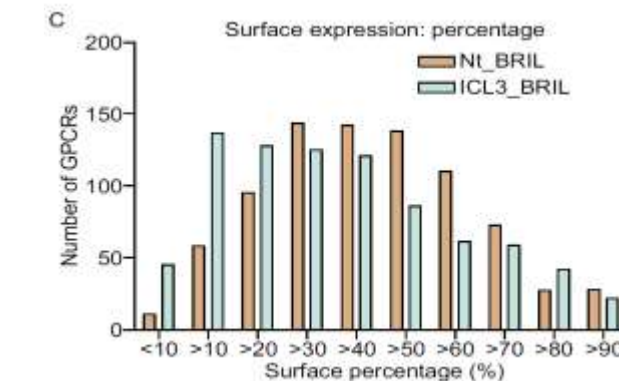
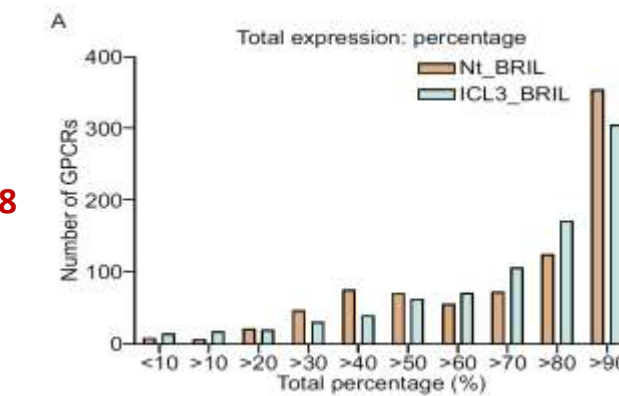
* Extended if structured (Cys bonds, ECD etc)

**For shorter ICL3 residues are added



Surface Expression >30%:

- 80% (718) of Nt_BRIL
- 60% (480) of ICL3_BRIL



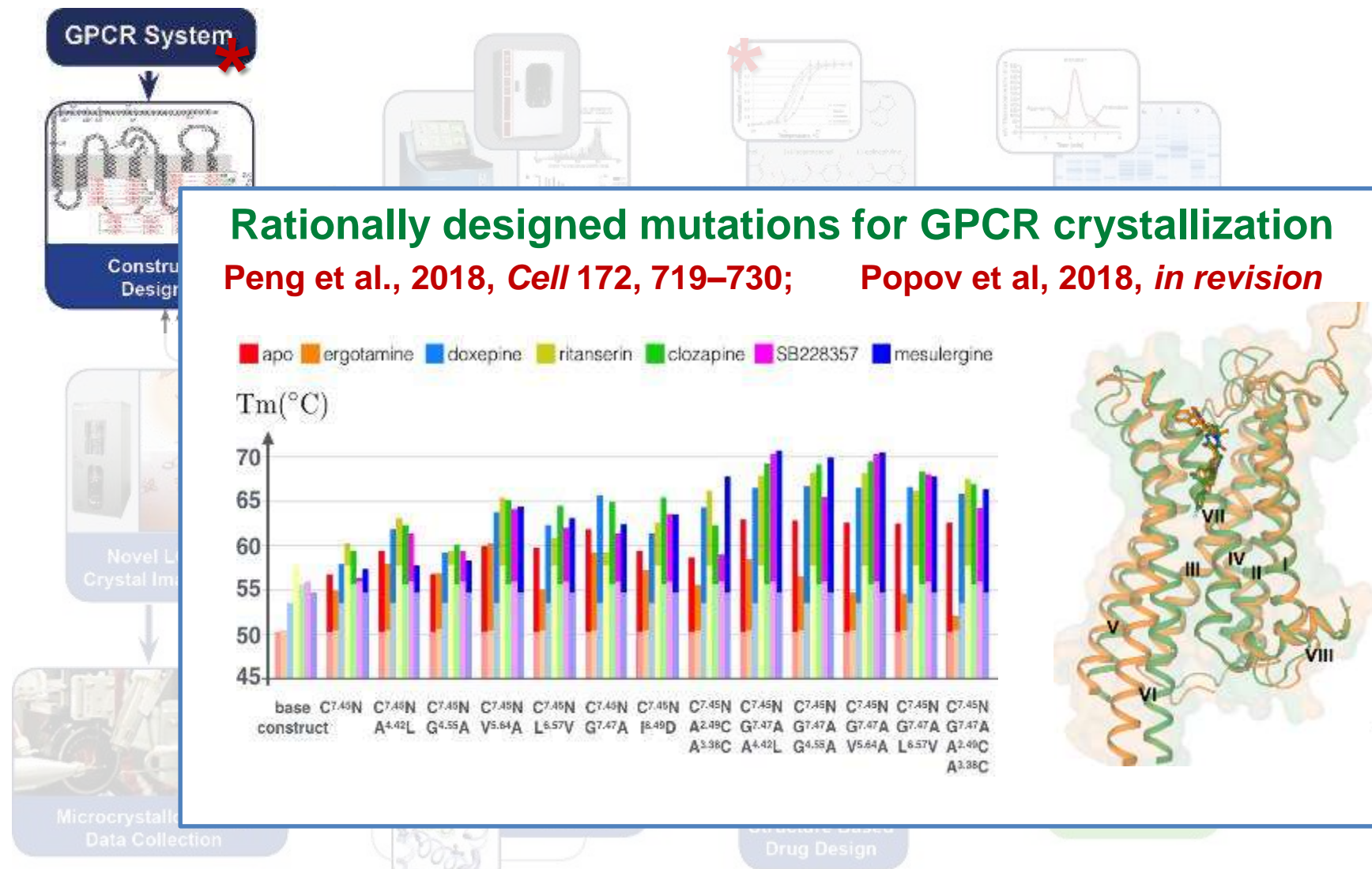
Xuechen Lv et al, Protein & cell (2016)

GPCR Network Structure-Function Process

CompoMug: Rationally Designed Mutations



GPCR
Consortium



Stabilizing mutations: Experimental approaches

Alanine/Leucine scanning

Number of mutants: 300-2000

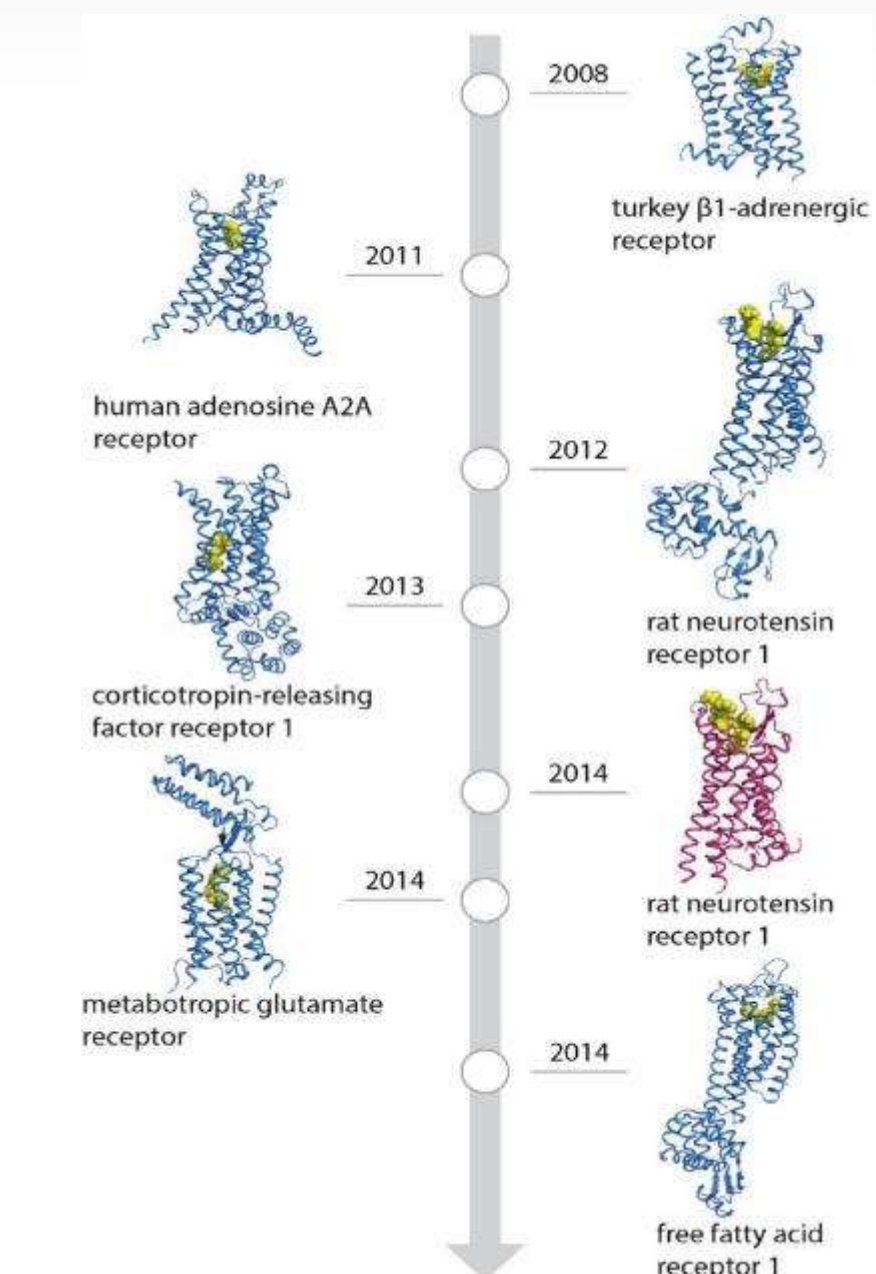
- β 1AR (Serrano-Vega et al., 2008, Warne et al., 2009)
- Adenosine A2A receptor (Magnani et al., 2008, Lebon et al., 2011, Robertson et al., 2011, Dore et al., 2011)
- Neuropeptide NTSR1 (Shibata et al., 2009, 2013)
- mGluR₅ (Dore et al., 2014)
- CRFR1 (Hollenstein et al., 2013)
- FFAR1 (Hirozane et al., 2014)

Directed evolution

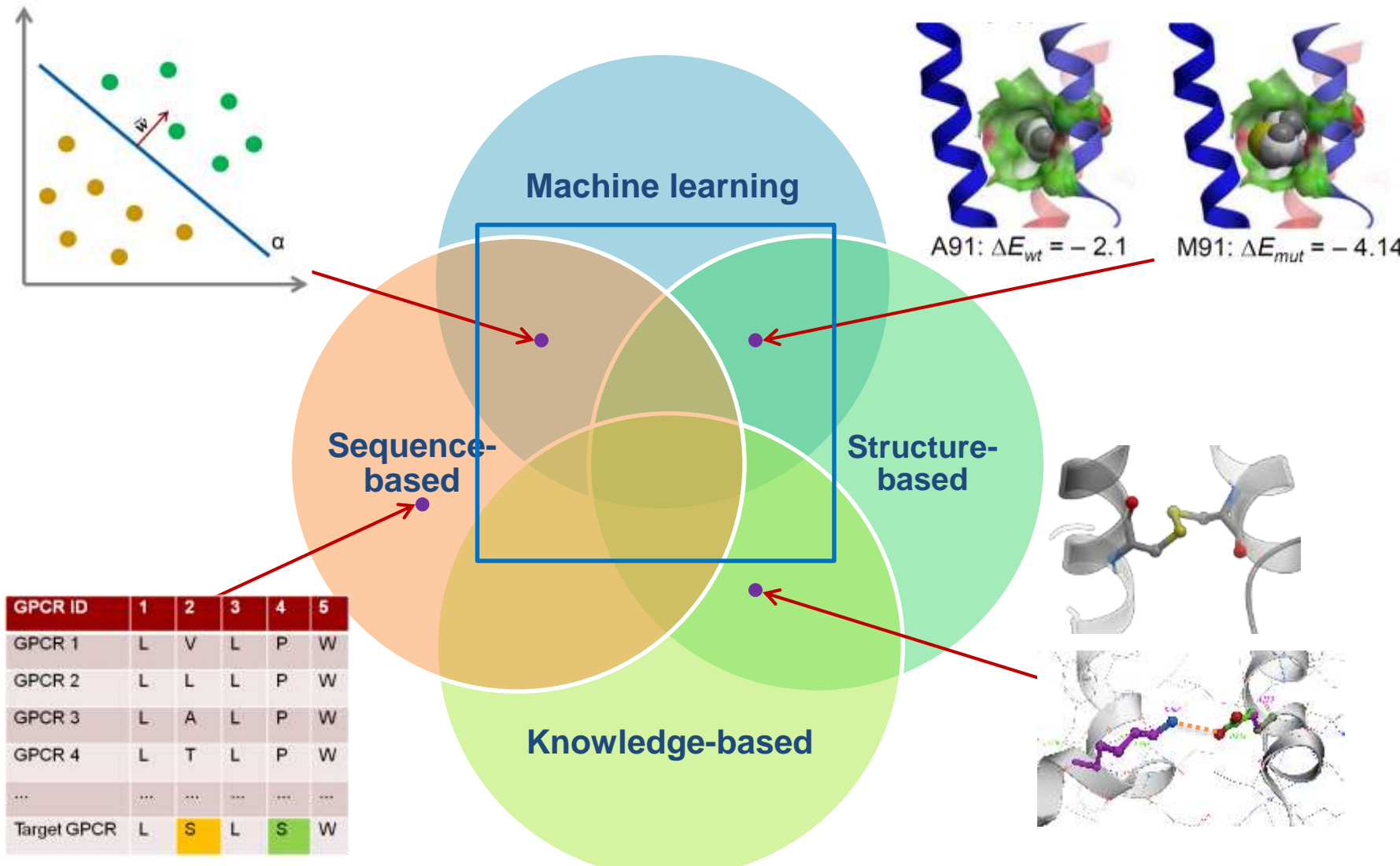
Number of mutants: > 1,000,000

- NTSR1 (Sarkar et al., 2008, Dodevsky et al., 2011)
- α 1AR, α 1BR (Dodevsky, Plückthun, 2011)
- Tachykinin receptor NK1 (Dodevsky, Plückthun, 2011)

One might hope that in the future it might be possible to design thermostabilizing mutations, computationally predict them or transfer them from other receptors ...



ComPOMuG: Computational Predictions of Optimizing Mutations in GPCRs

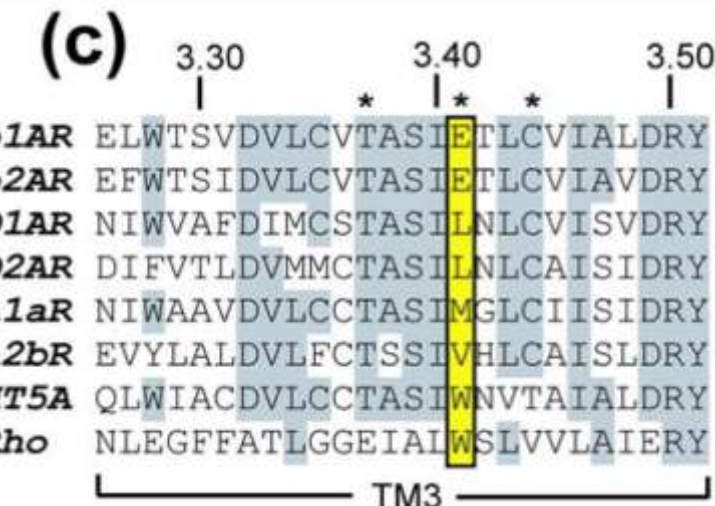
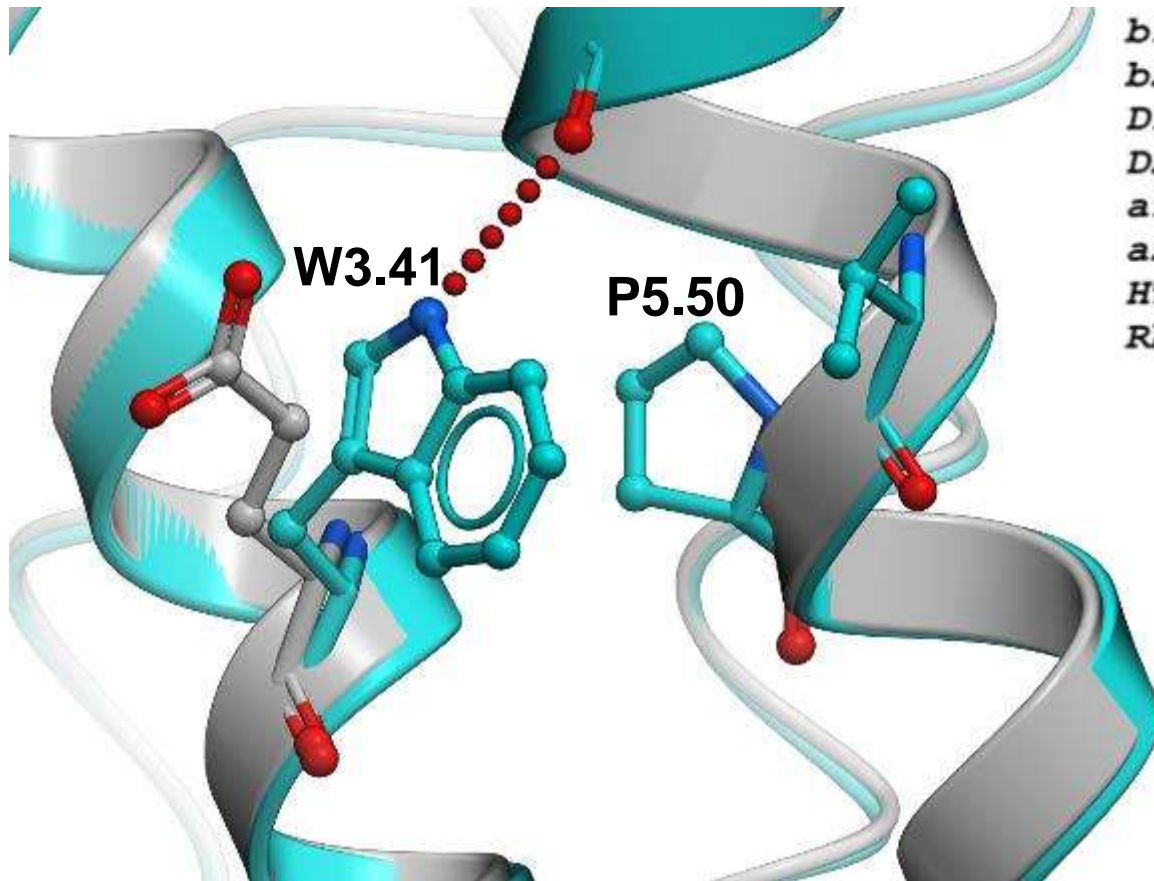


Knowledge Based (Class A only)

- 2 or more structures with this mutant
- Known transferable position
- Most of them destroy/modify a conserved **functional site**

| Position | Mutation | Role | Receptor (PDB ID) |
|----------|----------|--------------------------------------|---|
| 3.41 | X->W | stabilization of TM3 - TM5 interface | 5HT2B (4IB4), 5HT1B (4IAR), ADRB1 (5A8E), ADRB2 (3NY8), CXCR4 (3ODU), DRD3 (3PBL) |
| 2.50 | D->N | Sodium pocket | AA2AR (5WF5) |
| 3.39 | S->A | Sodium pocket | AA2AR (5WF5) |
| 7.49 | D->N | Sodium pocket | P2RY1 (4XNV), P2Y12 (4PXZ) |
| 3.40 | I->V, A | P-I-F microswitch motif | ADRB1 (4BVN), APJ (5VBL) |
| 3.49 | D,G->A | DRY motif | FFAR1 (5TZR), NTR1 (4XES) |
| 5.58 | Y-> A | Conserved activation microswitch | FFAR1 (5TZR), ADRB1 (4BVN) |
| 6.37 | L->A | Interferes with DRY motif function | AA2AR (5IU4), NTR1 (4GRV) |

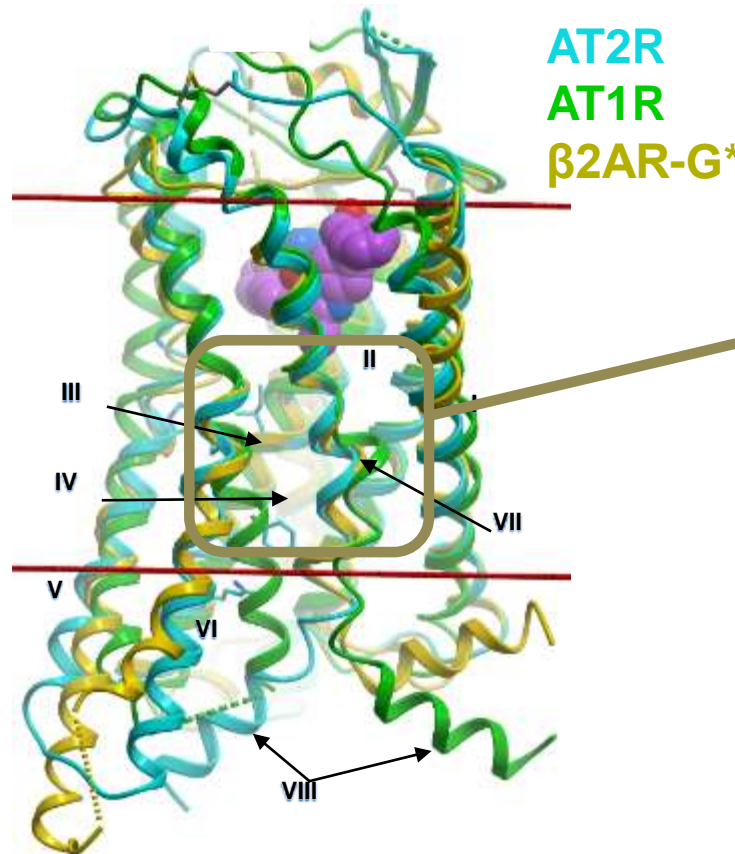
X3.41W – “Roth” Mutation



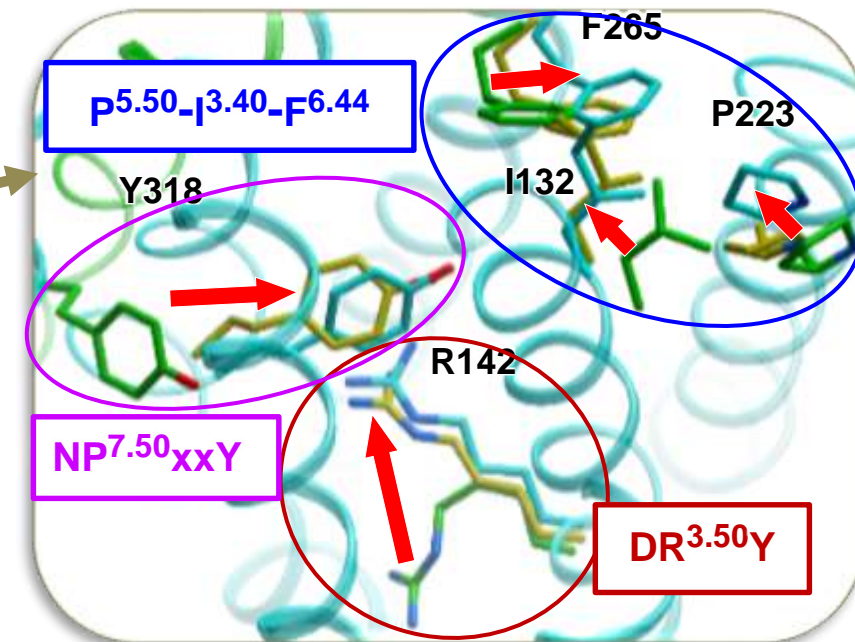
- Stabilizing or neutral in most Class A GPCRs
- Helped to solve >6 receptors, including 2 in active-like state

Activation Related Changes in Microswitches

Removing switches can decouple from agonist and limit natural motions of receptor

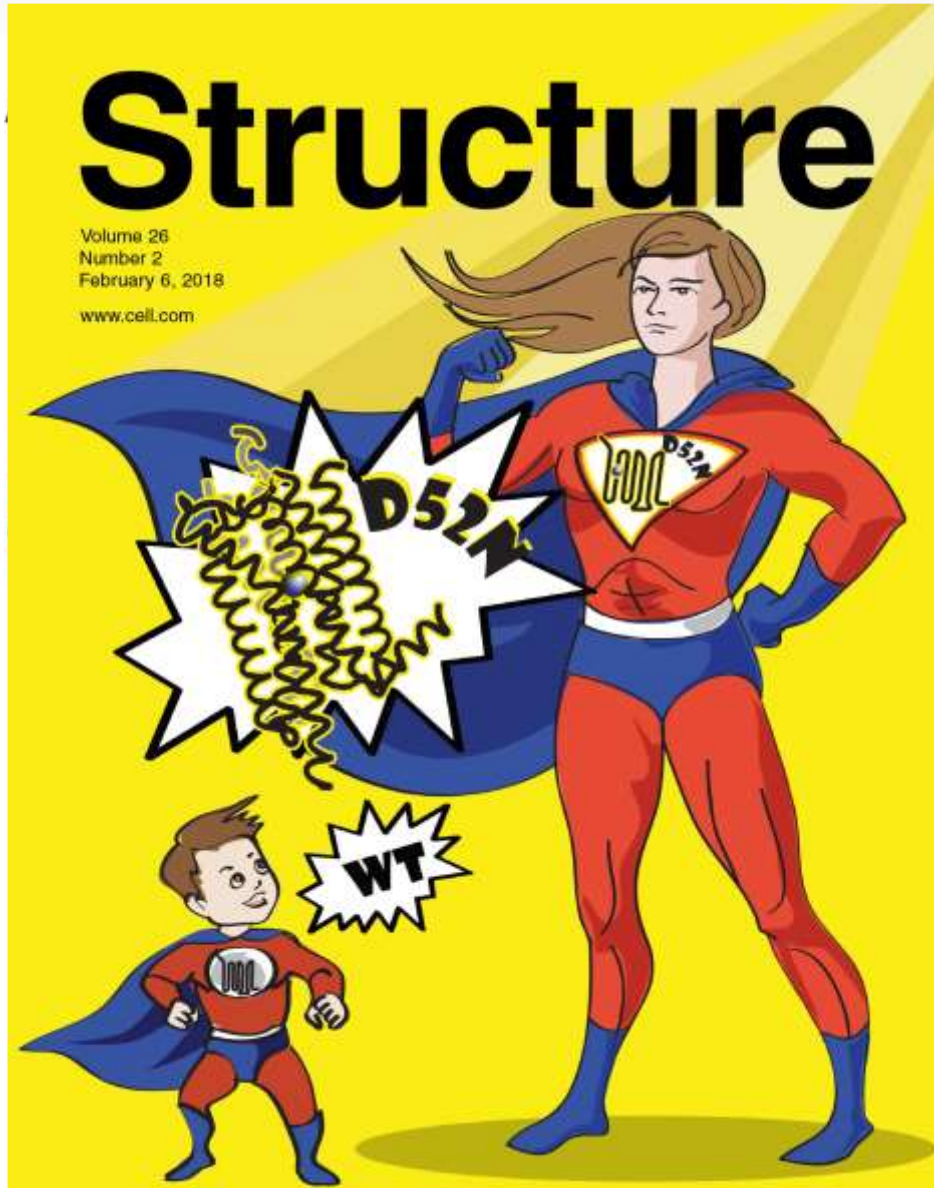


| | | |
|------|---------|------------------------------------|
| 3.40 | I->V, A | P-I-F microswitch motif |
| 3.49 | D,G->A | DRY motif |
| 6.37 | L->A | Interferes with DRY motif function |



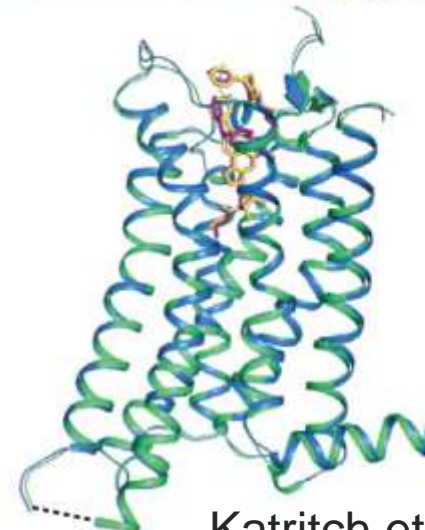
Zhang H et al, *Nature*. 2017;544:327-32.

Stabilizing mutations in conserved Na⁺ site



| | APO T _M °C | NECA T _M | Theophylline T _M | ZM241385 Tm |
|---------------|--------------------------|------------------------|--------------------------------|----------------|
| WT | 47 | 53 | 53 | 62 |
| D2.50A | 47 | 58 | 54 | 60 |
| S3.39A | 50 | 61 | 55 | 63 |
| N7.49A | 54 | 64 | 56 | 64 |
| D2.50N | 58 | 64 | 59 | 66 |

D52N–UK432097 (agonist)
S91A–UK432097 (agonist)



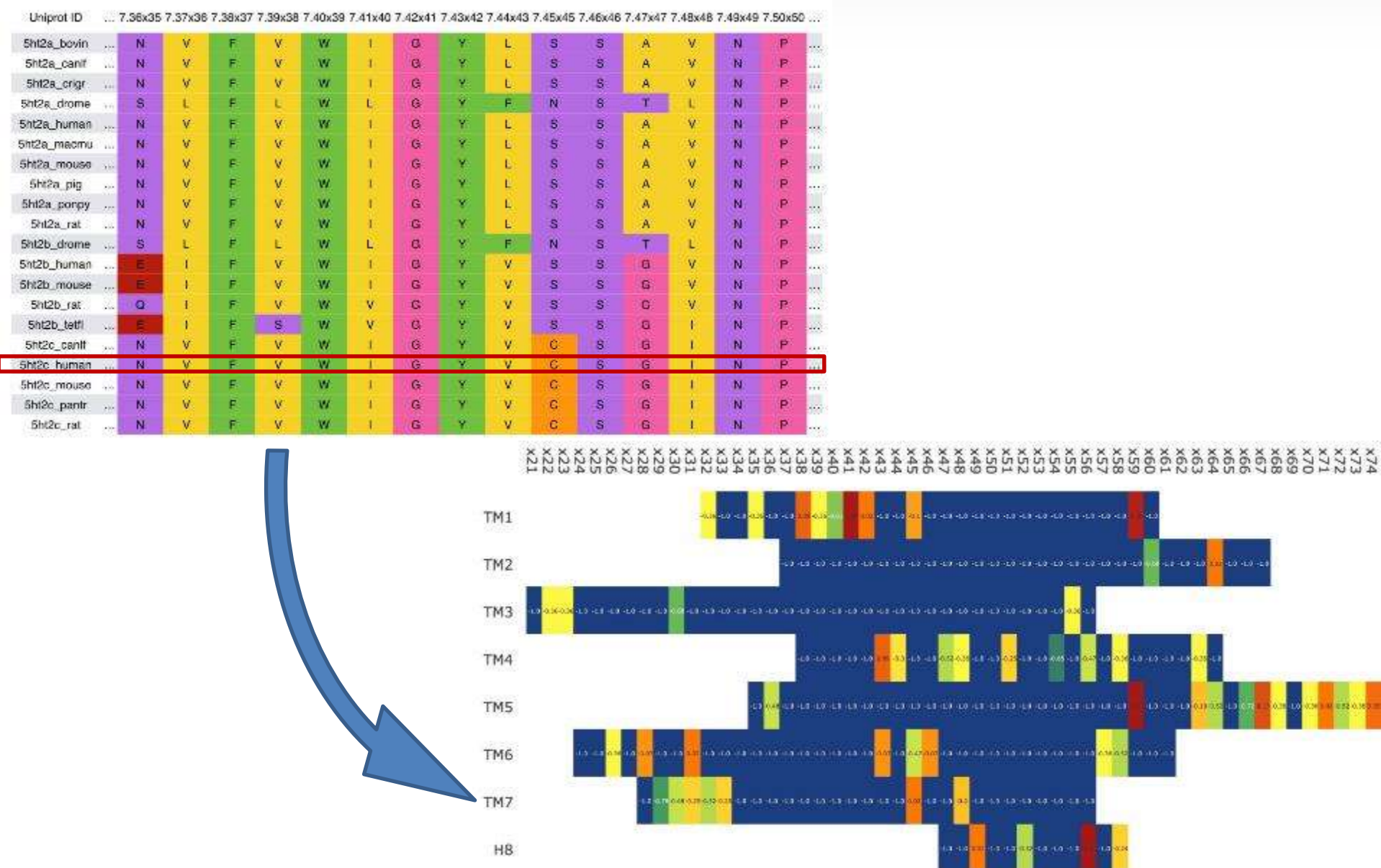
Katritch et al 2014, *TiBS*, **39**, 233
White et al 2018, *Structure* **26**, 259

Sequence-Based

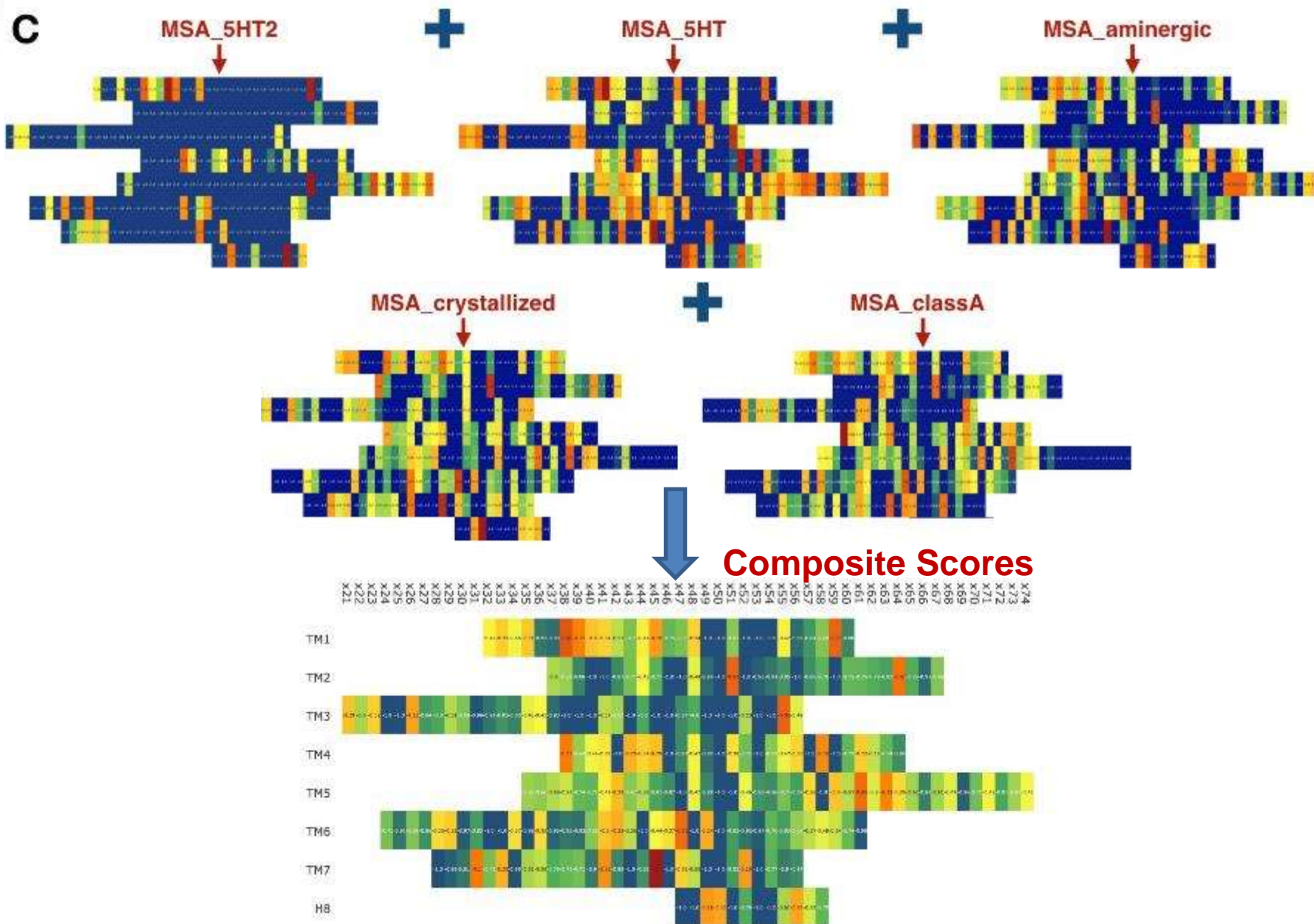
- Goal: identify (and replace) “outliers”: residues which are rarely observed at certain position
- Some positions are highly variable – take into account relative conservation
- Results depend on the GPCR set – use 3 levels of sequence clustering:
 - GPCR Class or branch (SI \geq 25%)
 - GPCR family (SI \geq 30%)
 - GPCR subfamily (SI \geq 35%)

| GPCR ID | 1 | 2 | 3 | 4 | 5 |
|-------------|-----|-----|-----|-----|-----|
| GPCR 1 | L | V | L | P | W |
| GPCR 2 | L | L | L | P | W |
| GPCR 3 | L | A | L | P | W |
| GPCR 4 | L | T | L | P | W |
| ... | ... | ... | ... | ... | ... |
| Target GPCR | L | S | L | S | W |

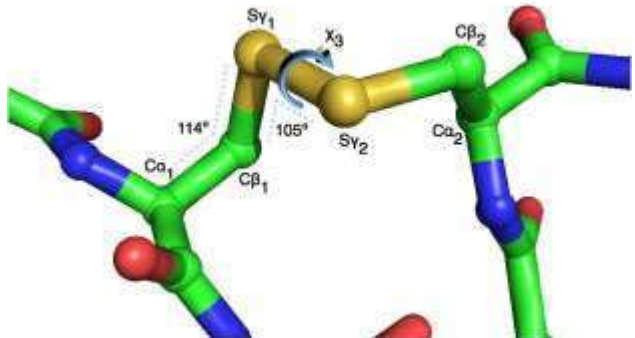
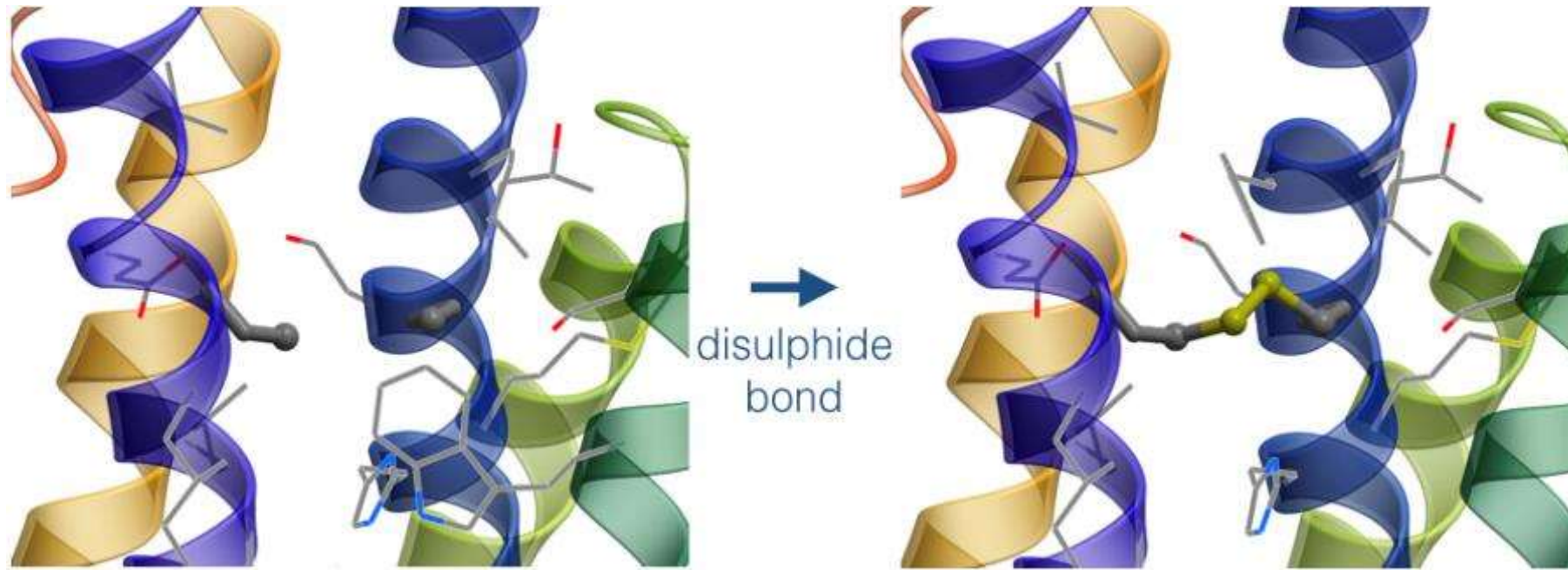
Sequence-Based: Building Scoring Matrix



Sequence-Based: Building Scoring Matrix

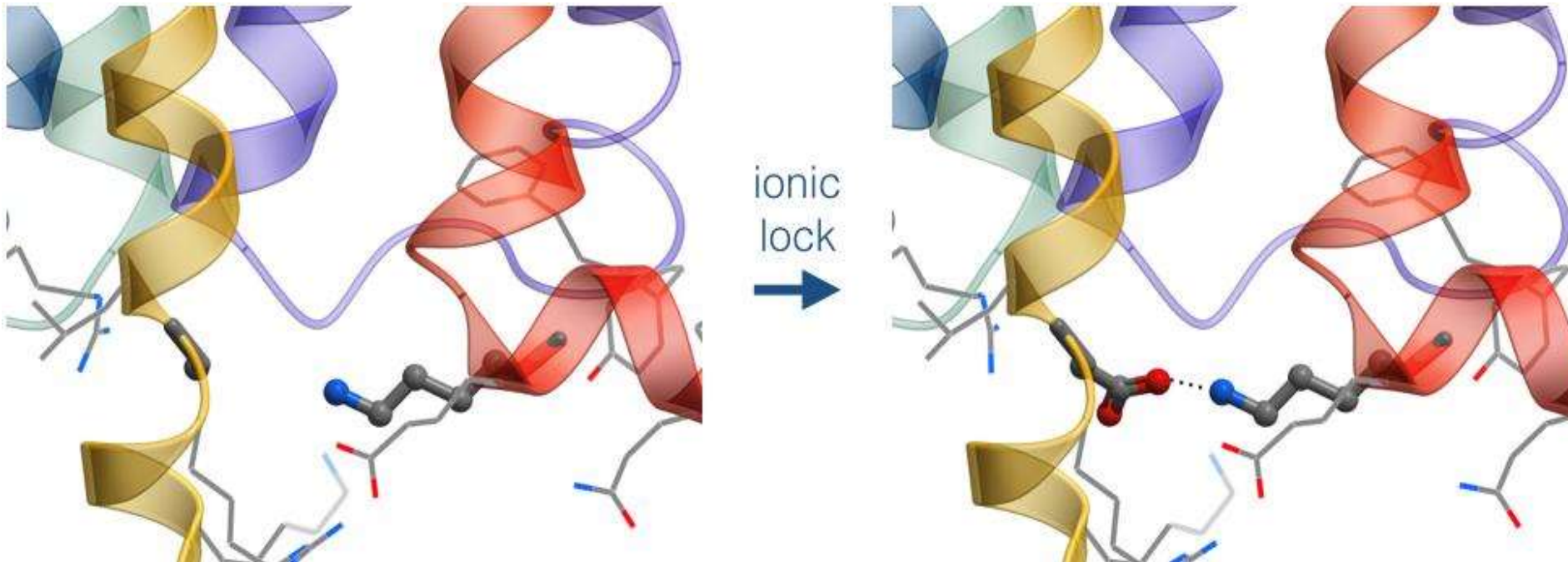


Structure-based: Design of Disulfide Bridges



- Find a pair of residues with permissive geometry
- Full energy optimization and scoring energy strain

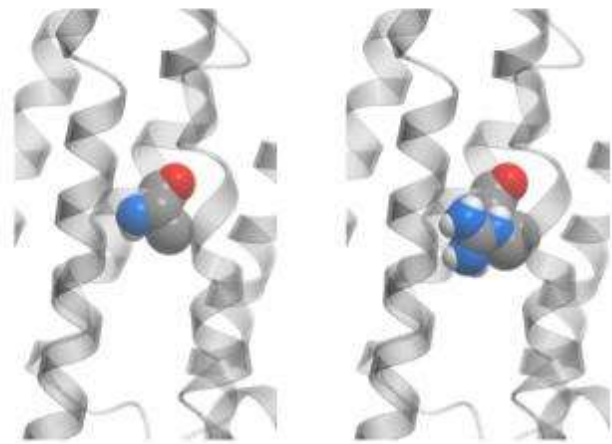
Structure-based: Design of ionic locks



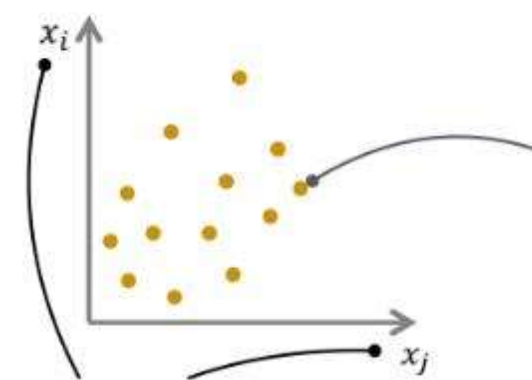
- Find a pair of residues with permissive geometry
- Full energy optimization and scoring energy strain

Machine Learning

A structural models of point mutations

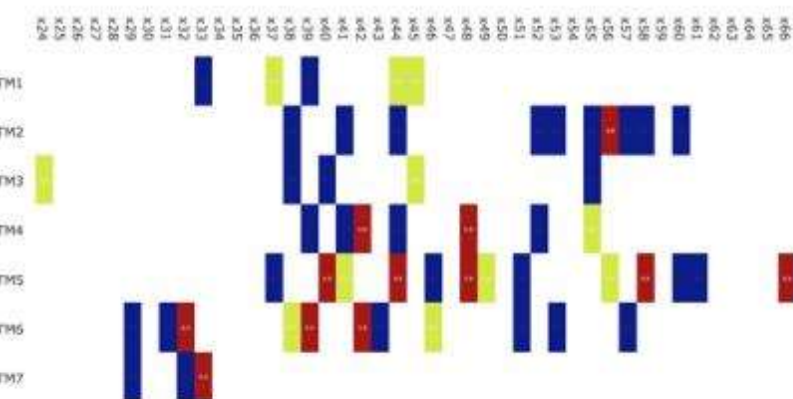


B projection into the feature space

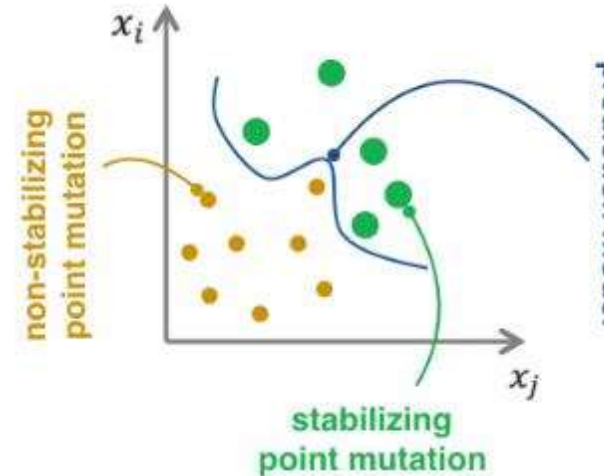


coordinate of the GPCR-specific feature space

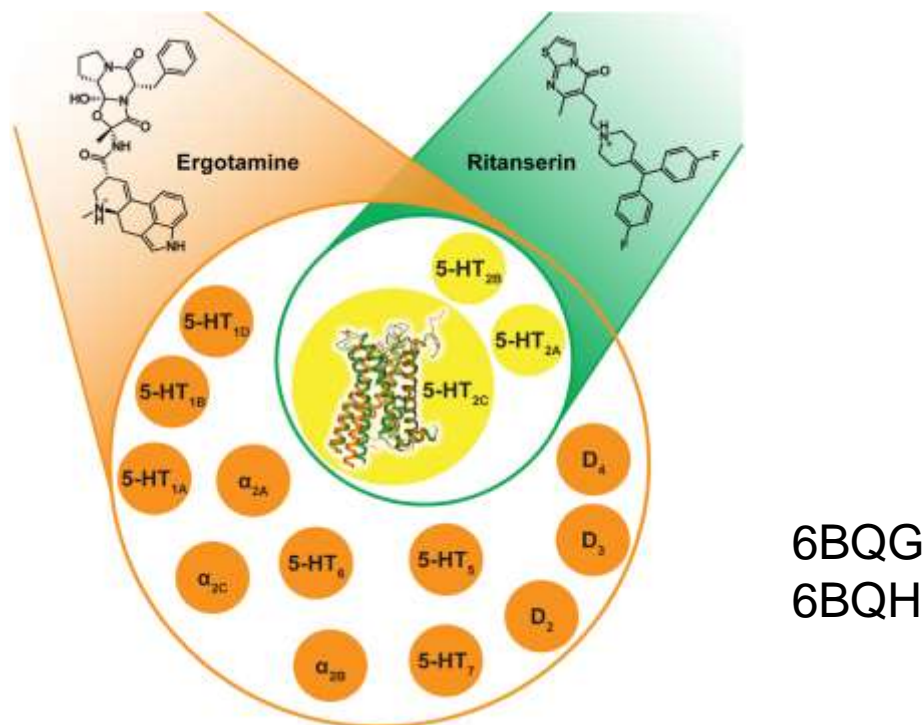
D scoring matrix



C applying of prediction model



Prospective Application to Mutant Discovery: 5HT_{2C} structures



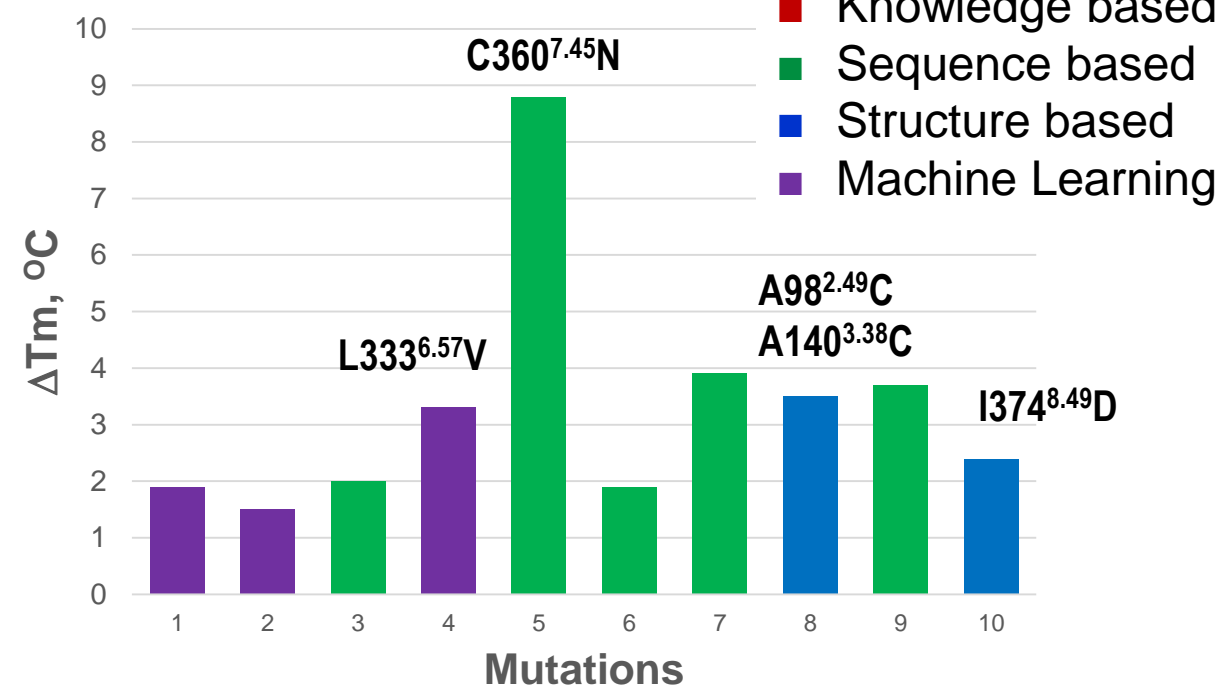
6BQG
6BQH

Peng Y et al. (2018) 5-HT_{2C} Receptor Structures Reveal the Structural Basis of GPCR Polypharmacology. Cell 172(4):719-30

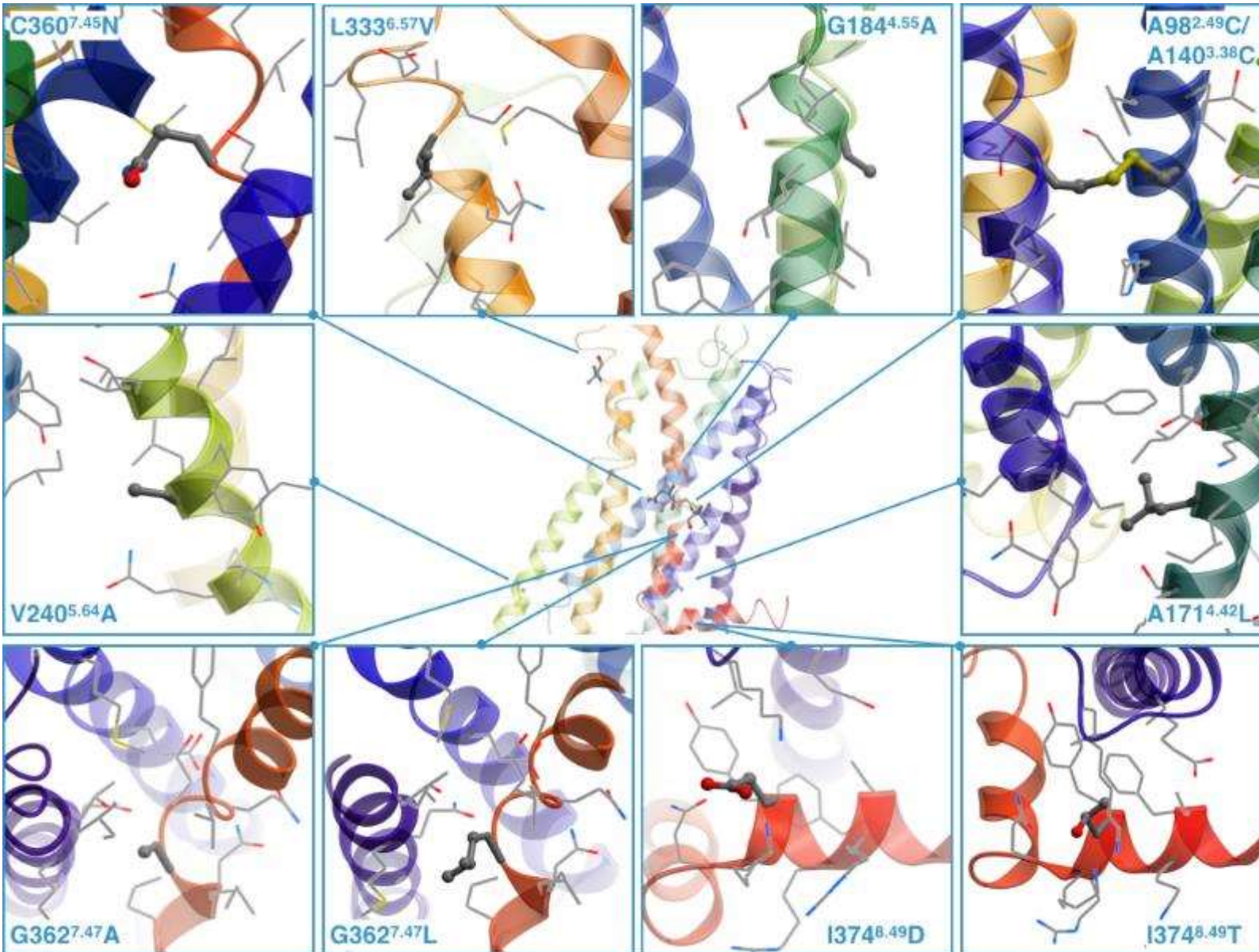
| Mutation | CompoMug Module | aSEC* quality | Tm (°C) ±SEM | ΔTm (C) |
|---|---------------------------|---------------|-------------------|------------|
| WT | | | 50.4 ± 0.8 | 0.0 |
| I62 ^{1.41} V | Seq-based | ~ | | -0.7 |
| G69 ^{1.48} A | Seq-based | - | | -1.4 |
| D99 ^{2.50} N | Knowledge | - | | - |
| H85 ^{12.51} E | Struct-based | N/A | | - |
| G103 ^{2.54} A | Seq-based | - | | -4.4 |
| Y125 ^{3.23} K | Seq-based | - | | -2.0 |
| Y125 ^{3.23} V | Seq-based | ~ | | -0.7 |
| M143 ^{3.41} W | Knowledge | - | | 0.6 |
| R157 ^{3.55} T | ML & Seq-based | - | | -1.8 |
| R157 ^{3.55} Q | Seq-based | - | | -2.0 |
| T169 ^{4.40} K | Seq-based | + | | 0.2 |
| A171^{4.42}L | ML | ~ | 52.3 ± 1.2 | 1.9 |
| I172 ^{4.43} A | Seq-based | - | | 1.1 |
| I172 ^{4.43} F | Seq-based | ~ | | 0.6 |
| G184^{4.55}A | ML | + | 51.9 ± 0.1 | 1.5 |
| N203 ^{ECL2} D | Struct-based | - | | -2.6 |
| F220 ^{5.45} I | ML | ~ | | 0.0 |
| F224 ^{5.48} Y | ML & Seq-based | - | | -3.3 |
| C235 ^{5.59} F | Seq-based | ~ | | 0.1 |
| L236 ^{5.60} R | ML & Seq-based | N/A | | - |
| V240^{5.64}A | Seq-based | + | 52.4 ± 0.5 | 2.0 |
| V240 ^{5.64} S | Seq-based | + | | 0.3 |
| G314 ^{6.38} A | ML | - | | -4.0 |
| L333^{6.57}V | ML & Seq-based | + | 53.7 ± 0.6 | 3.3 |
| K348 ^{7.32} A | Seq-based | - | | -4.4 |
| C360^{7.45}N | Seq-based | + | 59.2 ± 0.5 | 8.8 |
| G362^{7.47}L | Seq-based | + | 52.3 ± 0.7 | 1.9 |
| G362^{7.47}A | Seq-based | + | 54.3 ± 0.7 | 3.9 |
| L370 ^{7.55} D | Struct-based | - | | -2.3 |
| K373 ^{8.48} E | Struct-based | - | | -0.4 |
| I374^{8.49}D | Struct-based | + | 53.9 ± 0.8 | 3.5 |
| I374^{8.49}T | Seq-based | + | 54.1 ± 0.9 | 3.7 |
| Y375 ^{8.50} F | Seq-based | - | | -2.4 |
| N381 ^{8.56} R | Sequence-based | ~ | | 0.6 |
| T67 ^{1.46} C/G103 ^{2.54} C | Struct-based | - | | - |
| V74 ^{1.53} C/A96 ^{2.47} C | Struct-based | - | | - |
| A87 ^{2.38} C/A171 ^{4.42} C | Struct-based | ~ | | - |
| A98^{2.49}C/A140^{3.38}C | Struct-based | ~ | 52.8 ± 1.0 | 2.4 |
| T369 ^{7.54} C/Y375 ^{8.50} C | Struct-based | N/A | | - |

CompoMug prospective screening: 5HT_{2C}

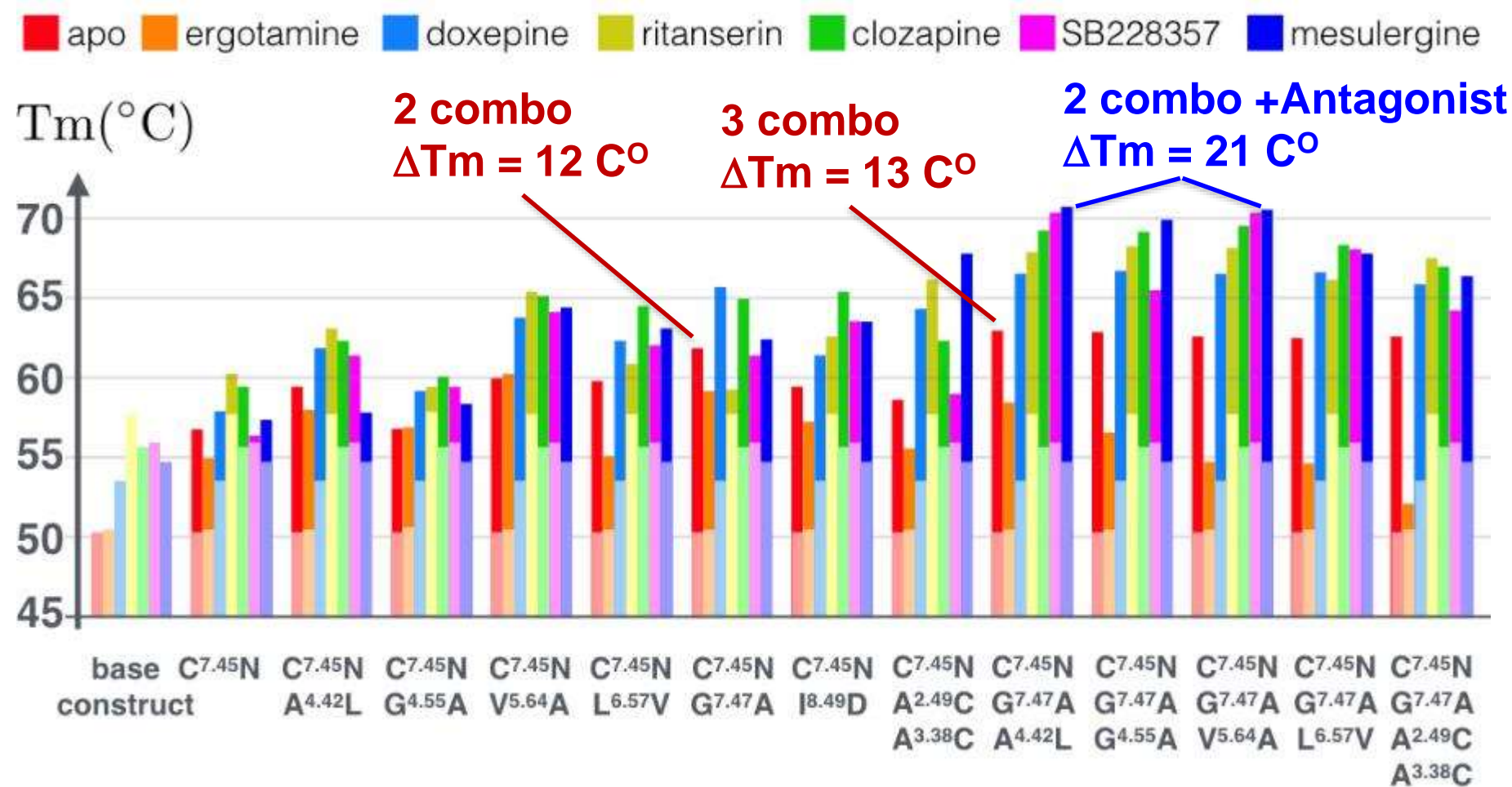
- 40 mutations tested
- 10 improved both Tm & SEC (~25%)
- Best shift ΔTm ~ 9°C
- 3 components contributed, but not Knowledge-based



5HT_{2C}: Mutations in the structural model

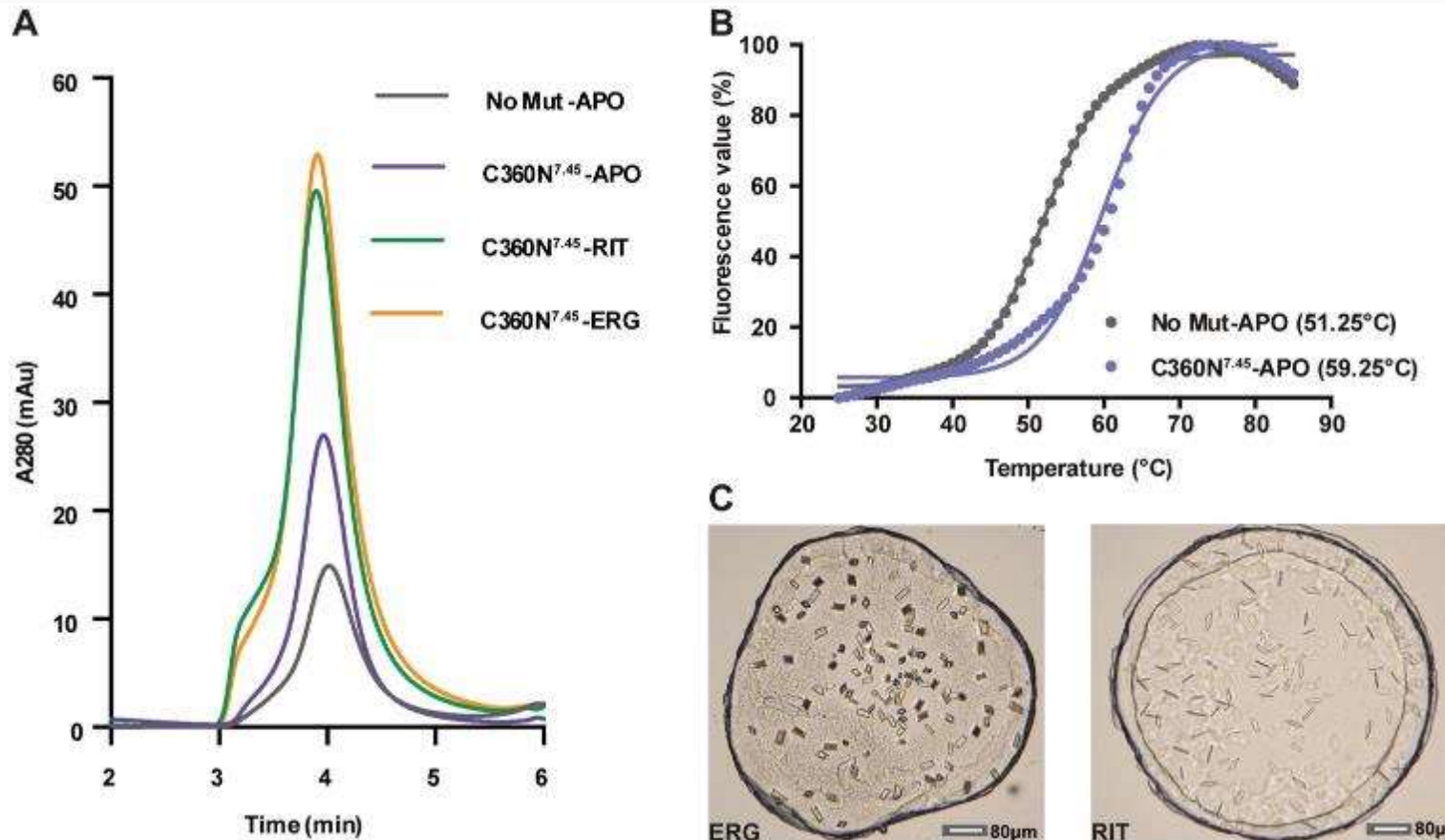


5HT_{2C}: Combined mutations in complex with ligands



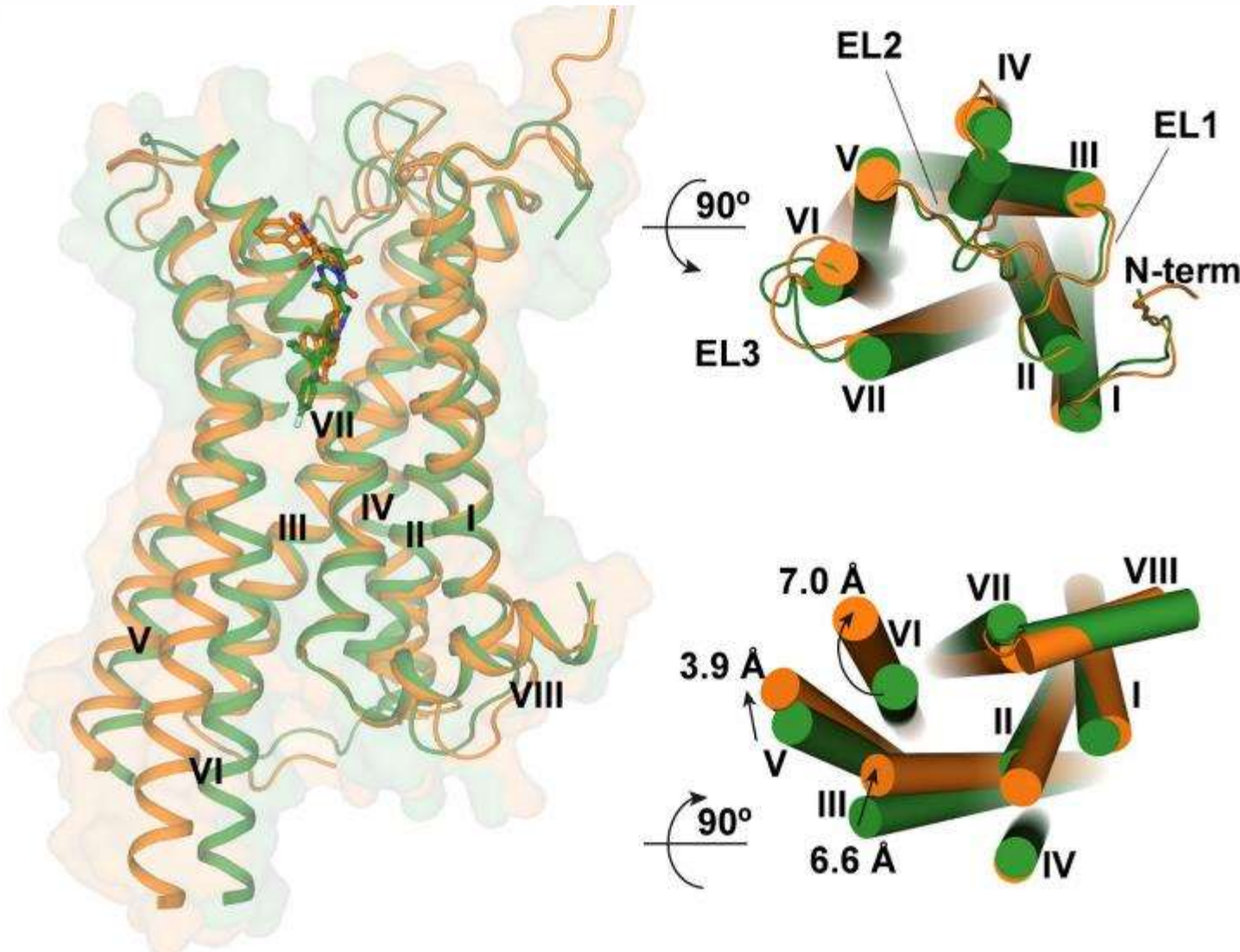
5-HT_{2C}: Crystals and structures

- Combo mutations yield first 5-HT_{2C} crystals with antagonists
- Single C360^{7.45}N allowed crystallization of both agonist and antagonists
- Structures for agonist Ergotamine (3.0 Å) and antagonist Ritanserin (2.7 Å)



Peng Y et al. (2018) Cell 172(4):719-30

5-HT_{2C} inactive and active-like structures



Peng Y et al. (2018) Cell 172(4):719-30

More CompoMug predictions tested

| Target | # tested single mutants | Hit rate | Best ΔT_m , C° | Best ΔT_m , C° combined mutations | Crystallized /Solved | Comment |
|-------------------|-------------------------------|----------|---------------------------|---|-------------------------|------------------------------|
| 5HT2C | 40 | 25% | 9 | 13 | Yes/Yes | 1 mutant in structure |
| Target #2 | 40 | 25% | 6 | 7 | Yes/Yes | 2+4 mutants in structure |
| Target #3 | 60 | 17% | 10 | | | |
| Target #4 | 36 | 30% | 5 | 9 | Yes/Yes | 5 mutations in structure |
| Target #5 | 40 | 20.0% | 4 | | | |
| Target #6 | 60 | 12% | 4 | | | |
| Target #7 | 40 | 10.0% | 3 | 4 | | |
| Target #8 | 60 | 7% | 4 | | | |
| Target #9 | 60 | 25% | 3 | 16 | Yes/Yes | non Class A; 4 mutants |
| Target #10 | 60 | 11% | 3 | | | |
| EP3 | 30 | 15% | 0 | | Yes/Yes | Only Improved Diffraction |
| Taste /Class C | 40-60 | 0% | | | | |

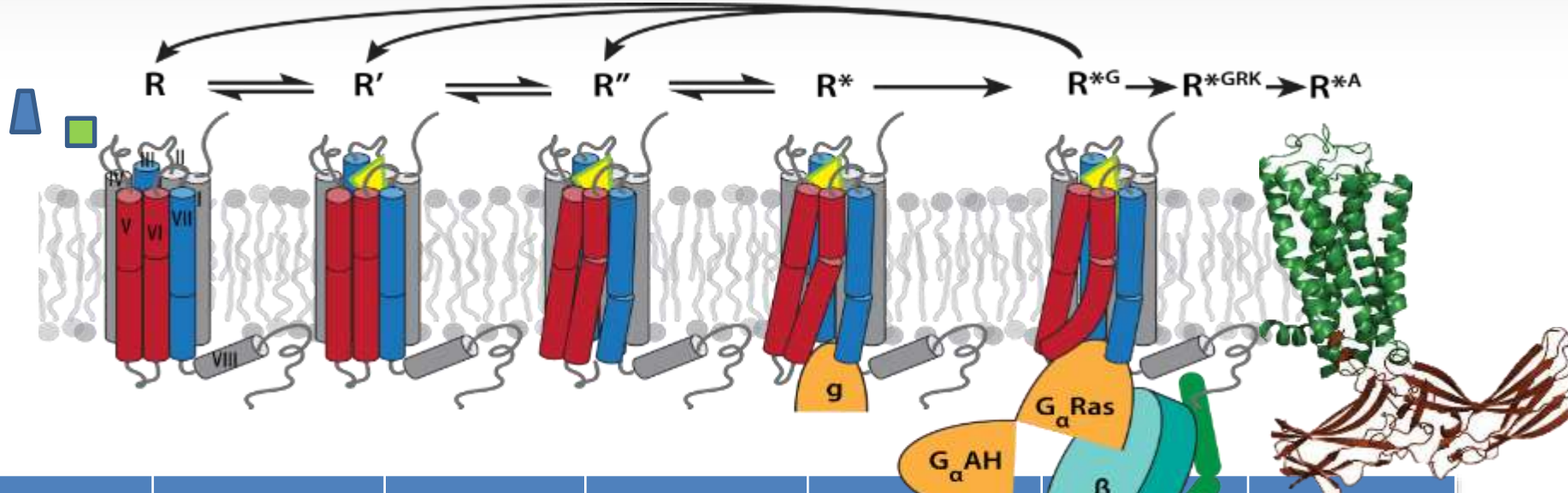
CompoMug: Summary & Outlook

- CompoMug already shows 15-30% “hit rate” for most GPCRs targets, and up to 16C° combined ΔTm
- Complementary to other engineering approaches
- All 4 modules make important contributions:
 - Sequence-based module most universally applicable
 - Energy-based predictions can improve with each GPCR structure (better homology models)
 - Machine learning continuously can improve with each new stability dataset obtained
- Utility for both SBDD and for assay development!

Outline

- Rational prediction of stabilizing mutations:
CompoMug
- New insights into GPCR function and allosteric mechanisms
- Structure-Based ligand discovery for GPCRs

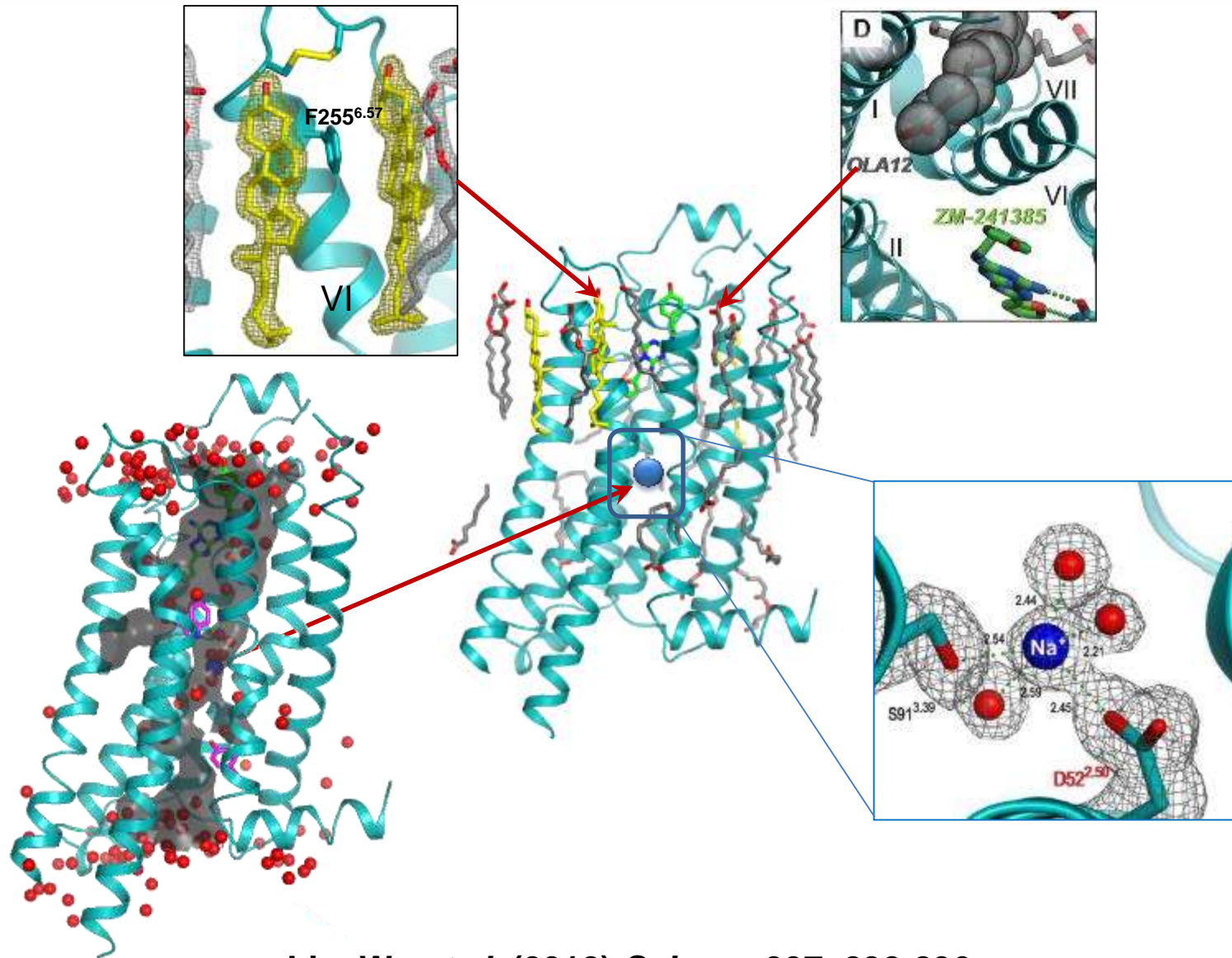
Dynamic Mechanisms of GPCR action on atomic level



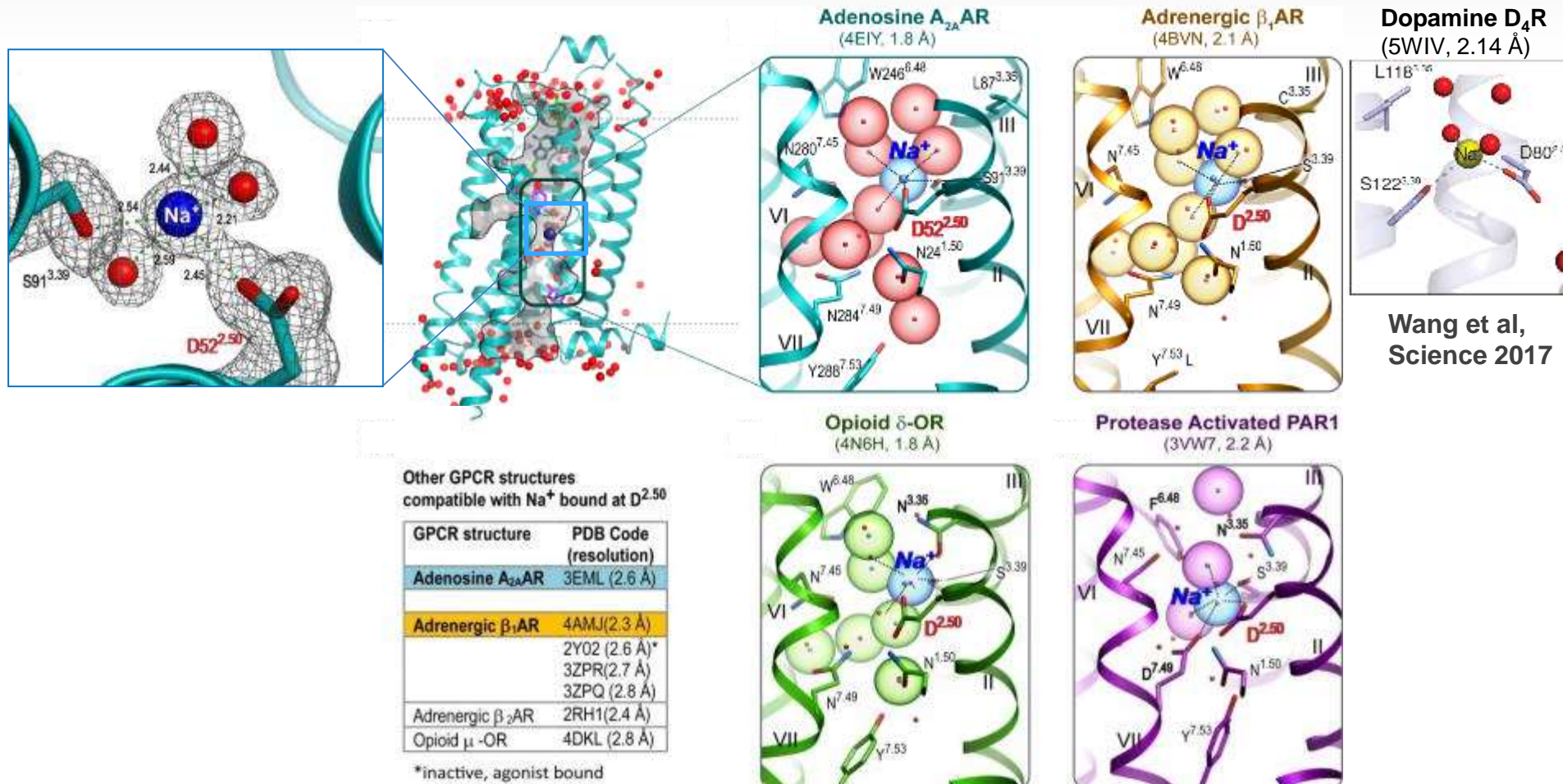
| Receptor | R Inactive Ground State | R' Inactive Agonist Bound | R'' Active-Like Agonist Bound | R* Active, G-protein or Mimic Binding | R*G G-protein Signaling | R*A β-arrestin Complex |
|---|---------------------------------------|------------------------------------|--|--|-------------------------------|--|
| Adenosine A _{2A} | 3EML,3REY, 3RFM, 3PWH, 4EIY | -- | 3QAK,2YDO,2YDV, 4UHR, 4UG2 | -- | 5G53 | |
| β ₁ -Adrenergic | 2VT4,2YCW,2YCX, 2YCY,2YCZ | 2Y00 -2Y04 | -- | -- | -- | |
| β ₂ -Adrenergic | 2RH1, 2R4R, 2R4S,3D4S | 3PDS | -- | 3P0G ^c (3.5) | 3SN6 | |
| Rhodopsin | 1F88,1U19 | 2G87, 2HPY | 3CAP ^f , | 3DQB,2X72,3PQR, 3PXO | -- | 4ZWJ |
| Muscarinic | 3UON | | | 4MGS,4MGT | | |
| Opioid | 4DKL | | | 5C1M, κ-OR | | |
| CB1 | 5U09 | | 5XRA | | | |
| P2Y12 | 4NTJ | 4PXZ | | | | |
| NTSR1, ETB ₄ 5HT1B, 5HT2B | | 5GLH | 4GRV, 4IAQ,4IAR, 4IB4 | | | Updated from Kardashev et al., Annual Rev. Pharmacol. |

Updated from Katritch, Stevens, Cherezov,
Annual Rev. Pharmacology & Toxicology, 2013

Endogenous allosteric molecules in 1.8 Å Structure of human A_{2A}AR



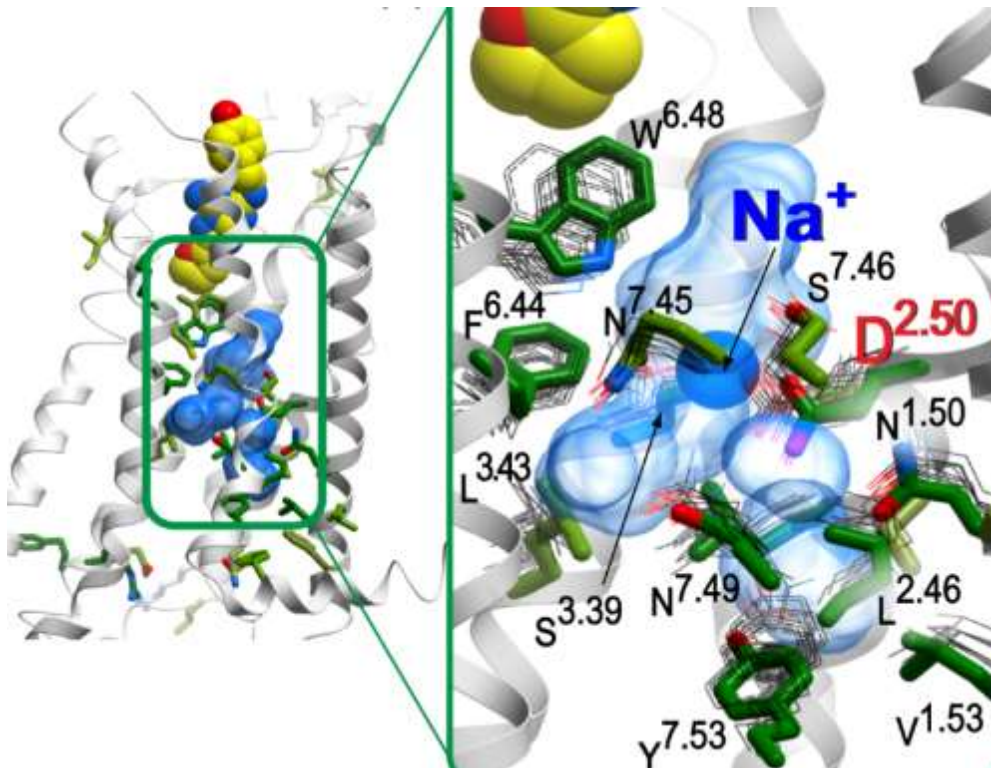
Allosteric Na⁺ site in class A GPCR structures



- Na⁺ crystallographically observed in α, δ, γ branches of Class A
- The pocket highly conserved in most class A GPCRs

Na⁺ Pocket Conservation in Class A GPCRs

- Largest conserved 3D cluster (15 residues of 34 most conserved residues)
- Includes NPxxY in helix VII and FxxCW in helix VI, but not DRY in helix III
- D2.50 conserved in 95% of GPCRs



(c)

| | N | V | L | A | D | L | S | L | F | W | N | S | N | P | Y | |
|---------------------|------|------|------|------|------|------|------|------|------|------|------|------|------|------|------|---|
| A ₂ AAR* | 1.50 | 1.53 | 2.46 | 2.49 | 2.50 | 3.35 | 3.39 | 3.43 | 6.44 | 6.48 | 7.45 | 7.46 | 7.49 | 7.50 | 7.53 | |
| β ₁ AR* | N | V | L | A | D | C | S | L | F | W | N | S | N | P | Y | |
| β ₂ AR | N | V | L | A | D | C | S | L | F | W | N | S | N | P | Y | |
| ACM2 | N | V | L | A | D | V | S | L | F | W | N | S | N | P | Y | |
| ACM3 | N | V | L | A | D | A | S | L | F | W | N | S | N | P | Y | |
| 5HT _{1B} | N | V | L | A | T | D | C | S | L | F | W | N | S | N | P | Y |
| 5HT _{2B} | N | V | L | A | D | F | S | L | F | W | S | S | N | P | Y | |
| H ₁ R | N | V | L | S | A | D | A | S | V | F | W | N | S | N | P | Y |
| D ₃ R | N | V | L | A | D | M | S | L | F | W | N | S | N | P | Y | |
| S1P ₁ R | N | V | L | A | D | G | A | S | L | F | W | N | S | N | P | Y |
| Rho | N | T | L | A | D | G | A | L | E | W | A | A | N | P | Y | |
| δ-OR* | N | V | L | A | D | N | S | L | F | W | N | S | N | P | Y | |
| κ-OR | N | V | L | A | D | N | S | L | F | W | N | S | N | P | Y | |
| μ-OR | N | V | L | A | D | N | S | L | F | W | N | S | N | P | Y | |
| NOP | N | V | L | A | D | N | S | L | F | W | N | S | N | P | Y | |
| CXCR4 | N | V | L | S | A | D | N | S | L | F | W | H | C | N | P | Y |
| NTSR1 | N | T | L | A | S | D | C | T | V | W | S | S | N | P | Y | |
| PAR1* | N | A | L | A | D | N | S | M | P | F | S | C | D | E | Y | |

Only 5% of Class A GPCRs lack D2.50

| | Uniprot ID | Description* | Protein name | #2.50 | Other Acid |
|----|-------------|--|---|-------|------------|
| 1 | VNRL4_HUMAN | PSEUDOGENE | Putative vomeronasal receptor-like protein 4 | H | |
| 2 | CCBP2_HUMAN | DECOY RECEPTOR D6 | Chemokine-binding protein 2 | N | |
| 3 | CCRL2_HUMAN | Non-signaling | C-C chemokine receptor-like 2 | N | |
| 4 | GNRR2_HUMAN | NON_FUNCTIONAL | Putative gonadotropin-releasing hormone II receptor | F | |
| 5 | GPR26_HUMAN | Orphan, Constitutively active | GPCR 26 | | |
| 6 | GPR78_HUMAN | Orphan, Constitutively active | GPCR 78 | | |
| 7 | GP161_HUMAN | Orphan, negative regulator of Shh pathway | GPCR 161 | N | |
| 8 | LGR4_HUMAN | ORPHAN, binds Frizzled and LRPCs | Leucine-rich repeat-containing GPCR 4 | N | |
| 9 | LGR5_HUMAN | ORPHAN, binds Frizzled and LRPCs | Leucine-rich repeat-containing GPCR 5 | N | |
| 10 | LGR6_HUMAN | ORPHAN, binds Frizzled and LRPCs | Leucine-rich repeat-containing GPCR 6 | N | |
| 11 | NTR2_HUMAN | Low_affinity to NT, constitutively active [19, 20] | Neurotensin receptor type 2 | G | |
| 12 | GP141_HUMAN | Probable GPCR | Probable G protein coupled receptor 141 | H | |
| 13 | GP146_HUMAN | Probable GPCR | Probable GPCR 146 | A | |
| 14 | GP148_HUMAN | Probable GPCR | Probable GPCR 148 | Y | |
| 15 | GP150_HUMAN | Probable GPCR | Probable GPCR 150 | F | |
| 16 | GP153_HUMAN | Probable GPCR | Probable GPCR 153 | V | |
| 17 | GP162_HUMAN | Probable GPCR | Probable GPCR 162 | V | |
| 18 | GP176_HUMAN | Probable GPCR | Probable GPCR 176 (HB-954) | I | |
| 19 | GPR21_HUMAN | Probable GPCR | Probable GPCR 21 | A | |
| 20 | GPR22_HUMAN | Probable GPCR | Probable GPCR 22 | V | |
| 21 | GPR33_HUMAN | Probable GPCR | Probable GPCR 33 | Y | |
| 22 | GPR52_HUMAN | Probable GPCR | Probable GPCR 52 | A | |
| 23 | GPR62_HUMAN | Probable GPCR | Probable GPCR 62 | A | |
| 24 | GPR75_HUMAN | Probable GPCR | Probable GPCR 75 | L | |
| 25 | GPR82_HUMAN | Probable GPCR | Probable GPCR 82 | N | |
| 26 | O10J6_HUMAN | Putative olfactory | Putative olfactory receptor 10J6 | K | |
| 27 | OR2G2_HUMAN | Olfactory | Olfactory receptor 2G2 | Y | E3.39 |
| 28 | OR4F6_HUMAN | Olfactory | Olfactory receptor 4F6 | N | E3.39 |
| 29 | OR5BH_HUMAN | Olfactory | Olfactory receptor 5B17 | G | E3.39 |
| 30 | OR8J1_HUMAN | Olfactory | Olfactory receptor 8J1 | N | E3.39 |
| 31 | OR8J2_HUMAN | Olfactory | Olfactory receptor 8J2 | N | E3.39 |
| 32 | OR8J3_HUMAN | Olfactory | Olfactory receptor 8J3 | N | E3.39 |
| 33 | GP143_HUMAN | Signals | GPCR 143 (Ocular albinism type 1) | A | D3.39 |
| 34 | GPBAR_HUMAN | Signals | G protein coupled bile acid receptor 1 | G | D7.50 |
| 35 | GNRHR_HUMAN | Signals | Gonadotropin-releasing hormone receptor | N | D7.49 |
| 36 | OPSB_HUMAN | Opsin, no Na ⁺ binding | Blue-sensitive opsin | G | |

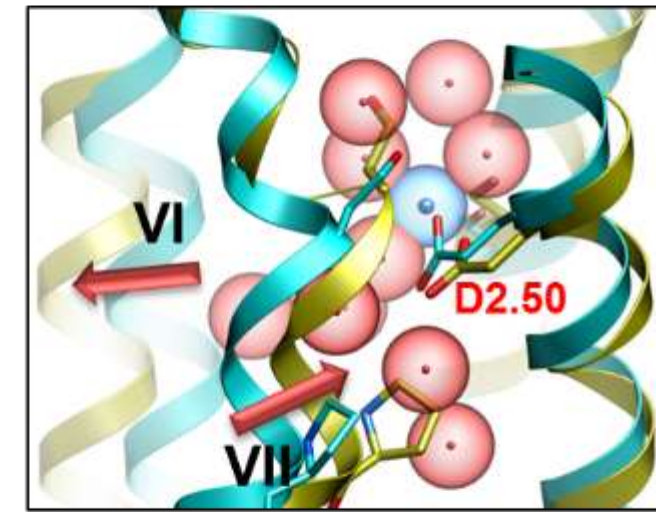
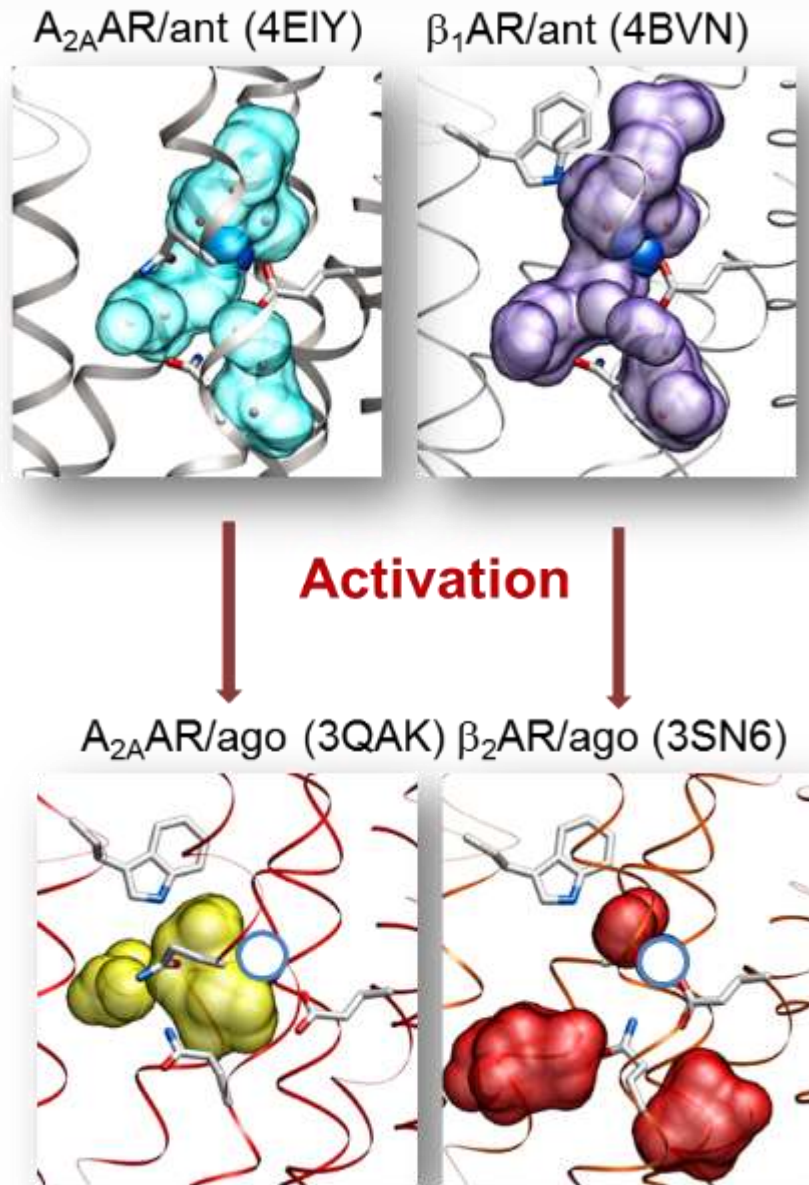
Orphans,
Constitutive,
Non-signaling

Probable/
Putative

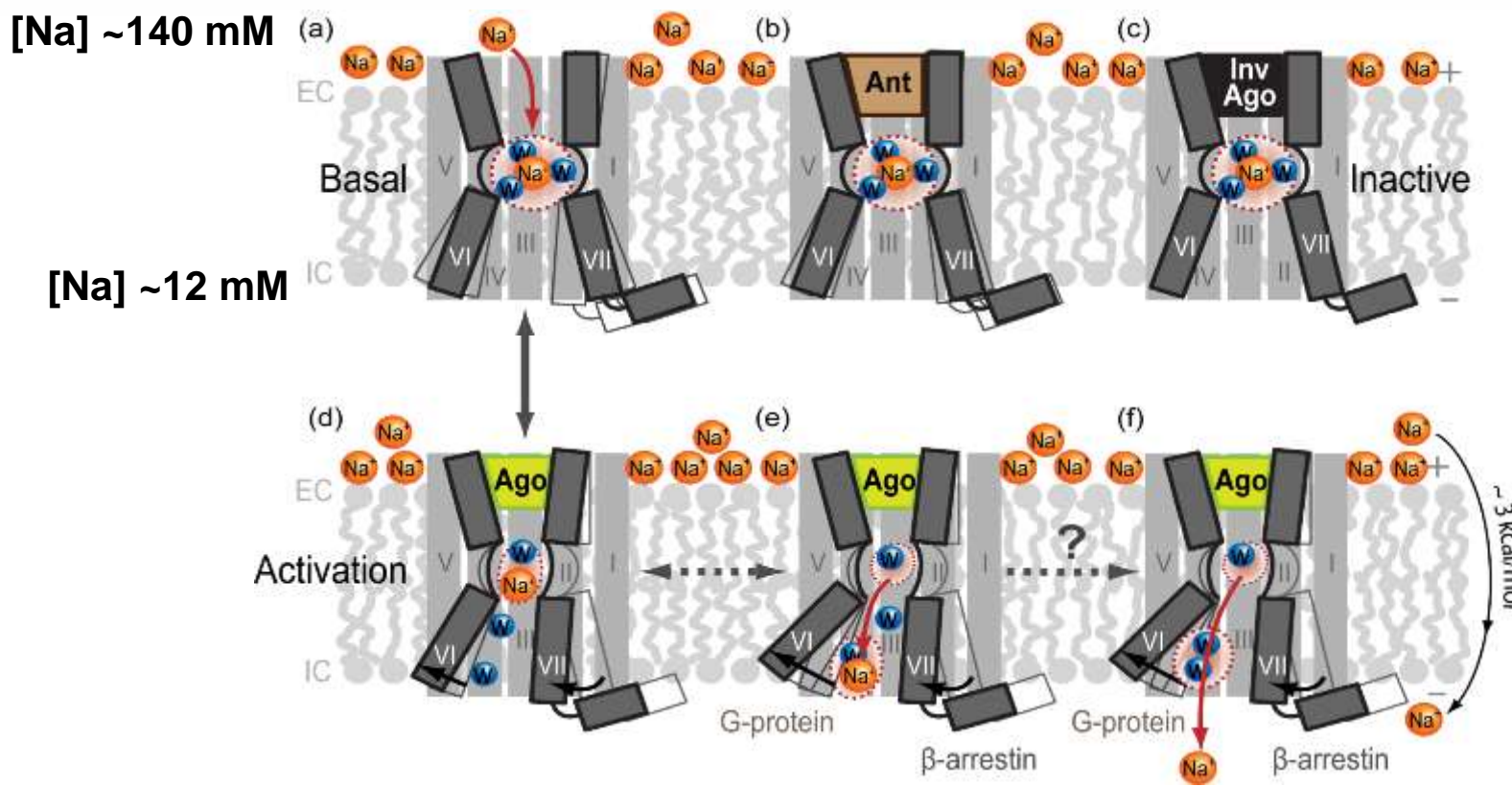
Have alternative
acidic side chain
In the pocket

BlueOpsin

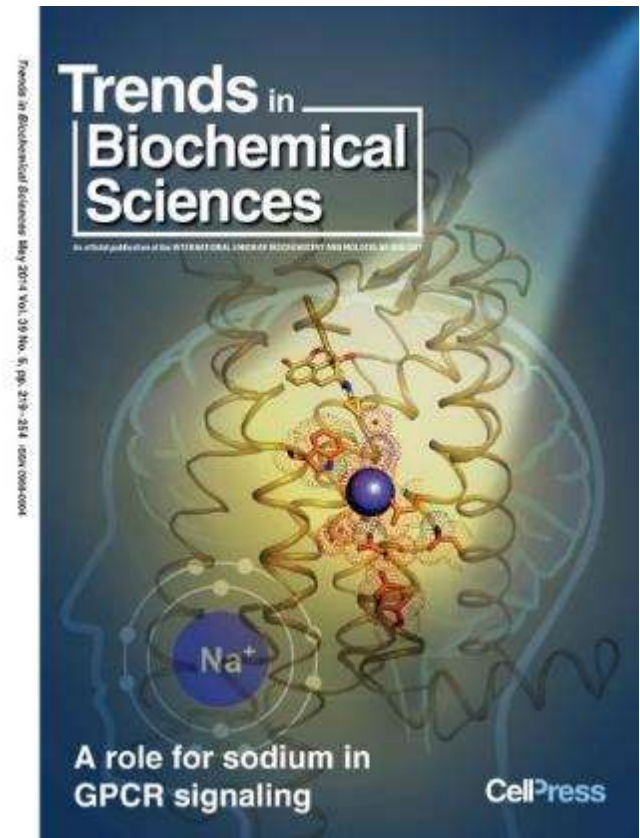
Collapse of the Na⁺ pocket in GPCR Activation



Na^+ Plays a Key Role in Activation Mechanism

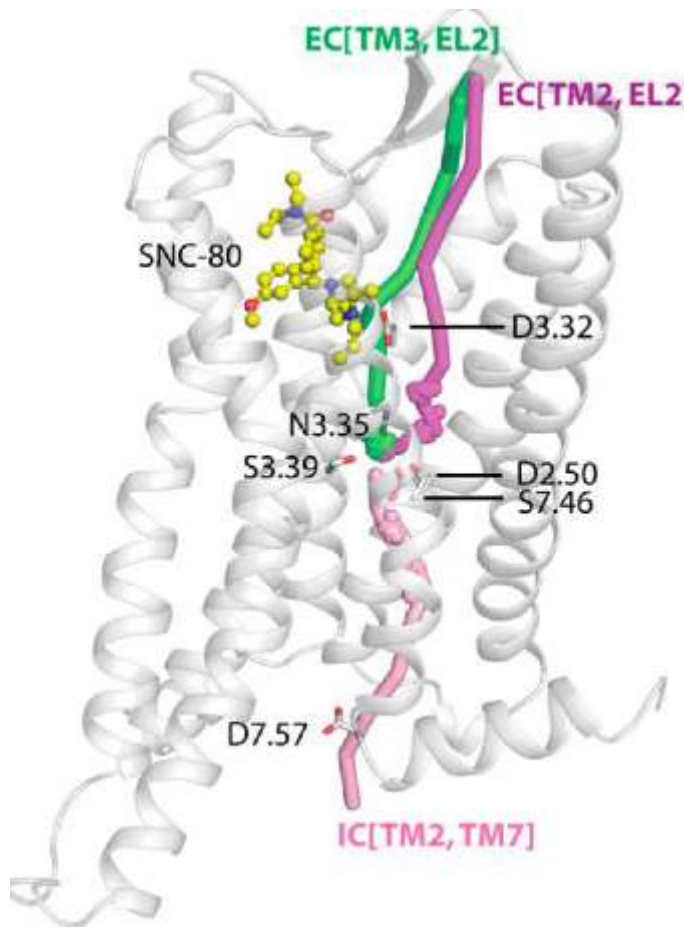


**Allosteric Sodium in GPCRs:
One of the ten Science Signaling “Breakthroughs of 2014”**



Fenalti et al. 2014, Nature 506, 191-196
Katritch et al. (2014) TiBS 39:233-44

But where does it go upon activation?



- “In MD simulations of activation transition, Na⁺ does not leave the allosteric pocket but rather kept its coordination with residues D2.50, N3.35, and S3.39”
- Used Accelerated MD, but only 15% follow the intracellular path

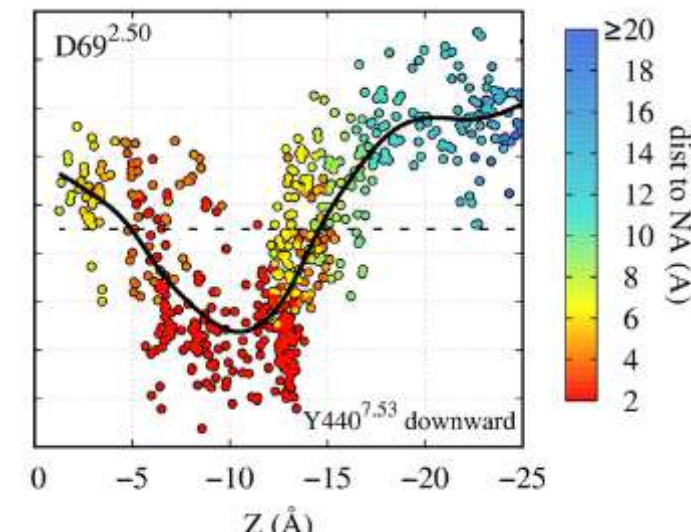
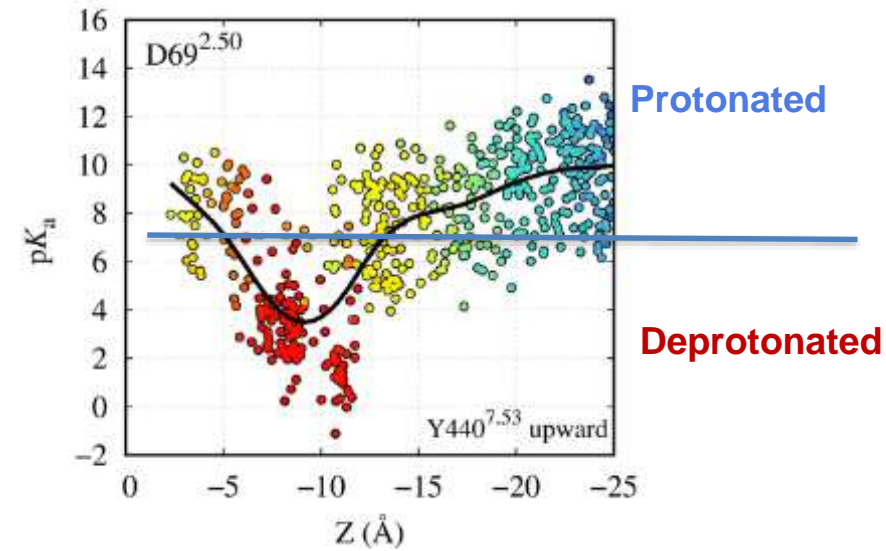
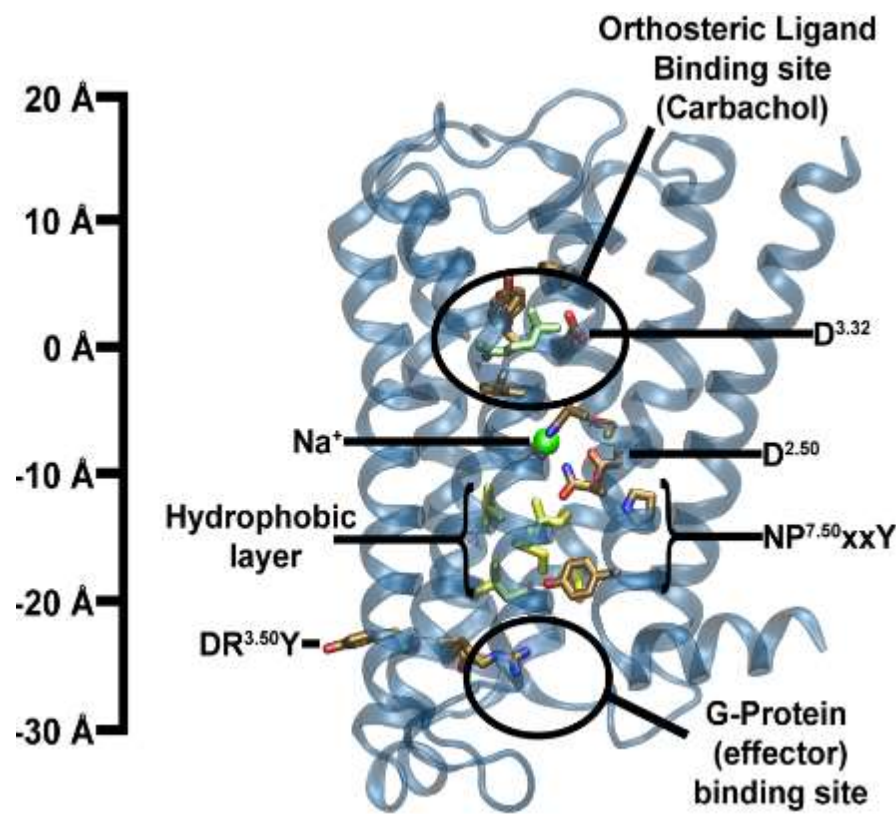
These MD simulations did not take into account:

1. Electrostatic and Na⁺ concentration gradient
2. Possibility of D2.50 protonation

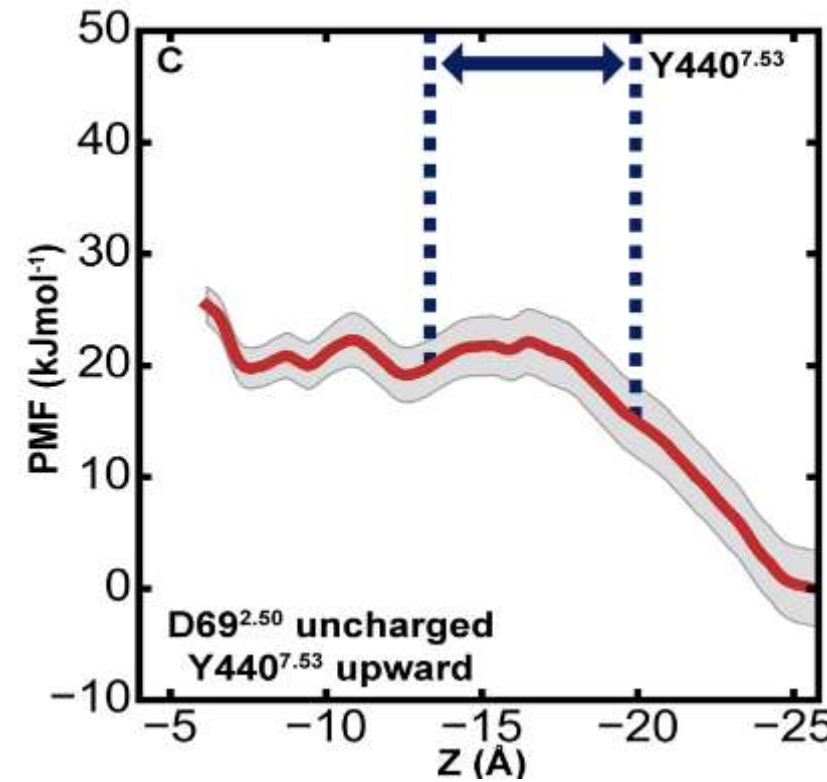
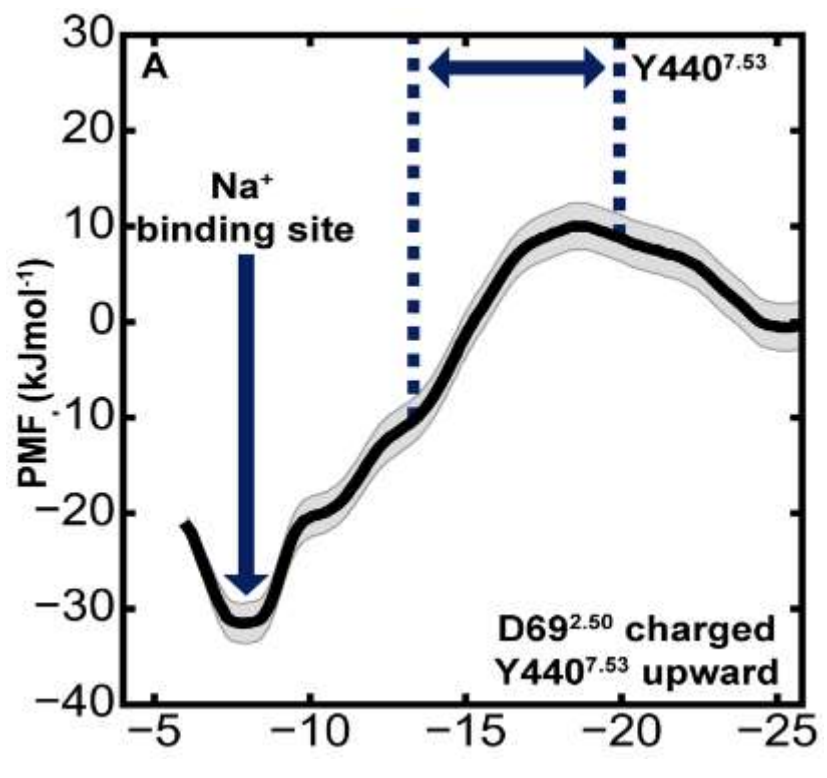
Is protonation of D2.50 involved in Sodium transition?



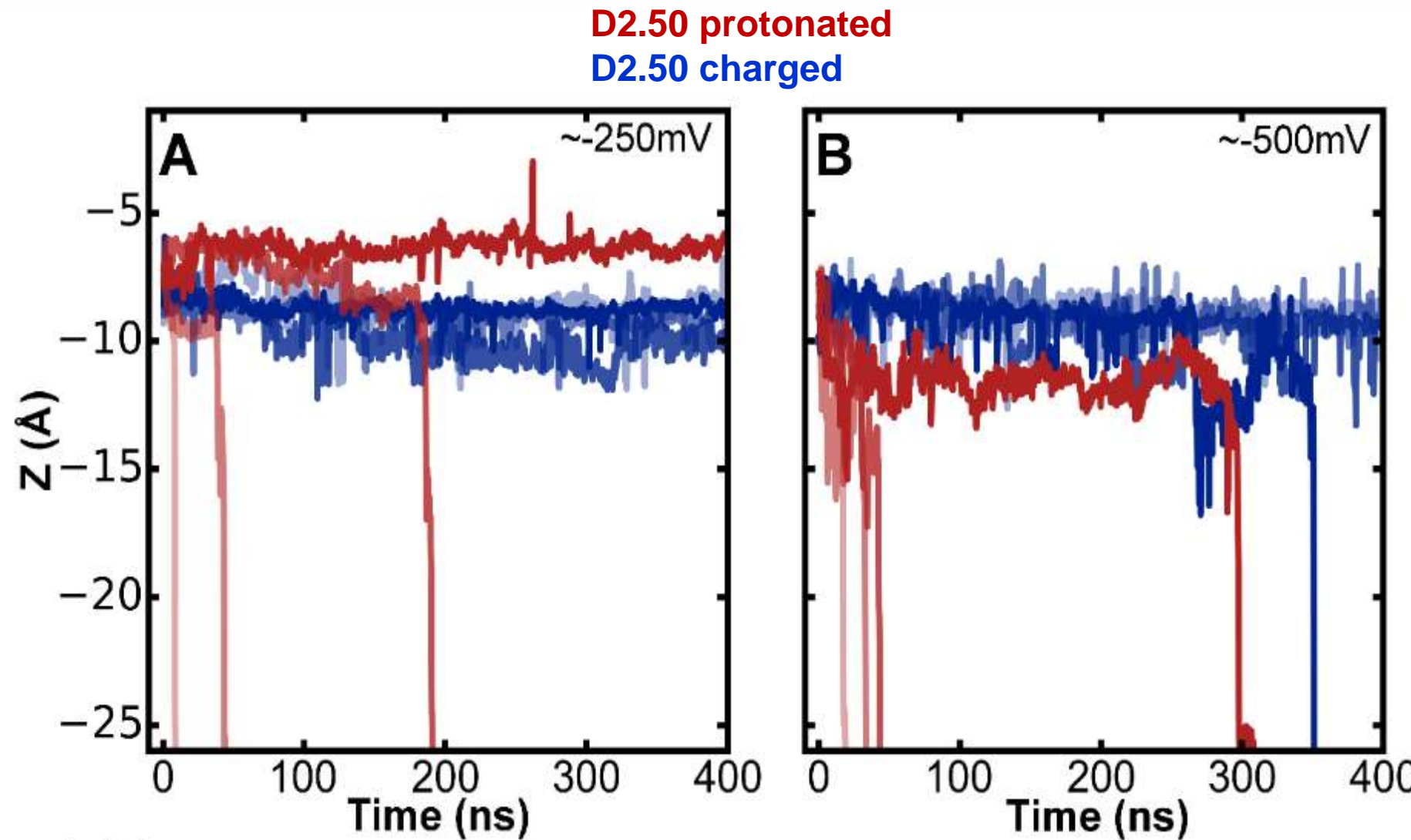
Calculated pK_a of D2.50 strongly depends on direct contact with Na^+



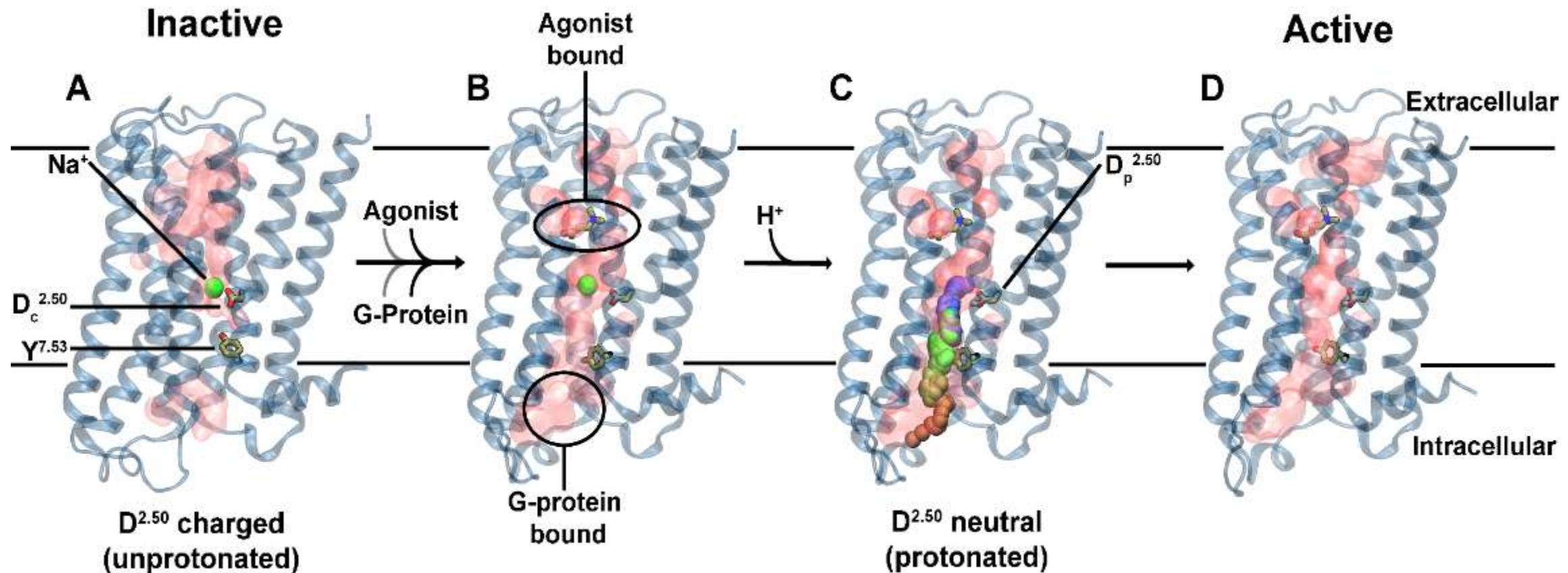
Protonation Changes Na⁺ Potential along the path



Na^+ ion egress to the intracellular side.



Updated Na⁺ mechanism



Summary & Outlook : Conserved Na⁺ site in GPCRs

- Sodium site conserved in most class A GPCRs
- Sodium coordinating residues and Na⁺ itself are involved in GPCR activation mechanism
- Sodium can travel through the GPCR “channel” along the voltage and concentration gradient (one Na⁺ at a time!)
- Sodium transfer may be coupled with D2.50 protonation
- Sodium site can be exploited in ligand discovery and receptor stability design

Outline

- Rational prediction of stabilizing mutations:
CompoMug
- New insights into GPCR function and allosteric mechanisms
- **Structure-Based ligand discovery for GPCRs**

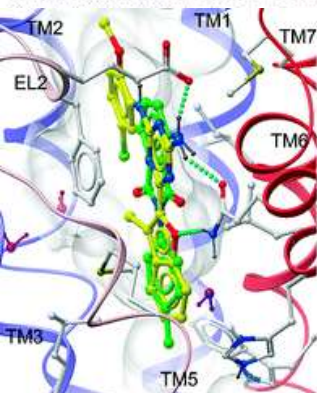
Can we use structures in GPCR ligand discovery?

Journal of
Medicinal
Chemistry
Article

J. Med. Chem. 2010, 53, 1793–1809 • 1799
DOI: 10.1021/jm901647p

Structure-Based Discovery of Novel Chemotypes for Adenosine A_{2A} Receptor Antagonists

Vsevolod Katritch,^{*†‡§} Veli-Pekka Jakkola,^{†§} J. Robert Lane,[†] Judy Lin,[†] Adrian P. Uzerman,[†] Mark Yeager,[†] Irina Kufareva,^{†§} Raymond C. Stevens,^{*,†} and Ruben Abagyan,^{*,†}



9, $K_i = 32 \text{ nM}$, LE = 0.37 Kcal/mol

21, $K_i = 5 \mu\text{M}$, LE = 0.38 Kcal/mol



Journal of
Medicinal
Chemistry

Optimization of Adenosine 5'-Carboxamide Adenosine Receptor Agonists Using Structure-Based Design and Fragment Screening

Dilip K. Tosh,[†] Khai Phan,[†] Zhan-Guo Gao,[†] Andrei A. Galakh,[†] Fei Xu,[†] Francesca Dellorian,[†] Ruben Abagyan,[§] Raymond C. Stevens,[‡] Kenneth A. Jacobson,^{*,†} and Vsevolod Katritch,^{*†}

[†]Molecular Recognition Section, Laboratory of Biophysical Chemistry, National Institute of Diabetes and Digestive and Kidney Diseases, National Institutes of Health, Bethesda, Maryland 20892, United States

[‡]Department of Molecular Biology, The Scripps Research Institute, 10550 North Torrey Pines Road, La Jolla, California 92037, United States

[§]University of California, San Diego Skaggs School of Pharmacy and Pharmaceutical Sciences, 9500 Gilman Drive, La Jolla, California 92093, United States

Supporting Information



Virtual Fragment Library Screening



ABSTRACT: Structures of G protein-coupled receptors (GPCRs) have a proven utility in the discovery of new agonists and inverse agonists modulating signaling of this important family of clinical targets. Applicability of active-state GPCR structures to virtual screening and rational optimization of agonists, however, remains to be assessed. In this study of adenosine 5'-derivatives,

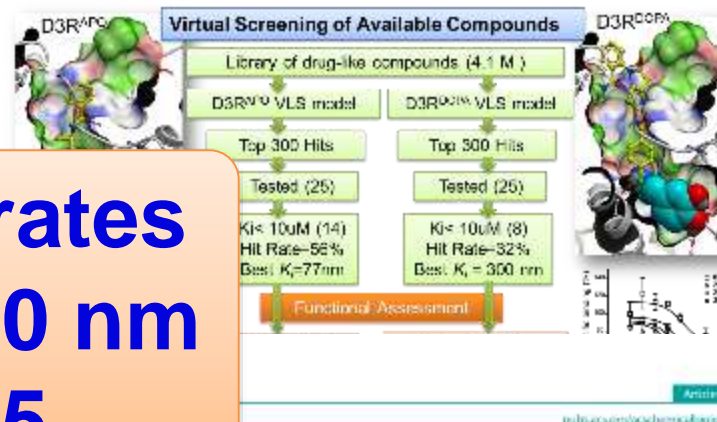
DOI: 10.1021/jm1001647p
Journal of Medicinal Chemistry, Vol. 53, No. 10, October 1, 2010
© 2010 by the American Association for Pharmacology and Experimental Therapeutics

Structure-Based Ligand Discovery Targeting Orthosteric and Allosteric Pockets of Dopamine Receptors^{1,2}

J. Robert Lane, Pavel Chubukov, Wei Liu, Meribell Canals, Vadim Cherezov, Ruben Abagyan, Raymond C. Stevens, and Vsevolod Katritch

Department of Integrative Structural and Computational Biology, Scripps Research Institute, La Jolla, California (P.C., W.L., V.C., R.C.S., R.K.); Drug Discovery Biology, Monash Institute of Pharmaceutical Sciences, Monash University, Parkville, Victoria, Australia (J.R.L., R.C.S.); and Skaggs School of Pharmacy and Pharmaceutical Sciences, and San Diego Supercomputer Center, University of California, San Diego, La Jolla, California (R.A.)

Received June 10, 2010; accepted September 10, 2010



Articles
pubs.acs.org/locpharmacology

Exploring a 2-Naphthoic Acid Template for the Structure-Based Design of P2Y₁₄ Receptor Antagonist Molecular Probes

Evgeny Kiselev,[†] Matthew O. Barrett,[†] Vsevolod Katritch,[‡] Silvia Paoletti,[†] Clarissa D. Weitzer,[†] Kyle A. Brown,[†] Eva Hamann,[†] Andrew L. Yin,[†] Qiang Zhao,[§] Raymond C. Stevens,[‡] T. Kendall Harden,[†] and Kenneth A. Jacobson,^{*,†}

[†]Molecular Recognition Section, Laboratory of Biophysical Chemistry, National Institute of Diabetes and Digestive and Kidney Diseases, National Institutes of Health, Bethesda, Maryland 20892, United States

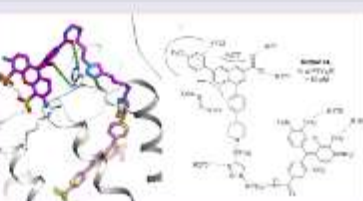
[‡]Department of Pharmacology, University of North Carolina, School of Medicine, Chapel Hill, North Carolina 27599, United States

[§]CAS Key Laboratory of Receptor Research, Shanghai Institute of Materia Medica, Chinese Academy of Sciences, 555 Zuchongzhi Road, Pudong, Shanghai 201203, China

[¶]Department of Integrative Structural and Computational Biology, The Scripps Research Institute, 10550 North Torrey Pines Road, La Jolla, California 92037, United States

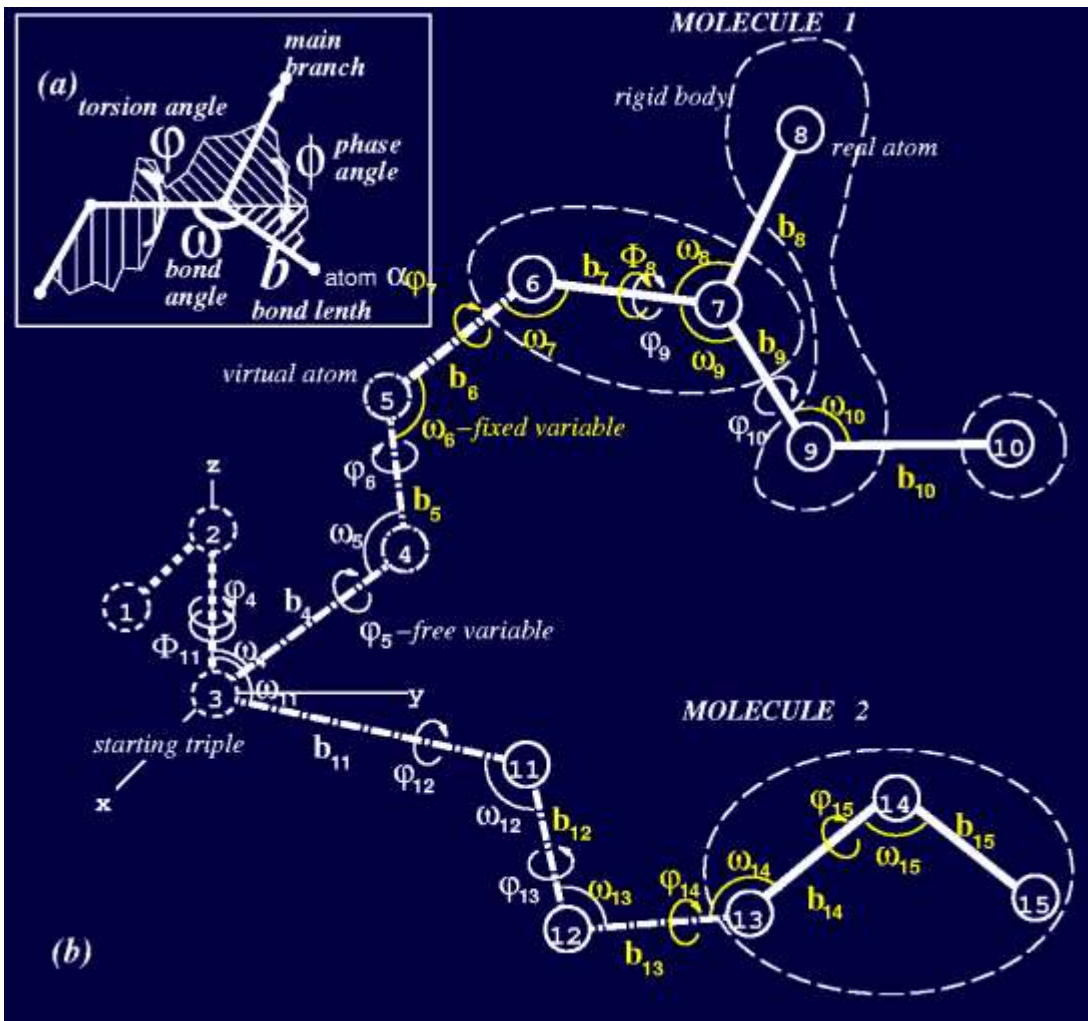
Supporting Information

ABSTRACT: The P2Y₁₄ receptor (P2Y₁₄R), one of eight P2Y G-protein-coupled receptors (GPCRs), is involved in inflammatory, endocrine, and lysosomal processes and is an attractive pharmaceutical target. The goal of this research is to develop high-affinity P2Y₁₄R fluorescent probes based on the potent and highly selective antagonist 4-(4-(pyridin-4-yl)-phenyl)-7-(4-(7-nitrobenzyl)-phenyl)-2-naphthoic acid (6, PPIN). A model of hP2Y₁₄R based on recent hP2Y₁₄R X-ray structure, together with simulated antagonist docking suggested that the piperidine ring is suitable for fluorophore conjugation while preserving affinity. Chain-extended alkyne or amide derivatives of 6 for click or amide coupling were



Core Modeling Technology: Internal Coordinate Mechanics (ICM)

$$E(\alpha) = \Delta E_{FF} + \Delta E_{EN} + \alpha_1 N_{at} + \alpha_2 \Delta E_{HB} + \alpha_3 \Delta E_{SE} + \alpha_4 \Delta E_{EL} + \alpha_5 \Delta E_{SO}$$



Internal coordinates:

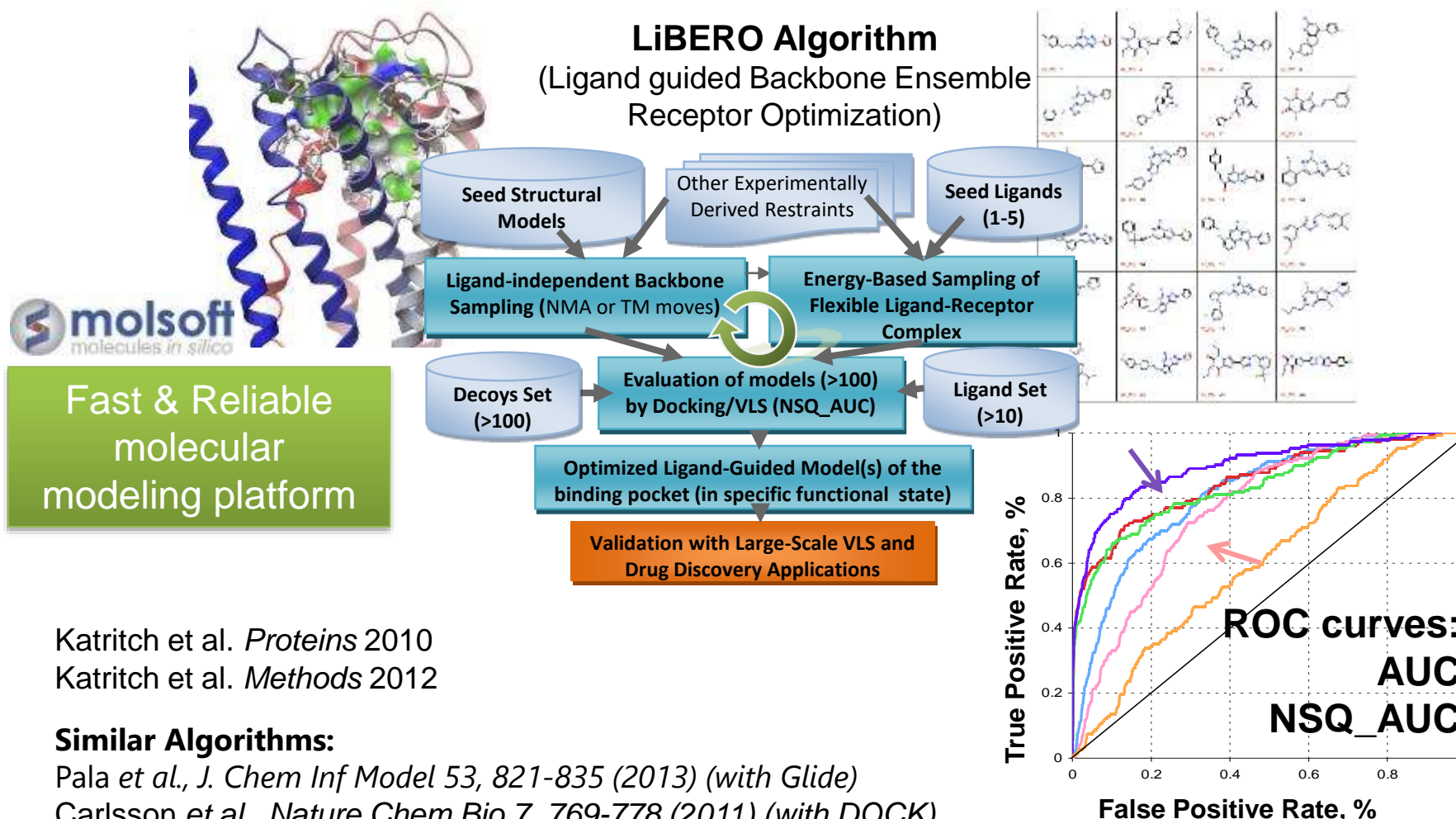
- + Eliminates “high frequency” modes
- + Efficient & fast global energy optimization algorithm
- + Large radius of convergence
- + Accurate force field and free energy func (solvation/entropy)
- + **Easy to perform sampling of both ligand and receptor conformations**

ICM References:

- Abagyan et al. (1994)
“ICM - a new method for protein modeling..”
J. Comp. Chem. 15, 488-506
- Katritch et al (2003).
ICFF: New Internal Coordinate Force Field
J Comp. Chem. 24:254-65

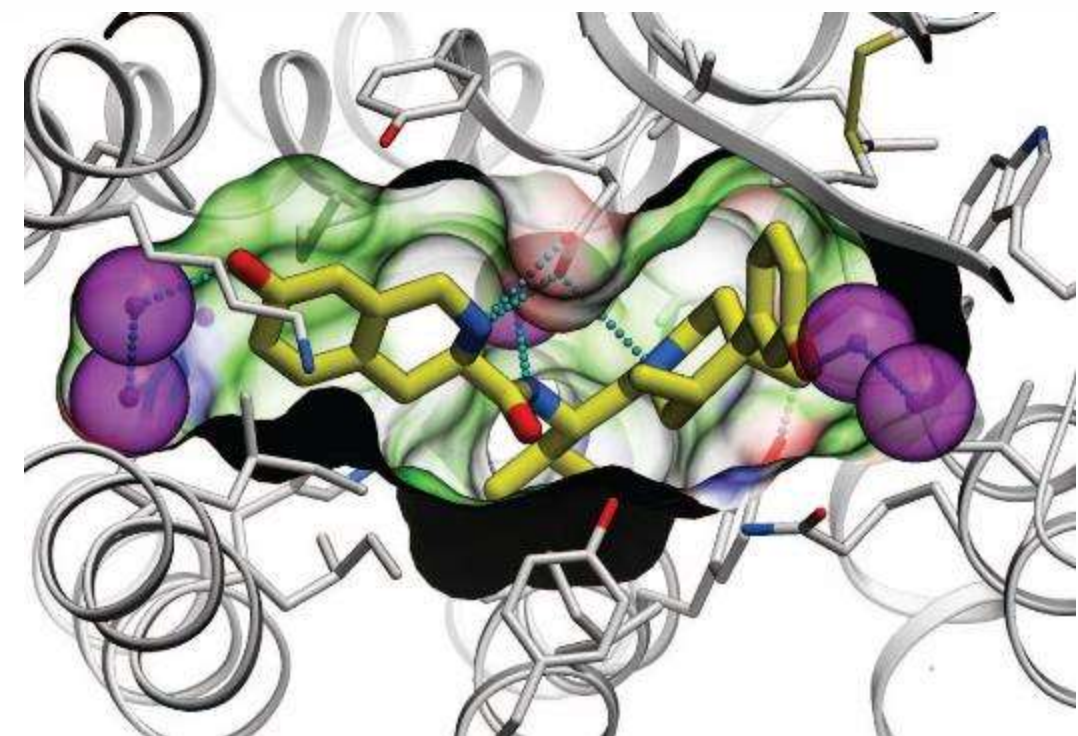
Ligand-Guided Model Optimization

- Improve accuracy and reliability of docking
- Improve VLS performance, especially for lower resolution structures or homology models
- Reduce ligand bias, or shift bias towards desirable ligand/scaffold
- Develop VLS models for different functional states



κ -Opioid Receptor as a Therapeutic Target

- κ -OR full agonists (e.g. SalA) lead to hallucination and dysphoria
- κ -OR antagonists: potential antidepressants, anxiolytics and anti-addiction drugs
- JDTic: high affinity selective antagonist, (but cardiac side effects in clinic)
- G-protein biased κ -OR agonists (no β -arrestin signaling): non-addictive analgesia
- **New κ -OR ligand chemotypes needed for both antagonist and biased agonist functional profiles**



κ -OR structure with JDTic (4DJH)
Wu et al 2012, Nature

Buda et al Neuropsychopharmacology 2015.
Carroll and Carlezon (2015) JMC 56: 2178–2195.

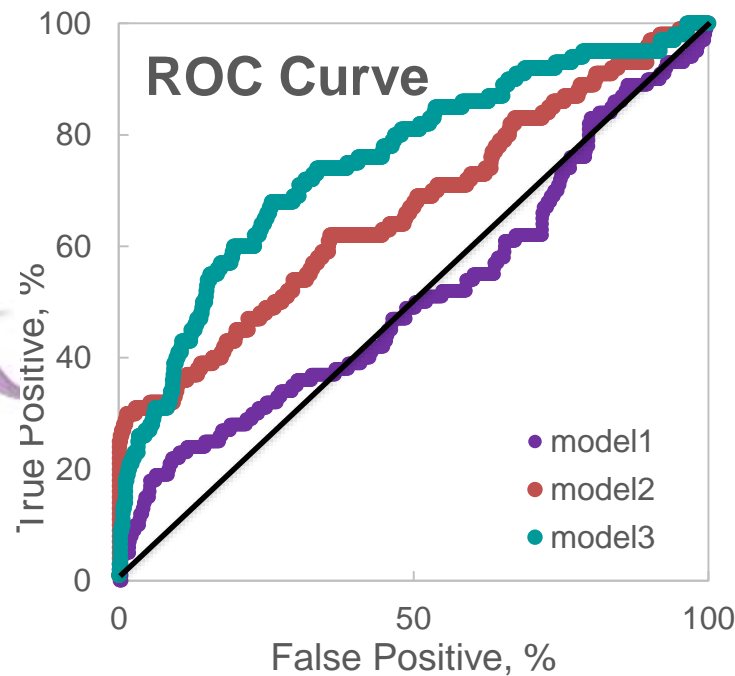
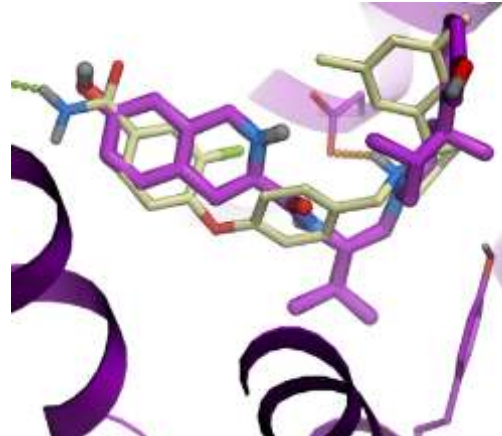
Hard target for VLS – few previously published VLS hits all $>\mu\text{M}$ range

Virtual Ligand Screening for κ -OR: Model Optimization



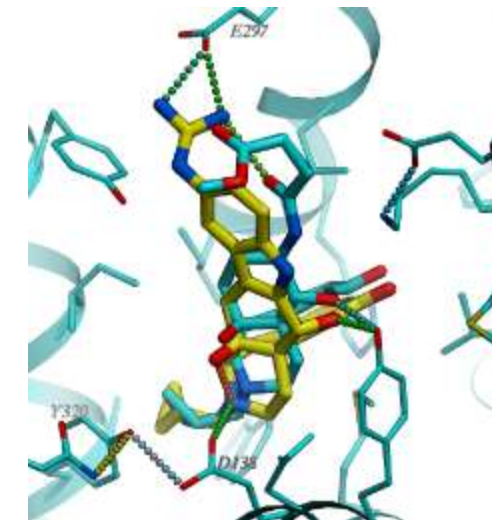
Model 1

JDTic-bound



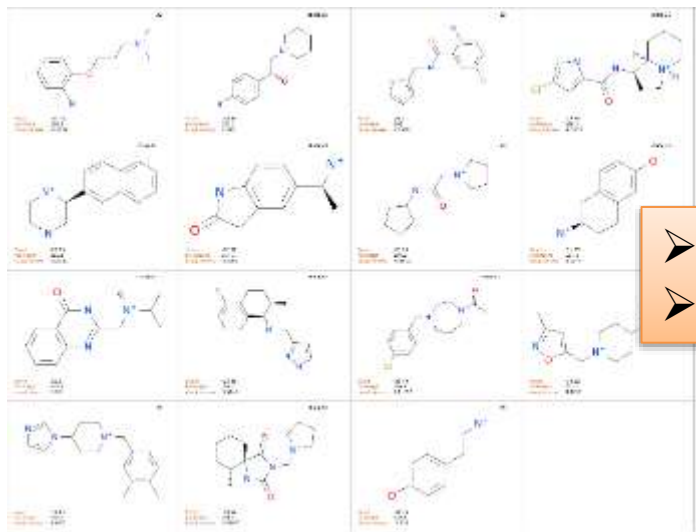
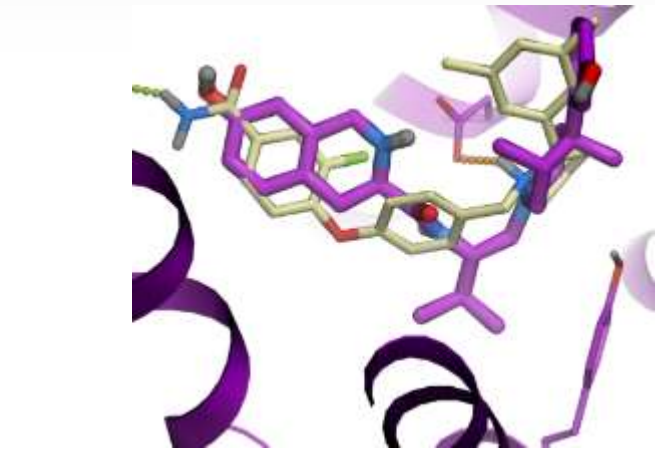
Model 3

Morphinan-bound



Virtual Ligand Screening for κ -OR

New Chemotype Discovery



Three Ligand-Optimized VLS models

Virtual Fragment-like and Lead-like Library
(5M compounds)

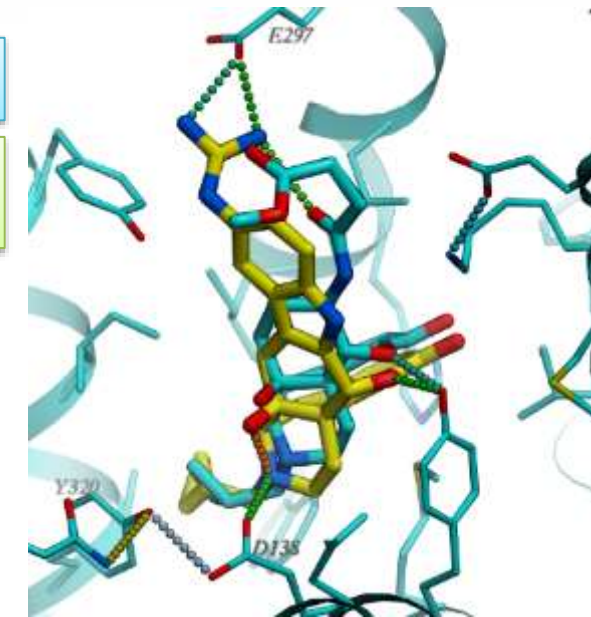
Novel Candidate hits with $\Delta\Delta G < 30$ (~200)

Ordered and tested (43)

$K_i(\kappa\text{-OR}) < 30 \mu\text{M}$ (27)

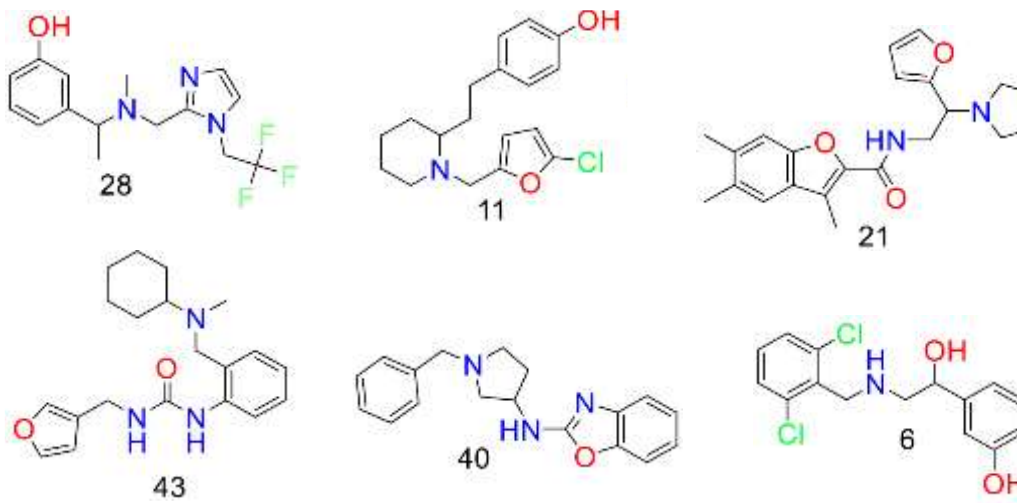
$K_i(\kappa\text{-OR}) < 10 \mu\text{M}$ (14)

- Best $K_i < 200$ nm, Ligand Efficiency **LE > 0.45**
- Agonists and antagonists, best $EC_{50} = 260$ nm

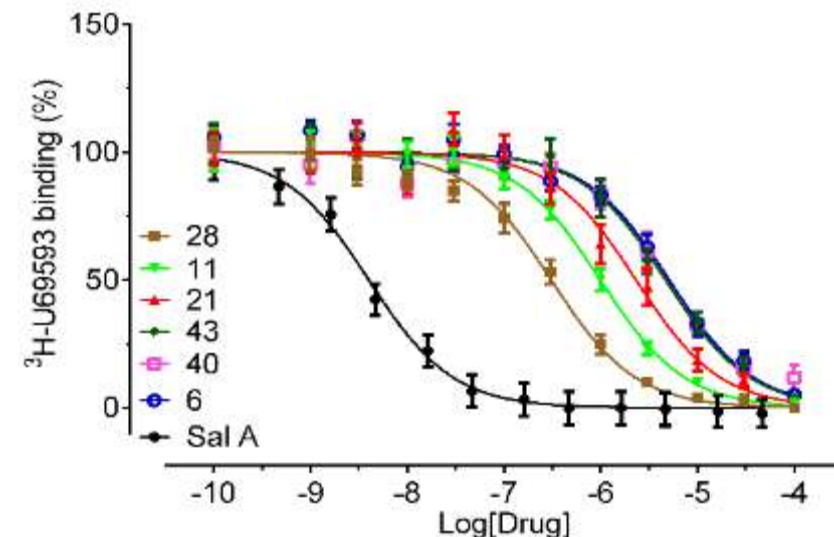
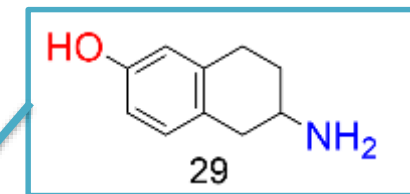


> 6 New Distinct Chemotypes of κ -OR Ligands

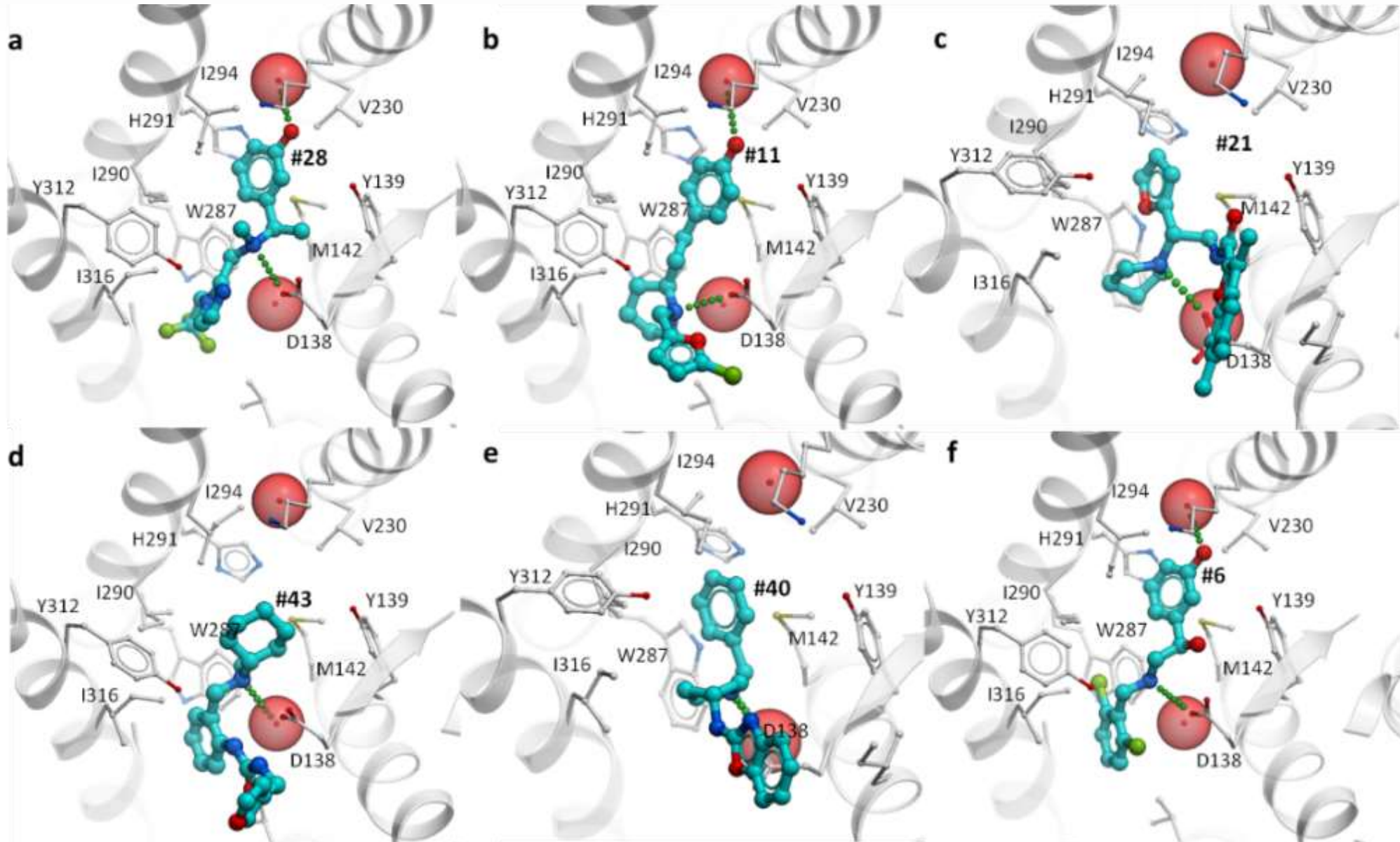
| Comp# | Model ^a | Inhibit% ^b | \pm | SEM ^c | pK_i | \pm | SEM | $K_i(\mu\text{M})$ | LE ^d | Tanimoto ^e |
|-----------|--------------------|-----------------------|-------|------------------|--------|-------|------|--------------------|-----------------|-----------------------|
| 28 | 1 | 96.9 | \pm | 1.2 | 6.82 | \pm | 0.16 | 0.2 | 0.43 | 0.42 |
| 11 | 1 | 95.3 | \pm | 2.5 | 6.30 | \pm | 0.12 | 0.5 | 0.40 | 0.19 |
| 21 | 3 | 77.5 | \pm | 6.8 | 5.95 | \pm | 0.26 | 1.1 | 0.31 | 0.29 |
| 43 | 2 | 76.5 | \pm | 4.7 | 5.64 | \pm | 0.16 | 2.3 | 0.32 | 0.39 |
| 40 | 3 | 77.5 | \pm | 5.6 | 5.59 | \pm | 0.22 | 2.6 | 0.36 | 0.40 |
| 6 | 1 | 80.1 | \pm | 4.2 | 5.58 | \pm | 0.17 | 2.6 | 0.39 | 0.39 |
| 17 | 2 | 53.0 | \pm | 7.8 | 5.52 | \pm | 0.12 | 3.0 | 0.32 | 0.52 |
| 16 | 2 | 60.7 | \pm | 14.7 | 5.52 | \pm | 0.17 | 3.0 | 0.37 | 0.38 |
| 20 | 2 | 49.1 | \pm | 16.4 | 5.21 | \pm | 0.14 | 6.2 | 0.30 | 0.42 |
| 35 | 2 | 49.8 | \pm | 8.4 | 5.19 | \pm | 0.17 | 6.4 | 0.36 | 0.51 |
| 3 | 1 | 70.2 | \pm | 3.9 | 5.18 | \pm | 0.18 | 6.6 | 0.36 | 0.26 |
| 8 | 1 | 73.7 | \pm | 4.0 | 5.09 | \pm | 0.22 | 8.1 | 0.29 | 0.34 |
| 29 | 2 | 48.6 | \pm | 9.6 | 5.08 | \pm | 0.12 | 8.3 | 0.59 | 0.15 |
| 22 | 2 | 47.3 | \pm | 7.7 | 5.01 | \pm | 0.13 | 9.8 | 0.28 | 0.39 |



“Similar” to JDTic core
tetrahydronaphthalene vs.
tetrahydroisoquinoline

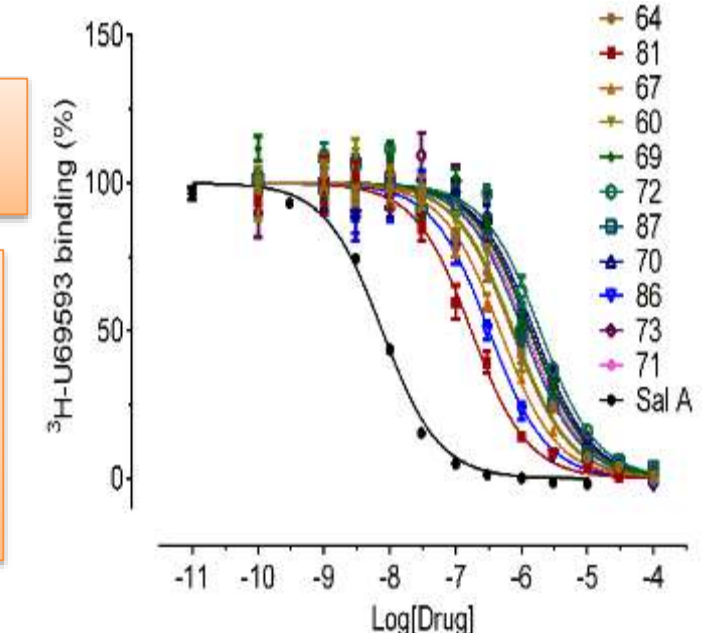
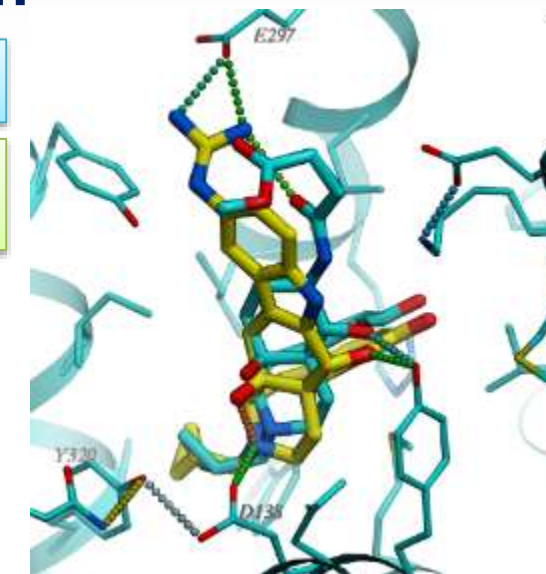
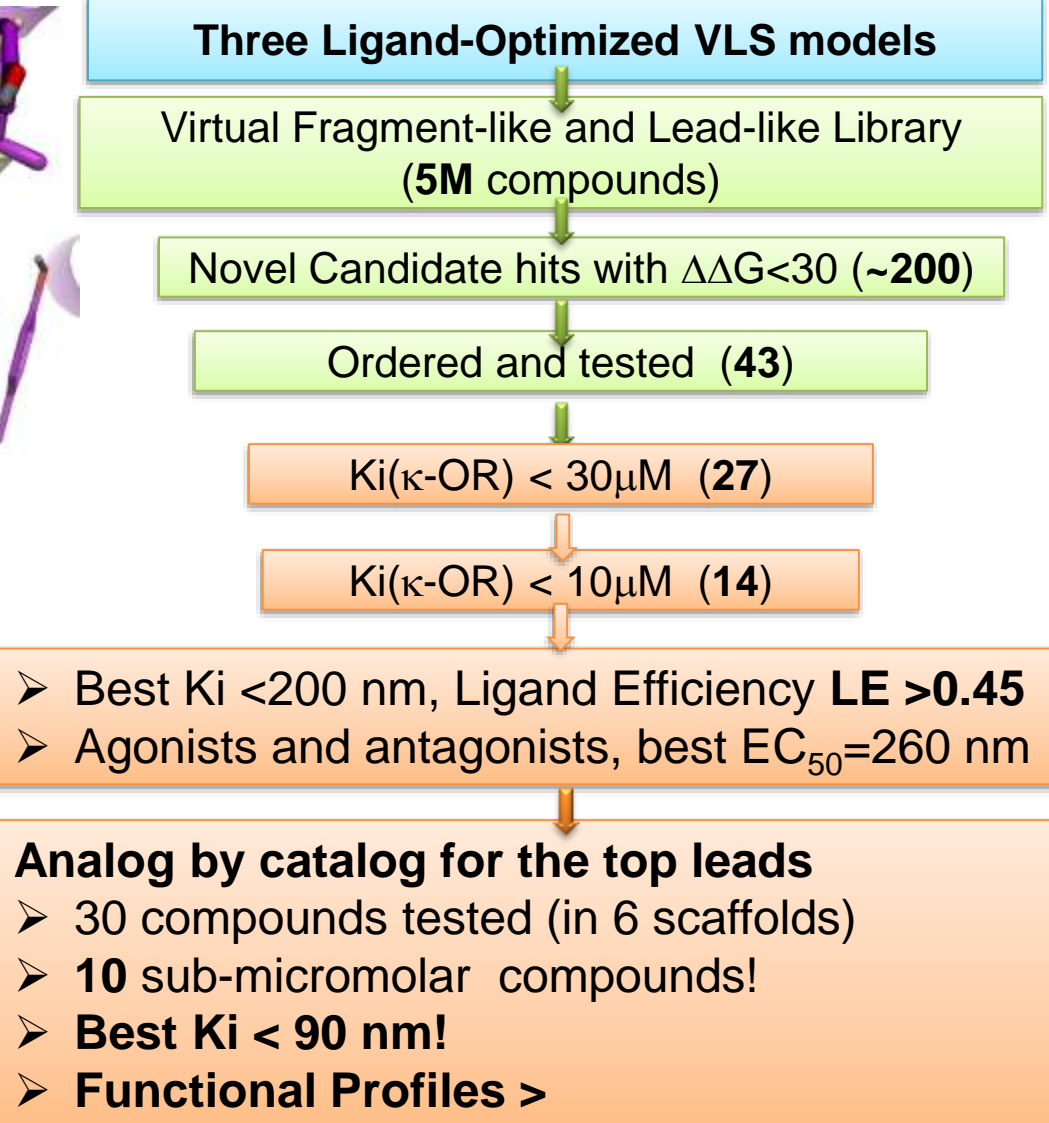
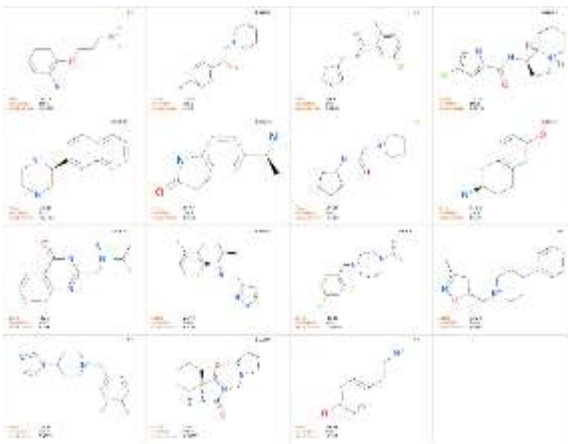
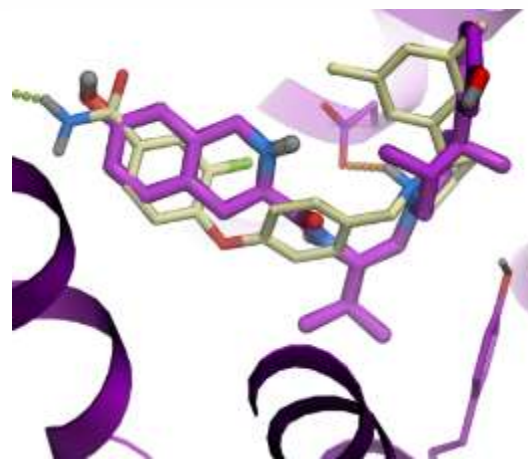


> 6 New Distinct Chemotypes of κ -OR Ligands

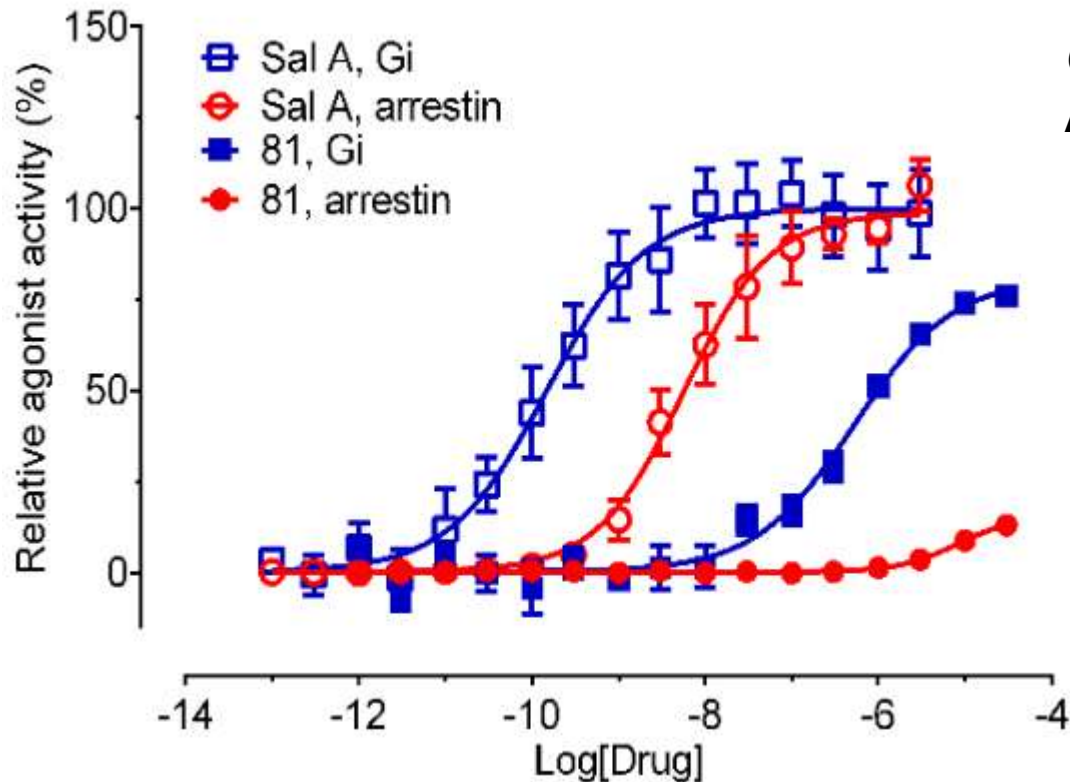


Virtual Ligand Screening for κ -OR

First Round of Optimization



Discovery of a new Biased Agonist



Comp #81:

Binding Affinity

$$K_i = 160 \text{ nM}$$

G_i pathway:

$$EC_{50} = 530 \text{ nM}$$

Arrestin :

$$EC_{50} > 10000 \text{ nM}$$

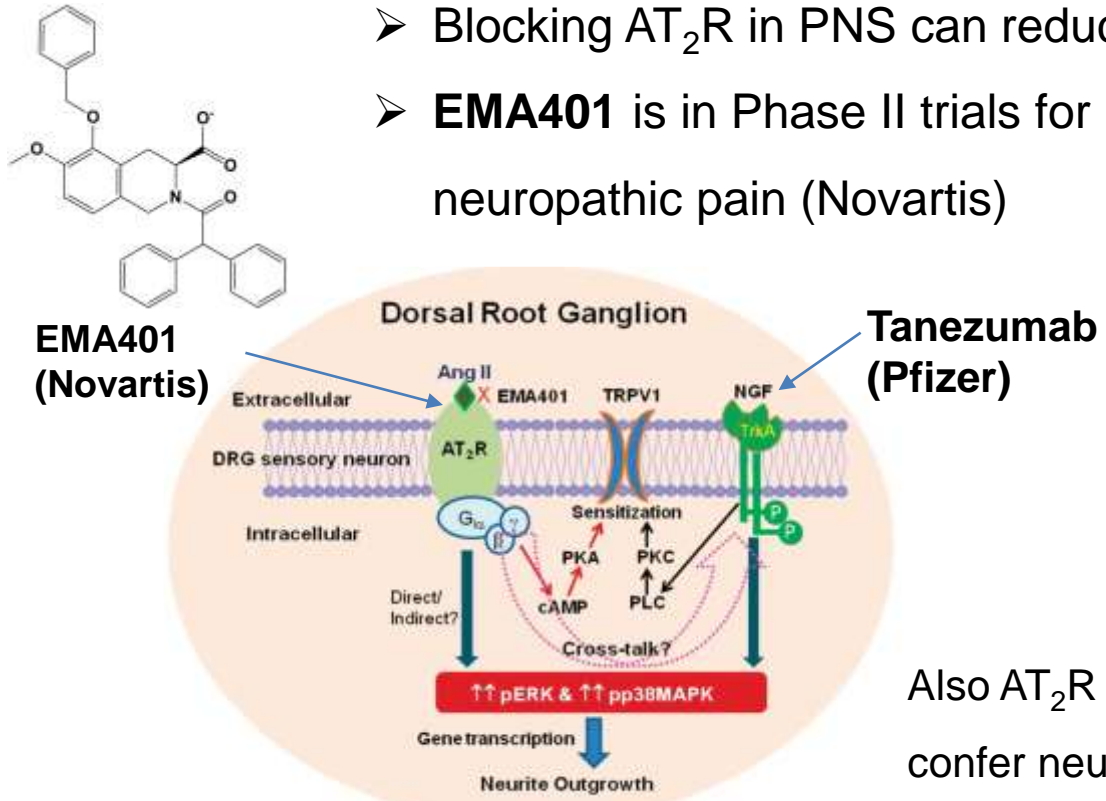
Bias factor: $\Delta\Delta\log(\tau/K_A) > 6.0$
(G_i vs arrestin pathways)

Ongoing optimizations of best scaffolds

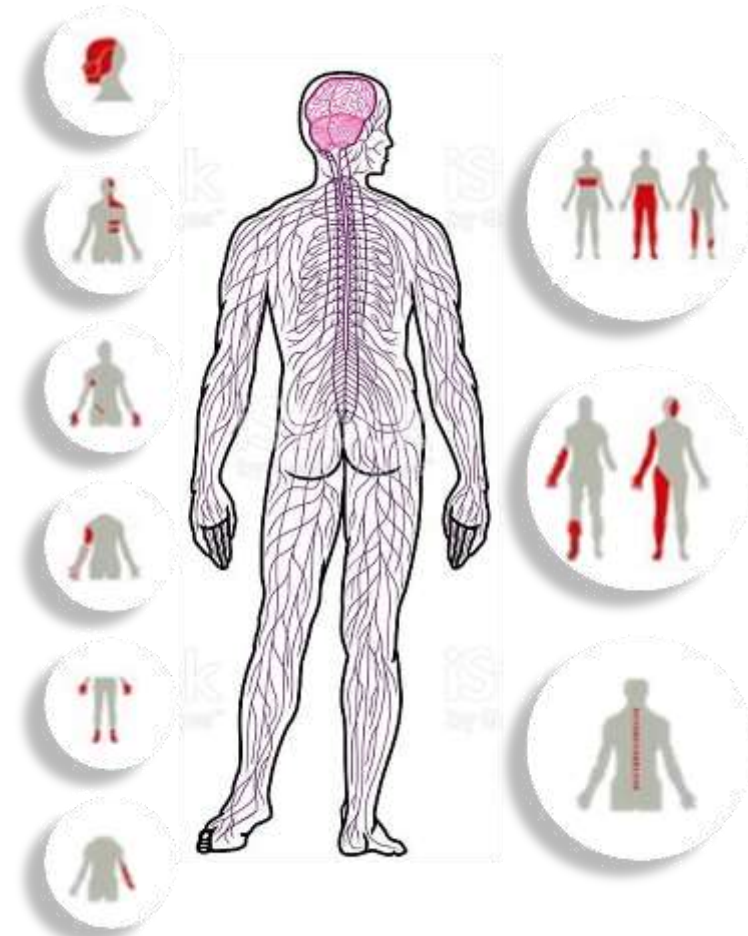
Angiotensin AT₂R antagonists for neuropathic pain relief



- AT₂R regulates nerve sensitization and neurite outgrowth in neuropathic pain
- Blocking AT₂R in PNS can reduce the pain
- **EMA401** is in Phase II trials for post-herpetic neuropathic pain (Novartis)

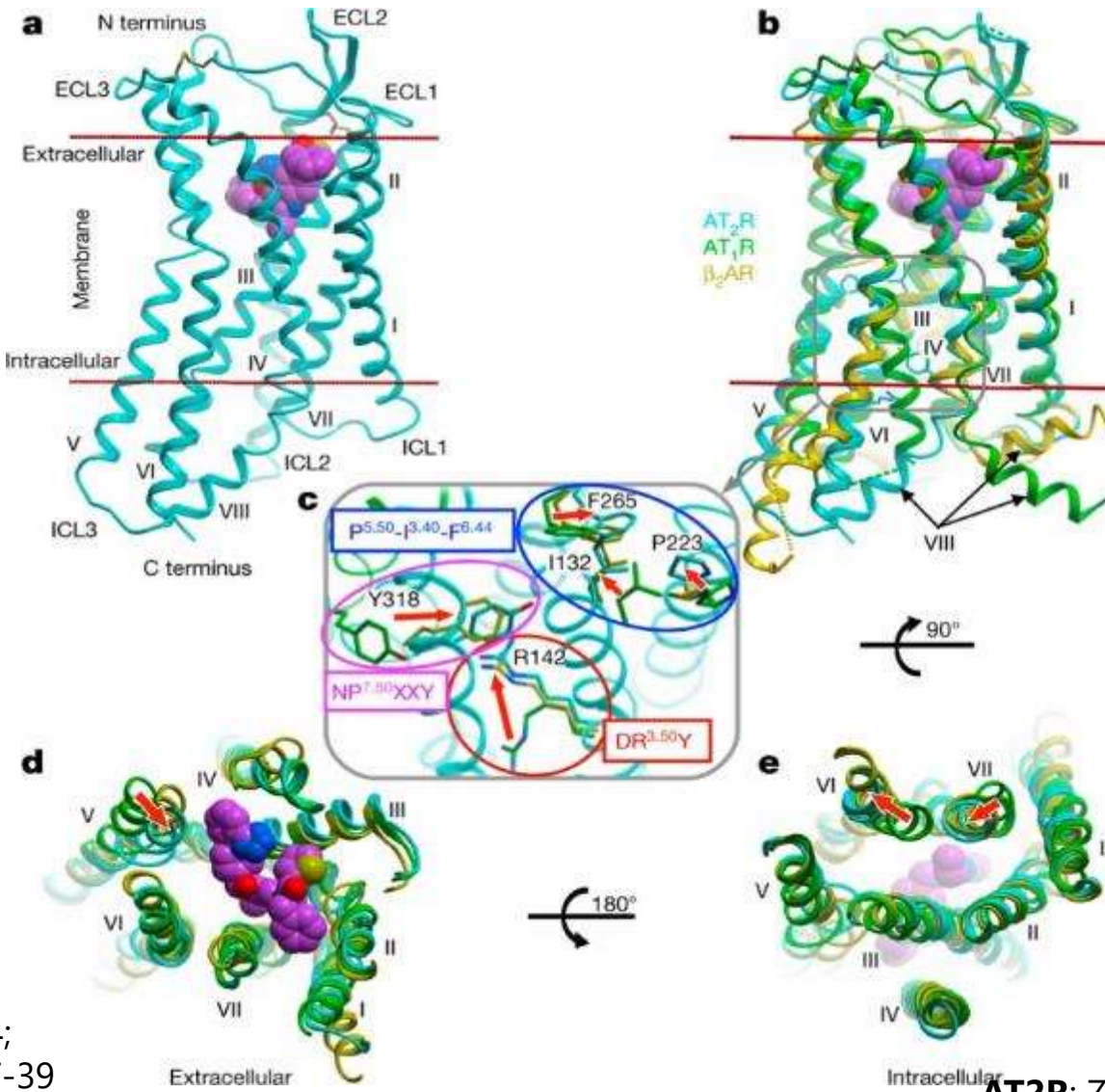


Also AT₂R agonists (C21)
confer neuroprotection in
CNS (stroke)





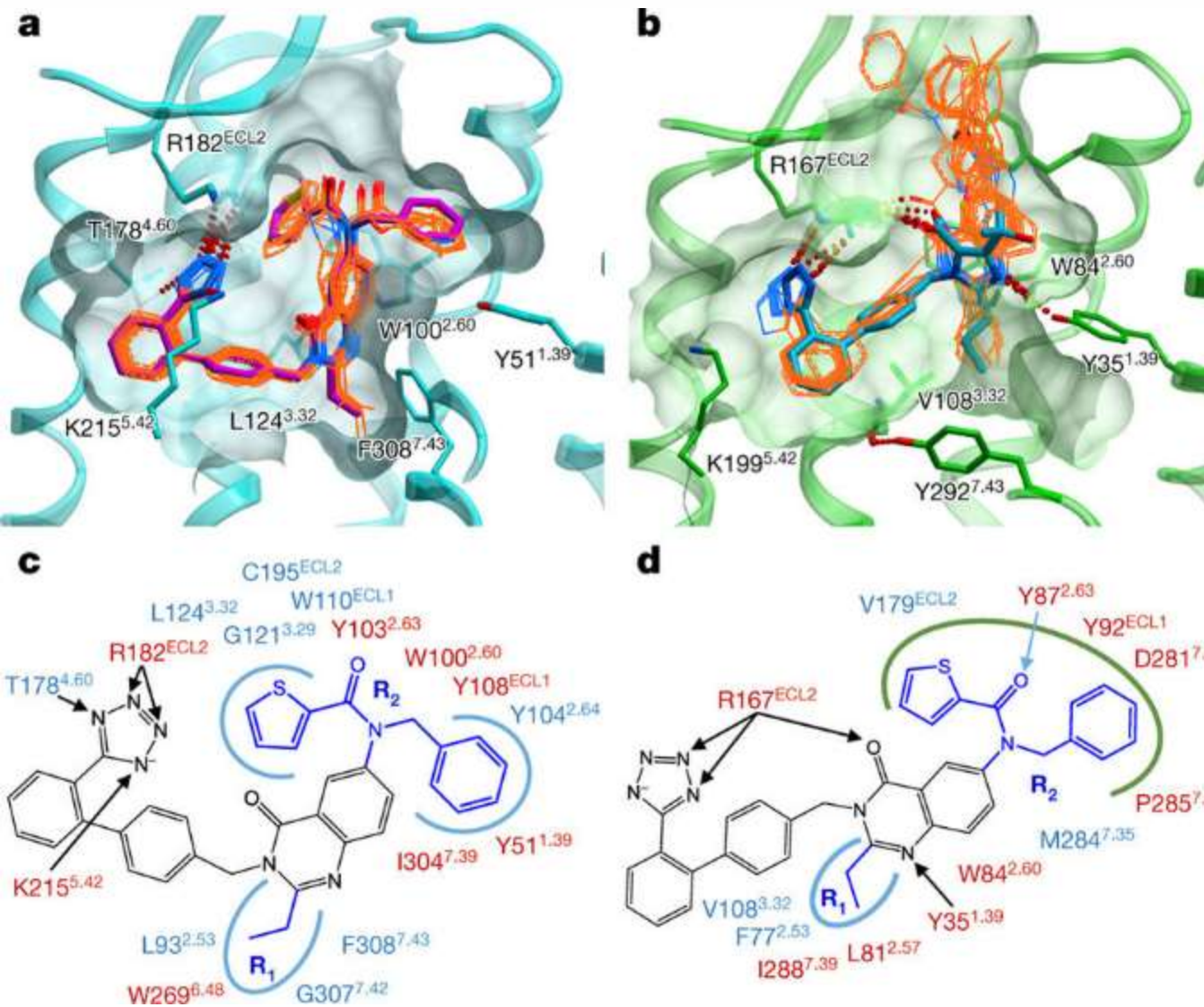
Crystal Structures of AT₁R and AT₂R give new insights into function ...



AT1R: Zhang H, *Cell.* 2015;161(4):833-44;
Zhang H, *JBC* 2015;290(49):29127-39

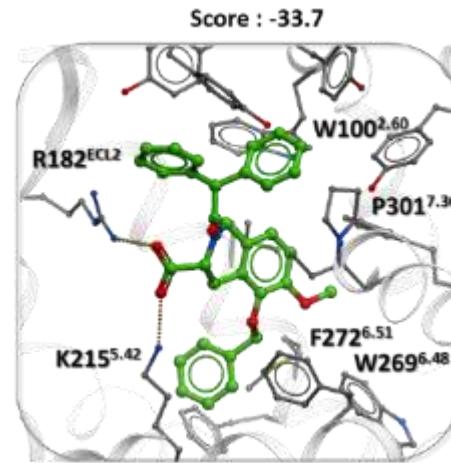
AT2R: Zhang H, *Nature.* 2017;544(7650):327-32;

... and AT₁R vs. AT₂R selectivity



Lead-like AT₂R selective hits from initial VLS

Model tested and refined with EMA401



- 1M • Lead Like Compounds
- 5K • Top rank analyzed for selectivity
- 52 • Purchased and tested
- 6 • Initial Validated Hits

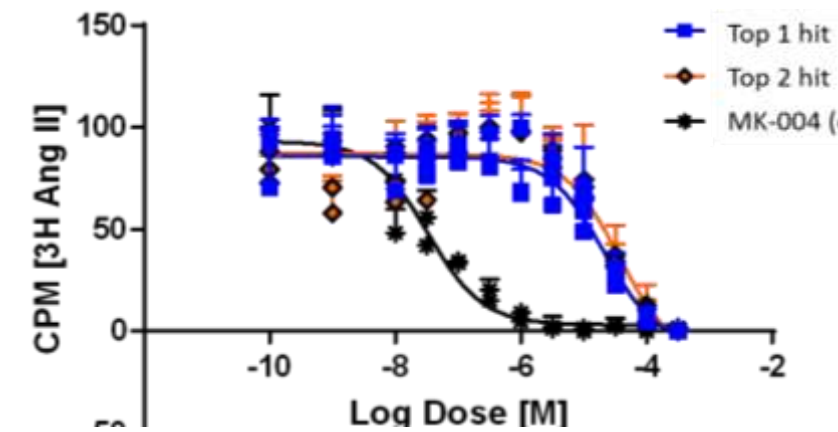
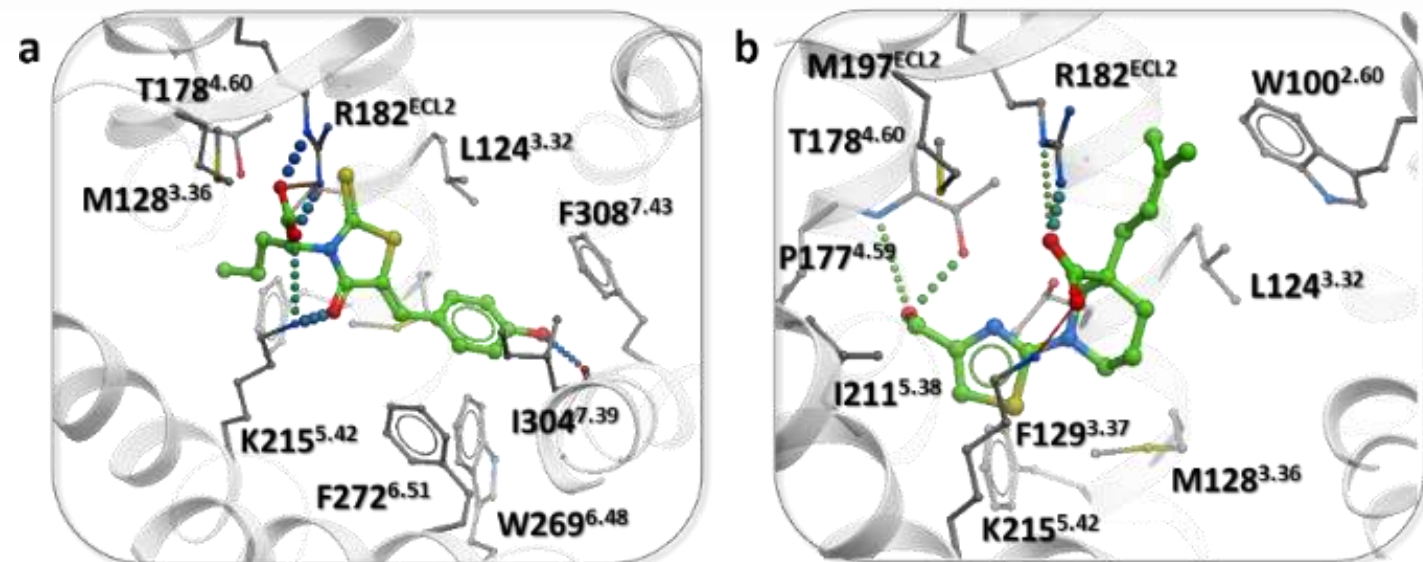
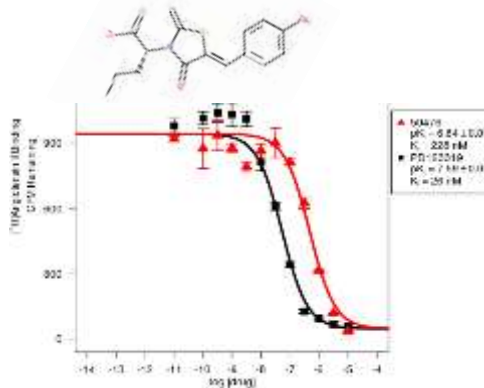


Fig.10 Radioligand competition binding assay for the MK-4 and top two hit compounds.

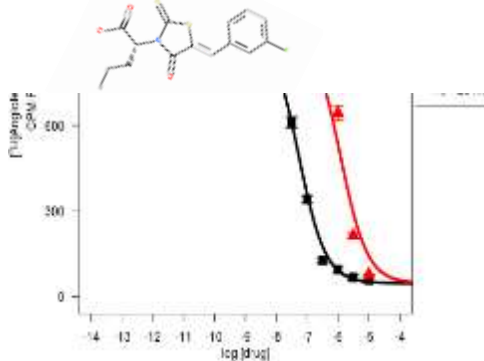
New SAR Results

Confidential

BRI-6001



BRI-6003



Compound #
(Name)

pKi ± SEM

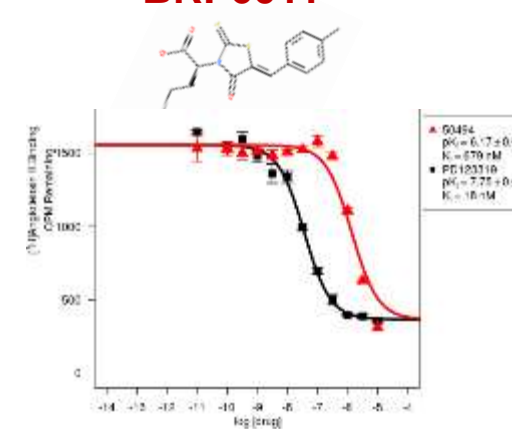
K_i, nM

LE

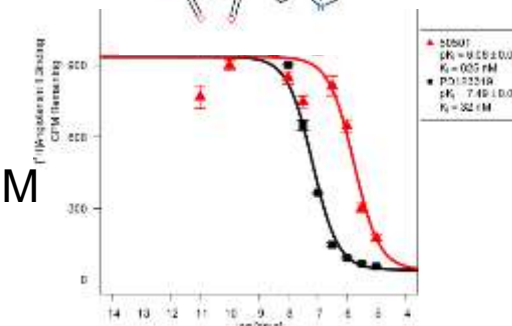
| | | | |
|-------------------------|--------------------|------------|-------------|
| 50476 (BRI-6001) | 6.64 ± 0.07 | 228 | 0.42 |
| 50486 (BRI-6103) | 6.24 ± 0.07 | 581 | 0.40 |
| 50491 (BRI-6108) | 5.65 ± 0.07 | 2254 | 0.36 |
| 50492 (BRI-6109) | 5.43 ± 0.08 | 3739 | 0.35 |
| 50494 (BRI-6111) | 6.17 ± 0.06 | 680 | 0.39 |
| 50501 (BRI-6118) | 6.08 ± 0.07 | 825 | 0.41 |
| 50502 (BRI-6119) | 5.25 ± 0.09 | 5681 | 0.32 |
| 50477 (BRI-6002) | 5.67 ± 0.08 | 2158 | 0.38 |
| 50533 (EMA401) | 7.60 ± 0.04 | 25 | 0.28 |
| 50534 (C21) | 7.44 ± 0.04 | 36 | 0.33 |

$$\text{Ligand Efficiency, LE} = 1.4 * pK_i / N_{atom}$$

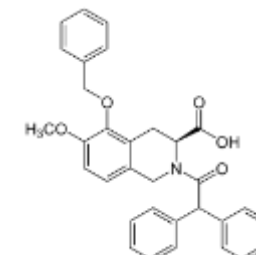
BRI-6011



BRI-6018

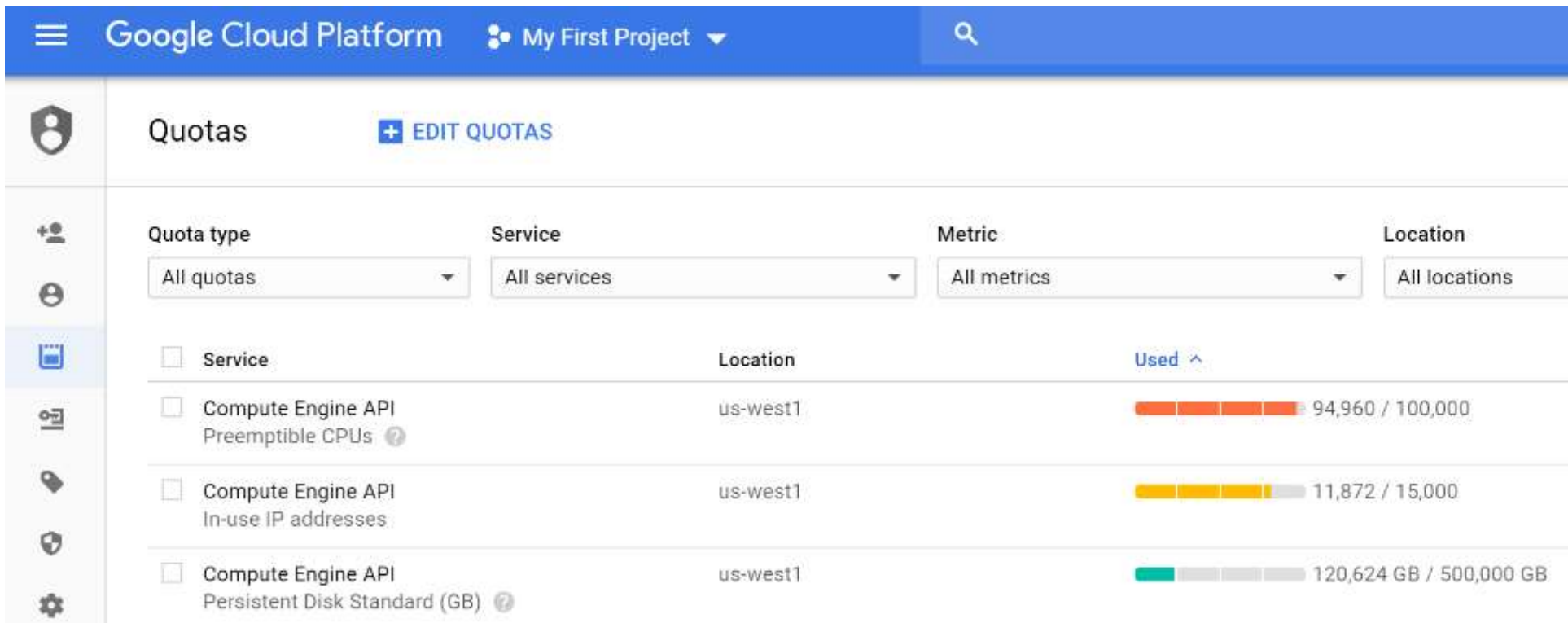


Control: PD123319 (**EMA401**)
 $N_{atom} = 38$



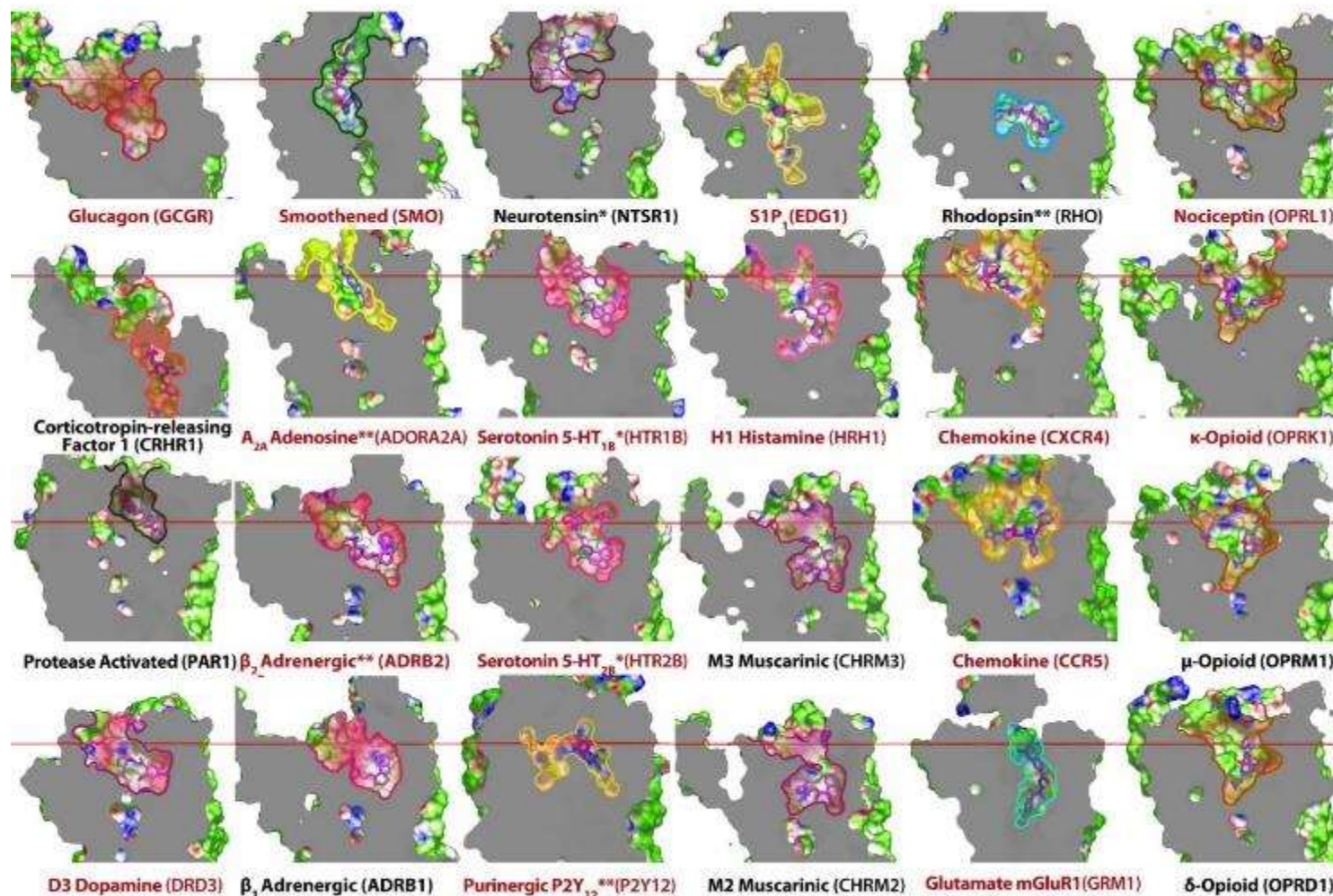
Google Cloud screening of 500M compounds (NIH Commons Pilot Project)

- Used new ZINC library of “Wait-OK” compounds (4-6 weeks, 80% success)
- Google Cloud screening used ~100,000 CPUs at once
- Completed in 24 hours
- Would take ~5 month on our servers



Other Hot GPCR Targets for Ligand Discovery

>50 GPCRs with structures solved and ~10 more coming this year...



Summary & Outlook : Structure-based VLS

- Structure-based VLS allows effective and fast discovery of novel chemotypes for GPCR targets
- High hit rates (20-40%), sub-uM affinities, high Ligand Efficiencies
- Subtype- and functional selectivity can be improved via SAR and lead optimization
- Targeting new allosteric pockets (e.g. sodium site)

Thanks!

GPCR
Consortium



R33 DA038858; P01 DA035764
R21 EY027620 (BRAIN Initiative)



Computational Group



Nilkanth Patel



Anastasiia Sadybekov



Barabara Zarzycka, PhD.



Saheem Zaidi, PhD



Jessica Grandner, PhD.



Petr Popov, PhD (+MIPT)



Arman Sadybekov, PhD



Natalie Binczewski

Collaborators:

- ❖ Bryan Roth (*UNC*)
- ❖ James Zhi-Jie (*iHuman*)
- ❖ Beili Wu & Quang Zhao (*SIMM*)
- ❖ Uli Zachariae (U. Dundee)
- ❖ Ken Jacobson (*NIH/NIDDK*)
- ❖ Patrick Giguere (*Ottawa U*)
- ❖ Rob Lane (*Monash U*)
- ❖ Ivy Carroll (*RTI*)
- ❖ Irene Coin (*Leipzig U*)
- ❖ Dirk Trauner (*NYU*)
- ❖ Ruben Abagyan (*UCSD/Molsoft*)

